

A new method for choosing the computational cell in stochastic reaction–diffusion systems

Hye-Won Kang · Likun Zheng · Hans G. Othmer

Received: 15 December 2010 / Revised: 23 June 2011
© Springer-Verlag 2011

Abstract How to choose the computational compartment or cell size for the stochastic simulation of a reaction–diffusion system is still an open problem, and a number of criteria have been suggested. A generalized measure of the noise for finite-dimensional systems based on the largest eigenvalue of the covariance matrix of the number of molecules of all species has been suggested as a measure of the overall fluctuations in a multivariate system, and we apply it here to a discretized reaction–diffusion system. We show that for a broad class of first-order reaction networks this measure converges to the square root of the reciprocal of the smallest mean species number in a compartment at the steady state. We show that a suitably re-normalized measure stabilizes as the volume of a cell approaches zero, which leads to a criterion for the maximum volume of the compartments in a computational grid. We then derive a new criterion based on the sensitivity of the entire network, not just of the fastest step, that predicts a grid size that assures that the concentrations of all species converge to a spatially-uniform solution. This criterion applies for all orders of reactions and for reaction rate functions derived from singular perturbation or other reduction methods, and encompasses both diffusing and non-diffusing species. We show that this predicts the maximal allowable volume found in a linear problem, and we illustrate our results

H.-W. Kang (✉) · L. Zheng
School of Mathematics, University of Minnesota, Twin Cities, MN 55455, USA
e-mail: hkang@math.umn.edu

L. Zheng
e-mail: zhen0107@math.umn.edu

H. G. Othmer
School of Mathematics & Digital Technology Center,
University of Minnesota, Twin Cities, MN 55455, USA
e-mail: othmer@math.umn.edu

with an example motivated by anterior-posterior pattern formation in *Drosophila*, and with several other examples.

Mathematics Subject Classification (2000) 80A30 · 92C45 · 60J28 · 35Q92

Keywords Biological networks · Noise · Stochastic reaction–diffusion systems · Discretization

Contents

1	Introduction	1
1.1	The description of reaction networks	1
1.2	The stochastic description of reactions	1
1.3	The master equation for a general system of reaction and diffusion	1
1.4	Overview of the paper	1
2	Linear stochastic reaction–diffusion networks	1
2.1	Measures of the fluctuations in a compartmental system	1
2.2	Example	1
3	An upper bound for the compartment size	1
3.1	Homogeneous Neumann conditions	1
3.2	Other types of boundary conditions	1
4	Applications	1
4.1	Example 2.2 revisited	1
4.2	Why network properties must be considered	1
4.3	The reaction $2A \rightleftharpoons C$ in a distributed setting	1
5	Discussion	1
	Appendices	
A	Proof of the mean first passage time for N walkers	1
B	Spectral representation of the reaction–diffusion matrix Ω	1
C	Proof of Proposition 1	1
D	Proof of Theorem 1	1
E	Proof of Theorem 2	1

1 Introduction

It is now widely-recognized that stochastic effects can play an important role in diverse processes such as gene expression and spatial pattern formation in development because many key biological molecules are present in low copy numbers. For example, gene transcription in some bacteria involves interactions between 1–3 promoter elements, 10–20 polymerase holoenzyme units, 10–20 copies of repressor proteins, 3000 RNA polymerase molecules, and approximately 1000 ribosomes (Kuthan 2001). Since chemical reactions occur in discrete steps at the molecular level, the processes are inherently stochastic and the inherent “irreproducibility” in these dynamics has been demonstrated experimentally for single cell gene expression events (Spudich and Koshland 1976; Ozbudak et al. 2002; Levsky and Singer 2003). In some contexts stochastic effects simply add noise to an output, but have no beneficial role, but in others, such as asymmetric cell division, their role is essential. In general organisms show a remarkable degree of resilience or robustness in the face of noise, and thus understanding the time-dependent behavior of a system of interacting species and how

noise influences the outcome is important in numerous contexts, including temporal gene expression profiles, signal transduction, and other biochemical processes. Of course when the numbers of molecules of all species are large enough, a ‘law of large numbers’ argument shows that for finite times the stochastic formulation described later converges to the mass-action based deterministic description commonly used, at least in well-mixed systems (Kurtz 1972).

One of the earliest investigations of stochastic effects in reactions is due to Delbrück (1940), who studied the distribution of the number of molecules for a single reacting species in a one-component, enzyme-catalyzed system. It was assumed there that the substrate is in excess and thus the process is effectively first-order. There are many other examples of first-order reaction networks that involve a small number of molecules, including transcription and translation modeled as first-order catalytic reactions (Thattai and van Oudenaarden 2001), for which stochastic analysis is necessary. The evolution of the surface morphology during epitaxial growth involves the nucleation and growth of atomic islands, and these processes may be described by first-order adsorption and desorption reactions coupled with diffusion along the surface. Proteins exist in distinct conformational states, and the reversible transitions between states can be described as first-order conversion processes (Mayor et al. 2003). Fluctuating protein conformations are important in the movement of small molecules through proteins such as myoglobin; hence it is important to understand the distribution of these states (Di Iorio et al. 1991; Austin et al. 1975). RNA also exists in several conformations, and the transitions between various folding states follow first-order kinetics (Bokinsky et al. 2003). In Gadgil et al. (2005) the linear problem for an arbitrary number of components is more or less completely solved, in that it is shown there how to obtain the evolution equations for the mean and variance in closed form. These results also address the problem of understanding how the interplay between the nature of the individual steps and the connectivity or topology of the entire network affects the dynamics of the system, irrespective of whether a deterministic or a stochastic description is the most appropriate, but this problem remains unsolved for general nonlinear reaction schemes.

In the context of biological pattern formation, robustness or resilience is frequently defined with respect to the precision and sensitivity of the determination of boundaries between different cell types in a developing tissue (Umulis et al. 2008). A classical paradigm for this process is the French flag model, in which a one-dimensional domain is to be divided into three equal-size sub-domains (Umulis et al. 2008). In the simplest deterministic version of this model, either specialized source and sink cells located at the boundary of the developmental field maintain the concentration of a signaling molecule, called a morphogen, at appropriate fixed levels, or boundary cells produce the morphogen at a fixed rate. In the former case, when there is no degradation of the morphogen in the interior of the domain a linear distribution can be established in a one-dimensional system of about 1 mm in length in the time that is normally available for commitment to differentiation (Wolpert 1971; Crick 1970). Given fixed thresholds between different cell types, the tissue can be proportioned into any number of cell types and the determination of the boundaries is robust with respect to changes in the size of the system. In the latter case we consider a simple version in which the flux at the boundary is specified, and degradation by first-order reaction occurs through-

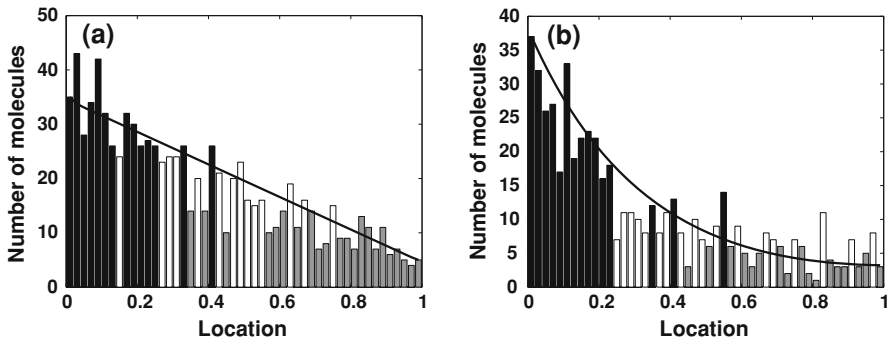


Fig. 1 Two examples of the French flag model with stochastic dynamics. In each case the system is $1 \times 0.01 \times 0.01 \text{ mm}^3$, the x -length is discretized into 50 compartments, the diffusion coefficient is $1,000 \mu\text{m}^2 \text{min}^{-1}$, and one realization is shown at 100 mins. **a** The distribution for fixed concentrations at the boundaries: 35 molecules at the left and 5 at the right, with diffusion and no degradation throughout. The *color* indicates the thresholds: *black* greater than 25 and *gray* less than 15 molecules. **b** The distribution when there is an influx from a source at the left end at a rate $0.1 \text{ nM } \mu\text{m} \text{min}^{-1}$, and diffusion and degradation at a rate 0.01 min^{-1} throughout. Initially, each compartment has 10 molecules of morphogen. The *color* indicates the thresholds: *black* greater than 12 and *gray* less than 6 molecules

out the domain—generalizations will be discussed later in the context of *Drosophila* patterning.

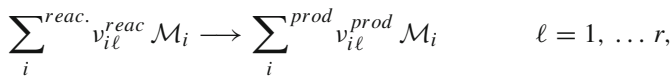
However a deterministic description of either of these models ignores the possible effects of stochastic fluctuations in the signaling and gene control networks and the effect stochastic fluctuations may have on the precision of patterning. Figure 1a shows one realization of a stochastic model of a linear chain of compartments with fixed numbers of molecules at the endpoints of the domain, and Fig. 1b shows one realization for the second scheme, in which the input flux is fixed at the left. In both panels the solid line shows the mean of the distribution, which can be computed directly since the equations are linear (Gadgil et al. 2005). These curves also represent the steady-state distribution for the corresponding deterministic system. Since each developing embryo represents one realization of the stochastic patterning process, the results illustrate the difficulty in determining the location of the boundaries between cell types in the face of such fluctuations. In embryonic patterning in *Drosophila*, the primary morphogen Dpp has signaling activity in the range of 10^{-10} to 10^{-9} M (Shimmi and O'Connor 2003), and at these concentrations there are very few Dpp signaling molecules available to the receptors. Thus fluctuations will be significant, and how the embryos cope with such noise and pattern reliably is still not fully understood. Preliminary work has shown that a postulated positive feedback mechanism (Serpe et al. 2008) increases the reliability of spatial patterning (Zheng et al. 2011). In any case, spatially-distributed systems add a new level of complexity to the problem of understanding the importance of noise in development.

1.1 The description of reaction networks

Throughout we deal with reacting systems that are not diffusion-limited, and thus a stochastic analysis and simulation of reaction and diffusion can be built around a

discretized or compartmentalized model of the system in which each compartment is well-mixed. We discuss the rationale for this approach and the method for choosing the compartment size in more detail later, but we begin by developing the chemical master equation that can be used to describe such systems. We begin with some background on a deterministic description of reacting systems, then derive the master equation for an arbitrary network of reacting species, and finally add diffusion. The formulation of the reaction component is described in more detail elsewhere (Othmer 1981; Gadgil et al. 2005; Lee and Othmer 2010).

Suppose that a reacting mixture contains a set \mathcal{M} of s chemical species \mathcal{M}_i that participate in a total of r reactions. Let $v_{i\ell}$ be the stoichiometric coefficient of the i th species in the ℓ th reaction. The $v_{i\ell}$ are non-negative integers that represent the normalized molar proportions of the species in a reaction. Each reaction is written in the form



where the sums are over reactants and products, respectively in the ℓ th reaction. Here the forward and reverse reaction of a reversible pair are treated as two irreversible reactions. There may be other species that do not react, but they play no role here. Once the reactants and products are specified the network topology of the associated reaction graph is defined. The linear combinations of species that appear as reactants or products in the various elementary steps are called complexes, and the relation defined by which complexes are connected by reaction gives rise to a directed graph \mathcal{G} in which each complex is identified with a vertex V_j in \mathcal{G} and a directed edge E_ℓ is introduced into \mathcal{G} for each reaction. Each edge carries a nonnegative weight $\hat{\mathcal{R}}_\ell(c)$ given by the intrinsic rate of the corresponding reaction. The topology of \mathcal{G} is in turn represented in its vertex-edge incidence matrix \mathcal{E} , which is defined as follows.

$$\mathcal{E}_{j\ell} = \begin{cases} +1 & \text{if } E_\ell \text{ is incident at } V_j \text{ and is directed toward it} \\ -1 & \text{if } E_\ell \text{ is incident at } V_j \text{ and is directed away from it} \\ 0 & \text{otherwise} \end{cases}$$

If there are p complexes and r reactions, then \mathcal{E} has p rows and r columns and every column has exactly one $+1$ and one -1 .

Once the complexes and reactions are fixed, the stoichiometry of the complexes is determined, and we let v denote the $s \times p$ matrix whose j th column encodes the stoichiometric amounts of the reacting species in the j th complex. Then the deterministic temporal evolution of the composition of a spatially-uniform reacting mixture is governed by

$$\frac{dc}{dt} = v\mathcal{E}\hat{\mathcal{R}}(c). \tag{1}$$

A special but important class of rate functions is that in which the rate of the ℓ th reaction can be written as

$$\hat{\mathcal{R}}_\ell(c) = k_\ell R_\ell(c).$$

This includes ideal mass action rate laws, for which the rate is given by

$$R_\ell = \prod_{i=1}^s (c_i)^{v_{i\ell}}. \quad (2)$$

As it stands, (1) includes all reacting species, but those whose concentration is constant on the time scale of interest can be deleted from each of the complexes in which it appears, and its concentration or mole fraction can be absorbed into the rate constant for reactions in which it participates as a reactant.¹ Furthermore, some complexes may not comprise any time-dependent species; these will be called null complexes and denoted by \mathcal{M}^0 , and each null complex gives rise to a column of zeroes in ν . The rate of any reaction in which the reactant complex is a null complex is usually constant. For instance, any transport reaction of the form $\mathcal{M}^0 \rightarrow \mathcal{M}_i$ introduces a null complex and the corresponding flux of \mathcal{M}_i represents a constant input to the reaction network, provided that the rate of the transport step does not depend on the concentration of a time-dependent species.

One can also base the description of a reacting system on the number of molecules, and to connect the deterministic and stochastic descriptions, we let $n = (n_1, n_2, \dots, n_s)$ denote the discrete composition vector whose i th component n_i is the number of molecules of species \mathcal{M}_i present in the volume \mathbf{V} . This is the discrete version of the composition vector c , and they are related by $n = \mathcal{N}_A \mathbf{V} c$, where \mathcal{N}_A is Avogadro's number. From (1) we obtain the deterministic evolution for n as

$$\frac{dn}{dt} = \nu \mathcal{E} \tilde{\mathcal{R}}(n)$$

where $\tilde{\mathcal{R}}(n) \equiv \mathcal{N}_A \mathbf{V} \hat{\mathcal{R}}(n/\mathcal{N}_A \mathbf{V})$. In particular, for mass-action kinetics

$$\begin{aligned} \tilde{\mathcal{R}}_\ell(n) &= \mathcal{N}_A \mathbf{V} k_\ell R_\ell(n/\mathcal{N}_A \mathbf{V}) = \mathcal{N}_A \mathbf{V} k_\ell \prod_{i=1}^s \left(\frac{n_i}{\mathcal{N}_A \mathbf{V}} \right)^{v_{i\ell}} \\ &= \frac{k_\ell}{(\mathcal{N}_A \mathbf{V})^{\sum_i v_{i\ell} - 1}} \prod_{i=1}^s (n_i)^{v_{i\ell}} = \hat{k}_\ell \prod_{i=1}^s (n_i)^{v_{i\ell}}. \end{aligned}$$

Care is needed in accounting for volume factors when one species in a bimolecular reaction is confined to a surface and the other to the adjacent fluid, as occurs in receptor–ligand interactions.

¹ Hereafter s will denote the number of species whose concentration may be time-dependent.

1.2 The stochastic description of reactions

In the stochastic description the evolution of the number of molecules of a species is modeled as a continuous-time Markov jump process. Let $N_i(t)$ be a random variable that represents the number of molecules of species \mathcal{M}_i at time t , and let N denote the vector of N_i s. The state of the system at any time is a point in \mathcal{Z}_0^s , where \mathcal{Z}_0 is the set of nonnegative integers. Let $P(n, t)$ be the joint probability that $N(t) = n$, i.e., $N_1 = n_1, N_2 = n_2, \dots, N_s = n_s$; then the master equation for the evolution of P is

$$\frac{d}{dt}P(n, t) = \sum_{m \in \mathcal{S}(n)} \mathcal{R}(m, n) \cdot P(m, t) - \sum_{m \in \mathcal{T}(n)} \mathcal{R}(n, m) \cdot P(n, t)$$

where $\mathcal{R}(i, j)$ is the probability per unit time of a transition from state i to state j , the ‘source’ set $\mathcal{S}(n)$ is the set of all states that can terminate at n after one reaction step, and $\mathcal{T}(n)$, the ‘target’ set, is the set all states reachable from n in one step of the feasible reactions. The sets $\mathcal{S}(n)$ and $\mathcal{T}(n)$ are easily determined using the underlying graph structure. It follows from the definition of v and \mathcal{E} that the ℓ th reaction $C(k) \rightarrow C(k')$ induces a change $\Delta n^{(\ell)} = v\mathcal{E}_{(\ell)}$ in the number of molecules of all species after one step of the reaction, where subscript ℓ denotes the ℓ th column of \mathcal{E} and $C(k)$ denotes the k th complex of species. Therefore the state $m = n - v\mathcal{E}_{(\ell)}$ is a source or predecessor to n under one step of the ℓ th reaction. Similarly, states of the form $m = n + v\mathcal{E}_{(\ell)}$ are reachable from n in one step of the ℓ th reaction.

Once the graph of the network and the stoichiometry are fixed, we can sum over reactions rather than sources and targets, and consequently the master equation takes the form

$$\frac{d}{dt}P(n, t) = \sum_{\ell} \mathcal{R}_{\ell}(n - v\mathcal{E}_{(\ell)}) \cdot P(n - v\mathcal{E}_{(\ell)}, t) - \sum_{\ell} \mathcal{R}_{\ell}(n) \cdot P(n, t).$$

However, the transition probabilities $\mathcal{R}_{\ell}(n)$ are not simply the macroscopic rates $\tilde{\mathcal{R}}$ if the reactions are second-order (or higher), but are given by (Gillespie 1976; Gadgil et al. 2005)

$$\mathcal{R}_{\ell} = c_{j(\ell)} h_{j(\ell)}(n).$$

Here $j(\ell)$ denotes the reactant complex for the ℓ th reaction, the factor $c_{j(\ell)}$ is the probability per unit time that the molecular species in the j th complex react via the ℓ th reaction, and $h_{j(\ell)}(n)$ is the number of independent combinations of the molecular components in this complex. Thus

$$c_{j(\ell)} = \frac{k_{\ell}}{(\mathcal{N}_A \mathbf{V}) \sum_i v_{ij(\ell)} - 1} = \hat{k}_{\ell} \quad \text{and} \quad h_{j(\ell)} = \prod_i \prod_{a_i=0}^{v_{ij(\ell)}-1} (n_i - a_i).$$

For a first-order reaction \hat{k}_{ℓ} is the probability per unit time per molecule of a transition, for a bimolecular step of the form $A + A \rightarrow C$ it represents the probability per

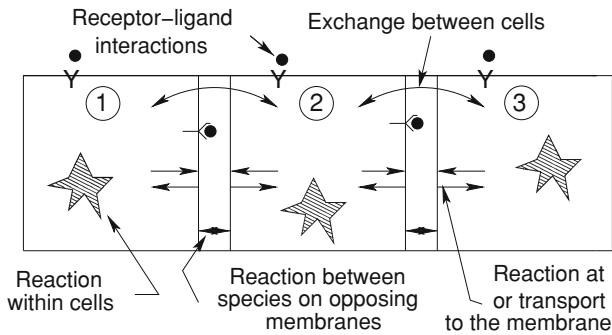


Fig. 2 A schematic of a 1D network of coupled cells in which cells can interact either at their opposing membranes or via transport between cells

unit time of a transition per ordered AA pair, and for a bimolecular step of the form $A + B \rightarrow C$ it represents the probability per unit time of a transition per AB pair. For a first-order reaction $1/\hat{k}_\ell$ represents a *bona fide* time scale, as in the deterministic case, whereas for bimolecular reactions it does not. We return to this point later.

1.3 The master equation for a general system of reaction and diffusion

Many biological problems involve more than just one well-mixed compartment, and this provides the motivation for describing a general framework for treating networks of cells or compartments that can communicate by various mechanisms, some of which involve material transport, and others of which merely involve signaling by, for instance, a ligand binding to a receptor. A schematic of an array of discrete cells that interact by several mechanisms is shown in Fig. 2. An example of a system that can be described by such a network is the developing wing disc in *Drosophila melanogaster*. We illustrate the types of interactions within and between cells, but there may also be transport by diffusion within the gaps between cells and in the surrounding fluid. We allow reaction within cells, reaction between species at the membranes with either species in the associated cell or on the membrane of the adjacent cell, and transport between cells.

If we associate a graph with only one class of nodes to the array, then ordering them so that the first N_c are cell labels and the remaining $2N_c$ (or smaller, depending on boundary conditions) are pairs of opposed membranes produces the cleanest separation, for then the incidence matrix has the form

$$\mathcal{E} = \begin{bmatrix} \mathcal{E}_{cc} & \mathcal{E}_{cm} \\ \mathcal{E}_{mc} & \mathcal{E}_{mm} \end{bmatrix}$$

where \mathcal{E}_{cc} , \mathcal{E}_{cm} , \mathcal{E}_{mc} , and \mathcal{E}_{mm} denote the cell–cell, the cell–membrane, the membrane–cell and the membrane–membrane connections, respectively.

It is not difficult to formulate a master equation for the general network in Fig. 2, since all the steps shown can be treated as chemical reactions, but the details depend

on the specific steps involved. When there is no interaction between membranes the matrix collapses to \mathcal{E}_{cc} , which encodes the connectivity of the cell network. It is clear that we can still allow receptor–ligand interactions, and an example of this is given later. In the remainder of the section we assume that transport is only by diffusion and that the network arises from the discretization of a reaction–diffusion problem.

In a stochastic description of reaction–diffusion systems in which the reactions are not diffusion-limited, the domain Ω containing the mixture can be discretized into spatially-uniform compartments, and diffusion can be treated as a jump process between compartments. How to correctly choose the computational cell or compartment size is a significant problem, and we deal with this in the following sections—here we simply derive the master equation for a reaction–diffusion system. In fact the compartments need not be computational cells that arise from the discretization of a domain; they could be compartments in the wider sense used above, as long as transport is diffusion-like, and we describe all cases as compartments hereafter. However, for simplicity we assume that transport between compartments is symmetric and linear in the concentration differences, so as to describe diffusion, and that all compartments are cubes of side-length h . We will comment later on how to generalize the resulting equation for other transport mechanisms and unequal compartment sizes.

Earlier we introduced the reaction graph \mathcal{G} and we indicated above that one can associate a graph with the cellular network as well. To distinguish between these we denote the former as \mathcal{G}_r and the latter as \mathcal{G}_c . We suppose that there are N_c nodes in \mathcal{G}_c , we define the incidence matrix \mathcal{E}_c , which was \mathcal{E}_{cc} in the general case, and the discrete Laplacian as $\Delta_c = -\mathcal{E}_c \mathcal{E}_c^T / 2$. When the network stems from a regular grid, the Laplacian is the discretization, modulo a scale factor of h^{-2} , of the spatial Laplacian (Othmer 1971).

Let $N(t) = (N^1(t), N^2(t), \dots, N^{N_c}(t))$ be the vector of random variables whose k th vector component represents the numbers of molecules of species in the k th compartment. Let $P(n, t)$ be the probability that $N(t) = n$, i.e., the joint probability that $N^1(t) = n^1 = (n_1^1, n_2^1, \dots, n_s^1)$, $N^2(t) = n^2 = (n_1^2, n_2^2, \dots, n_s^2), \dots, N^{N_c}(t) = n^{N_c} = (n_1^{N_c}, n_2^{N_c}, \dots, n_s^{N_c})$. Then $P(n, t) \equiv P(n^1, n^2, \dots, n^k, \dots, n^{N_c}, t)$, and in the absence of coupling between the compartments the master equation for $P(n, t)$ is

$$\frac{d}{dt} P(n, t) = \sum_{k=1}^{N_c} \left[\sum_{\ell} \mathcal{R}_{\ell}(n^k - \nu \mathcal{E}_{(\ell)}) \cdot P(n^1, \dots, n^k - \nu \mathcal{E}_{(\ell)}, \dots, n^{N_c}, t) - \sum_{\ell} \mathcal{R}_{\ell}(n^k) \cdot P(n^k, t) \right]$$

since this just involves the sum over all compartments of the changes in state of the individual compartments. Since the compartments evolve independently in the absence of coupling, the joint distribution can be factored into a product of N_c distributions, but this plays no role here.

In the absence of reaction but in the presence of diffusive coupling between compartments, the flux of the i th species from k to one of its neighbors k' is assumed to

be given by

$$J_i^{kk'} = \frac{D_i}{h^2} n_i^k,$$

while the reverse flux is

$$J_i^{k'k} = \frac{D_i}{h^2} (n_i^{k'} + 1).$$

The transfer of one molecule in the first step involves the change $n_i^k \rightarrow n_i^k - 1, n_i^{k'} \rightarrow n_i^{k'} + 1$ whereas the reverse flux involves the change $n_i^{k'} + 1 \rightarrow n_i^{k'}, n_i^k - 1 \rightarrow n_i^k$. Of course both steps conserve the particle number. Thus the evolution equation for $P(n, t)$ when diffusion alone is considered is

$$\frac{d}{dt} P(n, t) = \sum_{k=1}^{N_c} \sum_{k' \in \mathcal{N}(k)} \sum_{i=1}^s \left[\frac{D_i}{h^2} (n_i^{k'} + 1) P(n^1, \dots, n^k - e_i, \dots, n^{k'} + e_i, \dots, n^{N_c}, t) - \frac{D_i}{h^2} n_i^k P(n^k, t) \right]$$

where $\mathcal{N}(k)$ is the set of all neighbors of k in \mathcal{G}_c and $e_i = (0, 0, \dots, 1, \dots, 0)^T$ has a 1 in the i th position and zeroes elsewhere. To obtain the full equation we simply add the reaction and diffusion contributions; thus

$$\begin{aligned} \frac{d}{dt} P(n, t) = & \sum_{k=1}^{N_c} \left\{ \sum_{k' \in \mathcal{N}(k)} \sum_{i=1}^s \left[\frac{D_i}{h^2} (n_i^{k'} + 1) P(n^1, \dots, n^k - e_i, \dots, n^{k'} + e_i, \dots, n^{N_c}, t) \right. \right. \\ & \left. \left. - \frac{D_i}{h^2} n_i^k P(n^k, t) \right] + \sum_{\ell} \mathcal{R}_{\ell}(n^k - \nu \mathcal{E}_{(\ell)}) \cdot P(n^1, \dots, n^k - \nu \mathcal{E}_{(\ell)}, \dots, n^{N_c}, t) \right. \\ & \left. - \sum_{\ell} \mathcal{R}_{\ell}(n^k) \cdot P(n^k, t) \right\}. \end{aligned} \tag{3}$$

The formulation at (3) is based on the assumption that the domain is decomposed into equal-size compartments defined by a Cartesian grid. However this is not necessary, and a general formulation based on the compartment graph that allows for unequal volumes goes as follows. A first step is to generalize the foregoing to arbitrary topologies, albeit with equal-size compartments. This can be done using the Laplacian and the adjacency matrix A , which is defined via $\Delta = -d(\Delta) + A$, where $d(\Delta)$ is the diagonal matrix whose k th entry is the degree of the k th node. In the second step one incorporates unequal volumes of compartments and differences in the area for transfer between compartments. The latter is equivalent to allowing the diffusion coefficients to depend on the pair of compartments involved in the exchange. Finally, one has to scale the reaction rates differently in different compartments to account for

the fact that the volumes of the compartments are not equal. We leave the details to the interested reader.

1.4 Overview of the paper

If the compartment size used to develop the master equation (3) arises as a basic unit in the system, for example, a biological cell size, then no further analysis is needed, and a stochastic simulation based on (3) using the Gillespie's algorithm (Gillespie 1976) or one of its many modifications (Dobrzyński et al. 2007) is appropriate. However, if the system is described initially as a continuum and a reaction–diffusion equation of the form

$$\frac{\partial u(\mathbf{x}, t)}{\partial t} = \mathcal{D}\Delta u(\mathbf{x}, t) + \mathcal{R}(u(\mathbf{x}, t)) \quad (4)$$

is used, then the conversion to the master equation (3) requires a choice of compartment size. A numerical algorithm for the solution of the deterministic equation (4) would involve a discretization of space, and finer discretizations would produce more accurate solutions under suitable conditions. However this assumes that the solution is continuous in \mathbf{x} , but this is clearly not true when there are few molecules of any species present. One expects that for a fixed total number of molecules in a system, smaller compartments will produce larger variation in the number of molecules within a compartment, and the following example makes this precise.

Consider a closed system containing N molecules distributed in N_c compartments that are connected by diffusion. The steady-state distribution is spatially uniform, and it is known that it is multinomial (Gadgil et al. 2005) with mean and variance given by

$$M_i = \frac{N}{N_c} \quad \sigma_i^2 = M_i \left(1 - \frac{1}{N_c}\right) = \frac{N}{N_c} \left(1 - \frac{1}{N_c}\right).$$

Therefore, if we adopt the coefficient of variation, $CV = \sigma_i/M_i$ as a suitable measure of the noise, then one has

$$CV = \sqrt{\frac{N_c - 1}{N}}, \quad (5)$$

which is zero for $N_c = 1$ and which grows as $\sqrt{N_c}$ for large N_c . Thus choosing a very small compartment size leads to large fluctuations, as measured by the CV , in the amounts in various compartments. When reactions also occur the interaction between reaction and diffusion must be taken into account, and this will be done in later sections. Here we introduce some of the limitations of a compartmental analysis and then discuss previous work aimed at determining a suitable compartment size.

One problem that presents difficulties, both for a continuum description such as (4), as well as for the master equation approach, arises when one or more reactions are diffusion-limited. This applies only for bimolecular and higher-order reactions,

and refers to reactions of the type $A + A \rightarrow P$ or $A + B \rightarrow P$ in which the reaction occurs instantaneously when the reactants are in sufficiently close proximity. Thus formation of homo- and heterodimers, polymerization reactions, ligand-receptor interactions, and enzyme-catalyzed reactions are all potentially diffusion-limited. In this context neither (4) nor the conventional framework of a compartmentalized system can be used directly, and both require some modifications. The classical work of Smoluchowski (1917) dealt with coagulation reactions, but since then it has been extended by many others (for a review see Bamford et al. 1985). Suppose that the molecules are assigned a radius r_A and r_B , respectively, and assume that the molecules react at a rate k_0 when the distance between their centers is $r_A + r_B$. In a coordinate frame in which B is fixed, the concentration of A satisfies

$$\begin{aligned} \frac{\partial c}{\partial t} &= \frac{D}{r^2} \frac{\partial}{\partial r} \left(r^2 \frac{\partial c}{\partial r} \right) \quad \text{for } r \in (r_A + r_B, \infty) \\ 4\pi r^2 D \frac{\partial c}{\partial r} &= k_0 c \quad \text{at } r = r_A + r_B \\ \lim_{r \rightarrow \infty} c(r) &= c_0. \end{aligned}$$

In the strictly diffusion-limited case k_0 is infinite, and one finds that as $t \rightarrow \infty$, the effective reaction rate k_e reduces to

$$k_e = 4\pi(D_A + D_B)(r_A + r_B) = 4\pi DR$$

where $D = D_A + D_B$ and $R = r_A + r_B$ (Bamford et al. 1985). The units of k_e appear formally to be volume/time, but this is the rate per molecule of B , and therefore the units of k_e are

$$\left(\frac{\text{molecules of } B}{\text{volume}} \text{time} \right)^{-1}$$

as is necessary for a bimolecular rate constant. An associated time scale for a diffusion-limited reaction can be defined as

$$\tau_{dl} = (k_e \cdot c^*)^{-1} \quad (6)$$

where c^* is a characteristic concentration of B in molecules/unit volume.

An estimate obtained via a stochastic analysis begins with the problem of computing the mean first passage time for a random walker searching for a specified target. Suppose that the walker is confined to a spherical shell of inner radius r_0 and outer radius r_1 , that it cannot escape through the outer boundary and is annihilated upon hitting the inner boundary. The mean first passage time $\tau(r)$ for annihilation beginning

on a spherical surface of radius $r \in (r_0, r_1)$ is given by the solution of

$$\begin{aligned} \frac{D}{r^2} \frac{d}{dr} \left(r^2 \frac{d\tau}{dr} \right) &= -1 \\ \tau(r_0) &= 0 \\ \tau'(r_1) &= 0. \end{aligned} \tag{7}$$

One finds that the solution is

$$\tau(r) = \frac{1}{6D} \left(r_0^2 - r^2 + 2r_1^3 \left(\frac{1}{r_0} - \frac{1}{r} \right) \right)$$

and the average of this over the spherical shell is

$$\overline{\tau(r)} = \frac{r_1^2}{2D(1 - \xi^3)} \left[-\frac{2\xi^5}{15} + \frac{2\xi^2}{3} + \frac{2}{3\xi} - \frac{6}{5} \right]$$

where $\xi \equiv r_0/r_1$. If this ratio is sufficiently small, then to leading order

$$\overline{\tau(r)} = \frac{r_1^2}{3D} \frac{r_1}{r_0} = \frac{V_s}{4\pi D r_0}$$

where V_s is, to lowest order, the volume of the spherical domain. By identifying r_0 with $r_A + r_B$ one sees that the continuum and stochastic approaches agree to within the choice of a reference concentration in (6). When there are N non-interacting walkers in the shell, the spatially averaged mean first passage time for the first annihilation remains unchanged. A proof of this is given in Appendix A.

To estimate the magnitude of k_e and hence the time scale in a typical solvent, we use the Stokes–Einstein relation

$$D = \frac{k_B T}{6\pi \mu r'}$$

to estimate the diffusion coefficient, where k_B is Boltzmann’s constant, T is the absolute temperature, μ is the solvent viscosity, and r' is the hydrodynamic radius of the molecule. Assuming a solvent viscosity $\mu = 9$ poise, one finds that $k_B T/\mu = 4.5 \cdot 10^{-12}$ cm³/s, and if one assumes both molecules have the same encounter radius and a hydrodynamic radius equal to that radius, then

$$k_e = \frac{8}{3} \frac{k_B T}{\mu} = 1.2 \cdot 10^{-11} \text{ cm}^3/\text{s}$$

or in molar units

$$k_e = 7.2 \cdot 10^9 \text{ M}^{-1} \text{ s}^{-1}.$$

Table 1 On- and off-rates for second-order reactions

Receptor	Ligand	k_f ($M^{-1} s^{-1}$)	k_r (s^{-1})	Reference
Insulin	Insulin	1.6×10^5	3.3×10^{-3}	Lauffenburger and Linderman (1993)
EGF	EGF	3×10^6	2×10^{-3}	Lauffenburger and Linderman (1993)
Fibronectin	Fibronectin	1.17×10^4	1×10^{-2}	Lauffenburger and Linderman (1993)
Surface bound protein	BMP	1.67×10^7	3.33×10^{-2}	Umulis et al. (2006)
Type I/II BMP receptor	BMP	4×10^5	6.67×10^{-2}	Umulis et al. (2006)
Vkg	Dpp	3.92×10^3	2.90×10^{-3}	Wang et al. (2008)
Dcg1	Dpp	3.20×10^3	2.07×10^{-3}	Wang et al. (2008)
Human Collagen IV	BMP4	2.75×10^4	2.50×10^{-3}	Wang et al. (2008)
Cv-2 Receptor	BMP	1.67×10^6	3.33×10^{-3}	Serpe et al. (2008)
Receptor	BMP	4.0×10^5	4.0×10^{-4}	Serpe et al. (2008)
Receptor	BMP bound Cv-2	3.3×10^7	3.3×10^{-2}	Serpe et al. (2008)
Cv-2 Receptor	BMP bound receptor	3.3×10^5	3.3×10^{-2}	Serpe et al. (2008)

Based on this estimate, there appear to be few biochemical reactions that are severely diffusion-limited *in vitro*, since most of the available second-order rate constants lie in the range of 10^4 – 10^7 ($M s$) $^{-1}$ (cf. Table 1). It may be that *in vivo* measurements will show more diffusion influence on reaction rates.

When reactions are strictly diffusion-limited, rather than just diffusion-influenced, a precise description involves tracking individual particles as they diffuse in space, and algorithms for this have been developed (Andrews and Bray 2004; Dobrzyński et al. 2007). If one describes the motion of the Brownian particles A and B with stochastic differential equations, then in certain regimes the positions evolve according to

$$d\mathbf{x}_i = \sqrt{2D_i} dW_i \quad i = A, B,$$

where W_i are independent standard Wiener processes. This is a more fundamental approach that also indicates a shortcoming in the analysis discussed earlier, because that analysis assumes that the motion of the two particles is perfectly correlated, which is not true if each executes an independent Brownian motion.

Several different attempts to correctly treat diffusion-limited reactions via a compartment-based master equation have been made. Fange et al. (2010) first derive a discretized description using spherical shells around a single particle, and then lift this description to a compartmental model using modified diffusion kinetic coefficients that reflect the discretization. However, in deriving the modified rates the authors use a model in which the diffusing particle is confined to a spherical shell around the reaction

site, and thus implicitly assume that the particles will react with probability one. In 3D this is not strictly true, and in general it is an approximation that may be difficult to justify. Others have addressed the relationship between the continuum description (4) and the master equation for a diffusion-limited reaction (Isaacson 2009). It is shown that one cannot expect that the limit of the master equation is (4), since bimolecular reactions disappear in this limit. In Isaacson and Isaacson (2009) a pseudo-potential to capture the singular behavior is used, while the reaction rates in a compartmentalized model are modified so that the encounter probability of the molecules does not depend on the compartment size (Urban and Chapman 2009). A more fundamental approach is to derive the evolution equation for the pair distribution function, as was done in a continuum description (Sung et al. 1997), but the discretization problem was not addressed there.

Numerous authors have addressed the issue of how to choose a suitable compartment size h when reactions are not diffusion-limited. Most criteria are based on the premise that the compartment size should be small enough that all mobile species in a compartment can traverse the compartment on the time scale of the fastest reaction in a compartment, since only then a compartment can be considered spatially uniform. For bimolecular reactions this implies that all pairs of reactants have equal probability of reacting. Thus most criteria hinge on the relation between the diffusion time scale for a chosen compartment size and a characteristic reaction time. As noted earlier, reaction rates scale as $V^p \sim h^{pd}$ where $p = 1, 0, -1$, for zero-, first- and second-order reactions, respectively, V is the compartment volume, and d is the space dimension. Thus a characteristic reaction time scales with the compartment size as follows.

$$\tau_r \sim \begin{cases} \frac{c^*}{k_0 h^d} & : \text{ zero-order} \\ \frac{1}{k_1} & : \text{ first-order} \\ \frac{h^d}{k_2 c^*} & : \text{ second-order} \end{cases}$$

Here k_j is a concentration-based reference kinetic coefficient, usually the deterministic value, and c^* is a reference concentration.

A characteristic diffusion time scale is given by $\tau_d = h^2 / \min_i D_i$ and thus the following conditions on h

$$h^{2+d} < \frac{\min_i D_i}{k_0 (c^*)^{-1}} : \text{ zero-order}$$

$$h^2 < \frac{\min_i D_i}{k_1} : \text{ first-order}$$

$$h^{2-d} < \frac{\min_i D_i}{k_2 c^*} : \text{ second-order}$$

will ensure that $\tau_d \leq \tau_r$. Since no molecular interaction are involved in zero- and first-order reactions, one might conclude that the first two estimates are irrelevant.

However, they arise naturally in the criterion for convergence to spatial uniformity derived later, and they indicate the crossover in h from a regime in which diffusion is fast compared to reaction to one in which the reverse holds. Understanding these regimes plays a role in stochastic simulations using Gillespie's method, because if the compartment is too small the diffusion steps dominate the computations. A more detailed analysis using the known solutions for the mean and variance in systems of first-order reactions (Gadgil et al. 2005) will lead to a more precise characterization of this.

Stundzia and Lumsden (1996) describe diffusion as a jump process, but rather than using a constant jump rate, they use the inverse of the mean first passage time from a compartment to its neighbors. Baras and Mansour (1996) suggest that the compartment size should be smaller than a two-particle correlation length, but larger than a mean free path λ , defined as the average distance traveled by a particle between two reactive collisions. Since the correlation length is smaller than the mean free path in dilute solutions, they assert that the compartment size should be chosen with the order of mean free path i.e.,

$$h \approx \mathcal{O}(\lambda).$$

Since this only applies for gases we do not consider it further here. Bernstein (2005) applies Gillespie's algorithm to simulate diffusion with spatially-inhomogeneous coefficients in non-uniform Cartesian grids using a finite volume approximation with either Neumann or Dirichlet boundary conditions. To apply Gillespie's algorithm to reaction–diffusion networks the slowest diffusion time should be much less than the fastest reaction time, i.e., $\tau_d \ll \tau_r$.

Isaacson and Peskin (2007) suggest a lower and upper bound for the compartment size based on three facts: the compartment size should be much larger than the mean free path λ so that the system can be considered in local equilibrium in each compartment due to nonreactive collisions; the compartment size should be much smaller than the length scale of the system size L_x ; and the time scale for diffusion through each compartment should be faster than the time scale for the fastest bimolecular reaction. This leads to the condition

$$\max\left(\lambda, \frac{k}{D}\right) \ll h \ll L_x \quad (8)$$

but as we noted earlier, a reference concentration is needed to properly define a reaction time scale for bimolecular reactions.

Erban and Chapman (2009) suggest simulation algorithms for reaction–diffusion processes in which diffusion is treated as a jump process. They give a simple example of a bimolecular reaction for which the stationary distributions are explicitly known, and point out the limitations of current SSAs by comparing the stationary distributions. Using a modified algorithm, they show that if the compartment size is larger than a critical value, the multi-compartment model can reproduce the known stationary distribution correctly. The reactions considered are $\emptyset \rightarrow A$ and $A + B \xrightarrow{k} B$ with diffusing species, A and B , and k is the deterministic reaction rate of the bimolecular

Table 2 Previous criteria for the compartment size

Reference	Criteria
Bernstein	$\tau_d \approx \frac{h^2}{2dD} \ll \tau_r$
Isaacson and Peskin	$\max\left(\lambda, \frac{k}{D}\right) \ll h \ll L_x$
Erban and Chapman	$\frac{k}{4(D_A + D_B)} \leq h$

reaction. Then the lower bound on the compartment size is

$$h \geq h_{crit}$$

$$h_{crit} \approx \frac{k}{4(D_A + D_B)}.$$

All of these estimates implicitly assume that all reacting species also diffuse, but this is rarely the case in biological problems, since diffusible species may bind to receptors or other essentially immobile proteins. In addition, none of the criteria deal with the possibility of reactions on the boundary of the domain. In later sections we develop a criterion based on the full chemical network for a reacting system in which some species may be immobilized in the interior of the domain, and we compare the criteria in Table 2.

Another aspect inadequately addressed in previously-cited work is the effect of compartment size on the magnitude of the stochastic fluctuations, as measured by the coefficient of variation of solutions. As suggested by the example of diffusion alone, the noise can be expected to grow as the compartment size decreases, and this raises the question of how to choose h so as to ensure that the discretized system is accurate, and yet minimizes some measure of the noise. In the following section we analyze linear reaction networks to address this issue, and show that a certain scaling of the coefficient of variation stabilizes as h decreases, which leads to an optimal choice of h (in the sense that it is taken as large as possible). In Sect. 3 we develop a general criterion for the choice of compartment size that applies to all orders of reactions and both diffusing and non-diffusing species.

2 Linear stochastic reaction–diffusion networks

2.1 Measures of the fluctuations in a compartmental system

We consider a first-order chemical reaction–diffusion network, and from previous work we know that the reactions fall into one of four classes: production from a source, degradation, conversion, and catalytic production from a source (Gadgil et al. 2005). Production from a source is an input reaction of the form $\emptyset \rightarrow \mathcal{M}_i$; degradation is a reaction $\mathcal{M}_i \rightarrow \emptyset$; conversion is a reaction $\mathcal{M}_j \rightarrow \mathcal{M}_i$; and catalytic production from a source is a reaction $\emptyset \xrightarrow{\mathcal{M}_j} \mathcal{M}_i$. We assume that degradation, conversion, and catalyzed production from a source occur at all spatial positions, but production from

a source may be spatially nonuniform. Suppose that the domain Ω is a rectangular parallelepiped with dimensions $L_x \times L_y \times L_z$ of volume $\mathbf{V} = L_x L_y L_z$. We divide Ω into $N_c = N_x N_y N_z$ compartments, each of which has volume \mathbf{V}/N_c . Define the index $k = (k_1, k_2, k_3)$ to denote a compartment, where $k_1, k_2, k_3 = 1, \dots, N_x, N_y, N_z$, respectively, and set $\boldsymbol{\eta} = (k, i)$ where $i = 1, \dots, s$ denotes the species. Let $N_i^k(t) \equiv N^\boldsymbol{\eta}(t)$ be a random variable that represents the number of molecules of species \mathcal{M}_i in the k th compartment at time t , and let N^k denote the vector of N_i^k s. Several different measures of the noise will be introduced later to understand the dependence of noise on the discretization, all of which involve the means and variances of the components in the network, and thus we first analyze the evolution of these quantities.

The mean $M(t)$ is an sN_c -dimensional vector of first moments with elements defined by

$$[M(t)]_{\mathbf{i}(\boldsymbol{\eta})} = E[N^\boldsymbol{\eta}(t)], \quad (9)$$

where the index function \mathbf{i} , which is defined as $\mathbf{i}(\boldsymbol{\eta}) = i + ((k_1 - 1)N_y N_z + (k_2 - 1)N_z + (k_3 - 1)s)$, labels the components. Define $\boldsymbol{\zeta} = (q, j)$ as the index for the j th species in the q th compartment. Then the matrix of second moments $V(t)$ is an $sN_c \times sN_c$ matrix with elements

$$[V(t)]_{\mathbf{i}(\boldsymbol{\eta}), \mathbf{i}(\boldsymbol{\zeta})} = E[N^\boldsymbol{\eta}(t)N^\boldsymbol{\zeta}(t)] - E[N^\boldsymbol{\eta}(t)]\delta_{\{\boldsymbol{\eta}=\boldsymbol{\zeta}\}}.$$

The covariance matrix, $Cov(t)$, is defined as

$$[Cov(t)]_{\mathbf{i}(\boldsymbol{\eta}), \mathbf{i}(\boldsymbol{\zeta})} = E[N^\boldsymbol{\eta}(t)N^\boldsymbol{\zeta}(t)] - E[N^\boldsymbol{\eta}(t)]E[N^\boldsymbol{\zeta}(t)],$$

and therefore can be expressed in terms of $M(t)$ and $V(t)$ as

$$Cov(t) = V(t) - M(t)M(t)^T + M_d(t),$$

where $M_d(t) = \text{diag}[M(t)]$ is a diagonal matrix whose entries are those of $M(t)$.

As in [Gadgil et al. \(2005\)](#), let \mathcal{K} be the $s \times s$ reaction matrix for conversion or degradation of species within a compartment, let \mathcal{D} be the $s \times s$ diagonal diffusion matrix, let K^{cat} be the $s \times s$ matrix wherein the (i, j) th element is the catalytic production rate from a source of the i th species catalyzed by the j th species, and let K^S be the $sN_c \times sN_c$ diagonal matrix with the $\mathbf{i}(\boldsymbol{\eta})$ th diagonal element representing an input of the i th species from a source into the k th compartment.² Further, let Δ be the discrete Laplacian for the domain Ω with Neumann boundary conditions; Δ encodes the topology of the network, and more general topologies can be treated similarly ([Othmer 1971](#)). Finally, we let \mathbf{u} and I_{N_c} be a vector of length sN_c , all of whose entries are 1, and the unit matrix of dimension $N_c \times N_c$, respectively. We let \mathbf{k}^s be the

² This formulation can be generalized to allow catalyzed production from a source to be space-dependent as well, but we do not include this here.

vector whose components are the diagonal elements of K^S , and we define the rank one square matrix $S = [\mathbf{k}^s | \mathbf{k}^s | \dots | \mathbf{k}^s]$ whose columns are \mathbf{k}^s .

These definitions lead to a reaction–diffusion matrix defined as $\Omega \equiv \Delta \otimes \mathcal{D} + I_{N_c} \otimes \mathcal{K}$ (Gadgil et al. 2005), and we assume throughout that Ω is semi-simple, that the kinetic system is stable, and that the spectrum $\sigma(\Omega)$ lies in the closed left-half plane, denoted \overline{LHP} . A spectral representation of Ω is given in Appendix B. We consider two cases defined by whether Ω has a zero eigenvalue or not (multiple zero eigenvalues can be treated similarly). The presence or absence of a zero eigenvalue is determined solely by the kinetic matrix, and thus we exclude Turing-type instabilities that arise from the interaction of reaction and diffusion. If \mathcal{G}_c is strongly connected, as in the case treated here, the Laplacian has exactly one zero eigenvalue for Neumann boundary conditions, and $\sigma(\Omega) \subset LHP$ if the system is either closed with degradation or open with production from a source and degradation. In the absence of inputs the mean and variance decay to zero as $t \rightarrow \infty$, which is of no interest, and in the presence of inputs they are determined by the inputs as $t \rightarrow \infty$. On the other hand, if there is exactly one zero eigenvalue of Ω and no inputs, the steady-state probability distribution is determined by the eigenvector corresponding to the zero eigenvalue (Gadgil et al. 2005). Other cases may arise, but are not treated here.

The first and second moments $M(t)$ and $V(t)$ are solutions of the ordinary differential equations

$$\begin{aligned} \frac{dM(t)}{dt} &= \Omega M(t) + \mathbf{k}^s \\ \frac{dV(t)}{dt} &= \Omega V(t) + [\Omega V(t)]^T + C(t) + C(t)^T \end{aligned} \tag{10}$$

where $C(t) = W(t) + \mathbf{k}^s M(t)^T$ (Gadgil et al. 2005). Here $W(t)$ is a block-diagonal matrix with elements defined as

$$[W(t)]_{i(\eta), i(\zeta)} = \begin{cases} K_{ij}^{cat} [M(t)]_{i(\zeta)} & \text{if } k = q \\ 0 & \text{otherwise.} \end{cases}$$

Define indices l, m , and n which run over compartments, let μ, χ , and γ be indices that label species, and define the indices $\mathbf{l} = (l, \mu)$, $\mathbf{m} = (m, \chi)$, and $\mathbf{n} = (n, \gamma)$. The eigenvalues of $\Omega = \Delta \otimes \mathcal{D} + I_{N_c} \otimes \mathcal{K}$ can be computed once those of Δ , denoted by α_l , are known (Othmer 1971). They are eigenvalues of the matrix pencil $\mathcal{K} + \alpha_l \mathcal{D}$ and thus are the solutions of

$$|\mathcal{K} + \alpha_l \mathcal{D} - \lambda_1 I_s| = 0.$$

The corresponding eigenvectors of Ω are the tensor product of eigenvectors of Δ and those of $\mathcal{K} + \alpha_l \mathcal{D}$. Let ϕ_l and ϕ_l^* be the eigenvector and adjoint eigenvector of Δ for the eigenvalue α_l , and let φ_l and φ_l^* be the corresponding eigenvector and adjoint eigenvector of $\mathcal{K} + \alpha_l \mathcal{D}$ for λ_1 . Then $\phi_l \otimes \varphi_l$ is the eigenvector of Ω corresponding to

the eigenvalue λ_l , and the projection P_l associated with λ_l is defined as

$$P_l = (\phi_l * \overline{\phi_l^*}) \otimes (\varphi_l * \overline{\varphi_l^*}),$$

where $\overline{\phi_l^*}$ and $\overline{\varphi_l^*}$ are complex conjugates of ϕ_l^* and φ_l^* , respectively. Here $*$ is the dyad product defined operationally as $(u * v)w = \langle v, w \rangle u$. Given these, we can compute the solution for the first two moments in terms of λ_l and P_l in the semi-simple case.

Later we focus primarily on the steady-state level of fluctuations, and therefore we define

$$M_\infty \equiv \lim_{t \rightarrow \infty} M(t) \quad \text{and} \quad V_\infty \equiv \lim_{t \rightarrow \infty} V(t).$$

First, consider the case in which $\sigma(\Omega) \subset LHP$; then one finds that

$$\begin{aligned} M_\infty &= - \sum_l \frac{P_l}{\lambda_l} \mathbf{k}^s, \\ V_\infty &= \sum_m \sum_l \left[\frac{1}{\lambda_l(\lambda_l + \lambda_m)} P_m K^S (P_l S)^T + \frac{1}{\lambda_m(\lambda_l + \lambda_m)} P_m S K^S P_l^T \right. \\ &\quad \left. + \sum_n \frac{P_m \{ \text{diag}[P_n S] (K^{cat})^T + K^{cat} \text{diag}[P_n S] \} P_l^T}{\lambda_n(\lambda_l + \lambda_m)} \right], \end{aligned} \tag{11}$$

where the sums range over the eigenvalues of $\mathcal{K} + \alpha_l \mathcal{D}$.

To assess the fluctuations in the network we can use one of several forms of a coefficient of variation, defined as the standard deviation divided by the mean. The first measure results from defining the noise component- and compartment-wise, which may be appropriate when assessing the effect of fluctuations in a morphogen used to define the boundary between two tissue types. In this case one computes the standard deviation of the number of molecules for the i th species in the k th compartment divided by its mean, viz.,

$$(CV(t))^\eta \equiv \frac{\sqrt{E[N^\eta(t)^2] - E[N^\eta(t)]^2}}{E[N^\eta(t)]} \tag{12}$$

where $\eta = (k, i)$. This reflects the fluctuations of each species in each compartment, and thereby leads to a total of sN_c measures, but for our purpose a single global measure that averages over all species and compartments is more appropriate. There are many ways to do this—one could for instance use the average of the component measures in (12) or the maximum of these. However, we use a measure based on a

normalized covariance matrix (Tomioaka et al. 2004), which is defined as

$$\begin{aligned} [\Sigma_0(t)]_{i(\eta),i(\zeta)} &= \frac{E[N^\eta(t)N^\zeta(t)] - E[N^\eta(t)]E[N^\zeta(t)]}{E[N^\eta(t)]E[N^\zeta(t)]} \\ &\equiv (M_d(t)^{-1}Cov(t)M_d(t)^{-1})_{i(\eta),i(\zeta)}. \end{aligned}$$

We then define a generalized coefficient of variation as the square root of the maximum eigenvalue of $\Sigma_0(t)$, and denote it

$$CV^*(t) \equiv \sqrt{\lambda_{max}(\Sigma_0(t))}. \tag{13}$$

Since the covariance matrix is symmetric and at least positive semi-definite, this is well-defined.

We define other steady-state variables as

$$\begin{aligned} Cov_\infty &\equiv \lim_{t \rightarrow \infty} Cov(t) \quad M_{d,\infty} \equiv \lim_{t \rightarrow \infty} M_d(t) \quad (CV_\infty)^\eta \equiv \lim_{t \rightarrow \infty} (CV(t))^\eta \\ \Sigma_{0,\infty} &\equiv \lim_{t \rightarrow \infty} \Sigma_0(t) \end{aligned}$$

and then the steady-state CV^* is given by

$$CV^* = \sqrt{\lambda_{max}(\Sigma_{0,\infty})} = \sqrt{\lambda_{max}(M_{d,\infty}^{-1}(V_\infty - M_\infty M_\infty^T + M_{d,\infty})M_{d,\infty}^{-1})}.$$

In the following proposition, we express CV^* in terms of M_∞ alone when the eigenvalues of Ω are in the LHP and there are no catalyzed inputs to the system. When there is exactly one zero eigenvalue of Ω and no inputs, we express CV^* in terms of $M_{d,\infty}$, $M_d(0)$, and P_s , where P_s is the projection corresponding to the zero eigenvalue.

Proposition 1 *Suppose that the eigenvalues of Ω are in the LHP; then*

1. *If there are no non-catalyzed inputs ($K^S = 0$), then $M_{d,\infty} = Cov_\infty = 0$*
2. *If $K^S \neq 0$ then*

$$Cov_\infty = M_{d,\infty} + \sum_{l,m,n} \frac{P_m \{diag[P_n S](K^{cat})^T + K^{cat}diag[P_n S]\} P_l^T}{\lambda_n(\lambda_l + \lambda_m)}$$

and

$$\Sigma_{0,\infty} = M_{d,\infty}^{-1} + M_{d,\infty}^{-1} \left\{ \sum_{l,m,n} \frac{P_m \{diag[P_n S](K^{cat})^T + K^{cat}diag[P_n S]\} P_l^T}{\lambda_n(\lambda_l + \lambda_m)} \right\} M_{d,\infty}^{-1}.$$

If $K^{cat} = 0$, the second term vanishes and

$$CV^* = \sqrt{\frac{1}{\min_\eta [M_\infty]_{i(\eta)}}}. \tag{14}$$

3. Suppose that $\sigma(\Omega) \subset \overline{LHP}$ and there is exactly one zero eigenvalue of Ω and no inputs; then

$$Cov_\infty = M_{d,\infty} - P_s M_d(0) P_s^T$$

where P_s is the projection corresponding to the zero eigenvalue and

$$\Sigma_{0,\infty} = M_{d,\infty}^{-1} - M_{d,\infty}^{-1} P_s M_d(0) P_s^T M_{d,\infty}^{-1}. \tag{15}$$

Proof The proof is given in Appendix C. □

It is clear from the foregoing that CV^* is an increasing function of the number of compartments in the system, since the mean number of molecules of each species in each compartment decreases. However, as the following example illustrates, and as will be proven later, a scaled version of CV^* stabilizes as the compartment number increases. Define $V_c = \mathbf{V}/N_c$ and the scaled variables

$$\overline{M}_\infty \equiv \frac{M_\infty}{V_c}, \quad \overline{CV}^* \equiv \sqrt{V_c} CV^*, \quad (\overline{CV}_\infty)^\eta \equiv \sqrt{V_c} (CV_\infty)^\eta, \tag{16}$$

where $\eta = (k, i)$ and $(X)^{(k,i)}$ represents the component of X corresponding to the i th species in the k th compartment. Equation (14) shows that in the absence of catalyzed inputs, the least abundant species, evaluated over all compartments, determines CV^* , and one sees that convergence of \overline{M}_∞ implies convergence of \overline{CV}^* as $N_c \rightarrow \infty$. Convergence of the former as $N_c \rightarrow \infty$ is shown in Theorem 1 below.

Denote by \mathcal{K}' the reaction matrix for conversion or degradation of species in a compartment for systems with non-catalytic production of diffusing species, and rearrange the species order so that \mathcal{K}' can be partitioned into block matrices as

$$\mathcal{K}' = \begin{bmatrix} \mathcal{R} & \mathcal{S} \\ \mathcal{T} & \mathcal{W} \end{bmatrix}.$$

Here \mathcal{R} (\mathcal{W}) is the reaction matrix for conversion between diffusing (non-diffusing) species or degradation of diffusing (non-diffusing) species, and \mathcal{S} (\mathcal{T}) is the reaction matrix for conversion of non-diffusing (diffusing) species to diffusing (non-diffusing) species. We denote by $X(t)$ and $Y(t)$ the mean vectors for diffusing and non-diffusing species numbers, with each element defined as in (9), and write the governing equations for these means as follows:

$$\begin{aligned} \frac{dX(t)}{dt} &= (\Delta \otimes \mathcal{D} + I_{N_c} \otimes \mathcal{R}) X(t) + (I_{N_c} \otimes \mathcal{S}) Y(t) + \mathbf{k}^s, \\ \frac{dY(t)}{dt} &= (I_{N_c} \otimes \mathcal{T}) X(t) + (I_{N_c} \otimes \mathcal{W}) Y(t). \end{aligned} \tag{17}$$

Let X_∞ and Y_∞ be the steady-state solutions of (17). Assuming that $\sigma(\mathcal{W}) \subset LHP$, the steady-state mean vector for non-diffusing species can be expressed in terms of

X_∞ , where X_∞ is the solution of

$$(\Delta \otimes \mathcal{D} + I_{N_c} \otimes \mathcal{K}) X_\infty + \mathbf{k}^s = 0, \tag{18}$$

where $\mathcal{K} \equiv \mathcal{R} - \mathcal{S}\mathcal{W}^{-1}\mathcal{T}$. To show convergence of $X_\infty/(\mathcal{N}_A V_c)$ to the solution of the continuum deterministic reaction–diffusion system, we consider a 1-dimensional domain $[0, L_x]$ for simplicity, and we let $\tilde{\alpha}_l$ be the solution of the following scalar problem:

$$\begin{aligned} \frac{d^2 \tilde{q}(\mathbf{x})}{d\mathbf{x}^2} &= \tilde{\alpha} \tilde{q}(\mathbf{x}), & \mathbf{x} \in [0, L_x], \\ \tilde{q}'(\mathbf{x}) &= 0, & \mathbf{x} = 0, L_x. \end{aligned} \tag{19}$$

Theorem 1 *Let $\tilde{\mathcal{D}}$ be the diffusion matrix for the continuum problem, and suppose that*

$$\sigma(\Omega), \sigma(W), \sigma(\mathcal{K} + \alpha_l \mathcal{D}), \sigma(\mathcal{K} + \tilde{\alpha}_l \tilde{\mathcal{D}}) \subset LHP,$$

and that $\mathcal{K} + \alpha_l \mathcal{D}$ and $\mathcal{K} + \tilde{\alpha}_l \tilde{\mathcal{D}}$ are semi-simple. Assume that $K^{cat} = 0$ and assume that only diffusing species are produced from a source and production occurs only in the left-most compartment. Then,

- $[\overline{M}_\infty]_{\mathbf{i}(\eta)}$ converges to the steady-state solution of the corresponding continuum deterministic reaction–diffusion system as $N_c \rightarrow \infty$,
- \overline{CV}^* converges to the limit of $\sqrt{\frac{1}{\min_\eta [\overline{M}_\infty]_{\mathbf{i}(\eta)}}}$ as $N_c \rightarrow \infty$.

Proof The proof is given in Appendix D. □

For systems with no inputs, it follows from (15) that if we show that each element of $V_c \left(M_{d,\infty}^{-1} P_s M_d(0) P_s^T M_{d,\infty}^{-1} \right)$ converges to zero as $N_c \rightarrow \infty$, convergence of \overline{M}_∞ will imply convergence of \overline{CV}^* as $N_c \rightarrow \infty$, as stated in the following theorem, again under the assumption of a one-dimensional domain.

Theorem 2 *Suppose that there are no inputs, that $\sigma(\Omega) \subset \overline{LHP}$, and there is exactly one zero eigenvalue of Ω . Then,*

- $[\overline{M}_\infty]_{\mathbf{i}(\eta)}$ converges to the steady-state solution of the corresponding continuum deterministic reaction–diffusion system as $N_c \rightarrow \infty$,
- \overline{CV}^* converges to the limit of $\sqrt{\frac{1}{\min_\eta [\overline{M}_\infty]_{\mathbf{i}(\eta)}}}$ as $N_c \rightarrow \infty$.

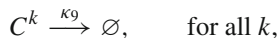
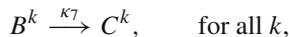
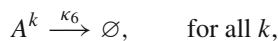
Proof The proof is given in Appendix E. □

In essence these results show that the concentration-based CV for the discretized problem stabilizes.

2.2 Example

The example in this section is motivated by the classical French flag paradigm of pattern formation in a one-dimensional system discussed earlier. In that context, a morphogen is produced at one end of a 1D domain, diffuses into the domain, and binds to receptors and is perhaps degraded by a first-order process (Wolpert 1969). The problem is to reliably partition the domain into 3 equal-size sub-domains (corresponding to blue, white and red, beginning at the staff) by setting thresholds that determine the extent of each domain. A system that exemplifies this arises in anterior-posterior pattern formation in the fruit fly *Drosophila melanogaster*. The *Drosophila* embryo is approximately ellipsoidal, and is surrounded by a thin fluid layer, called the perivitelline (PV) space, bounded by the outer membrane. The coordinate frame of the embryo is first established by gradients of inherited maternal factors in the anterior-posterior (AP) direction and by gradients of factors in the PV space in the dorsal-ventral direction. The first level of AP patterning is mediated by the morphogen Bicoid, which is a transcription factor that is transcribed from maternally-inherited mRNA localized at the anterior end of the embryo. Because production is localized at the anterior end, the concentration of the Bicoid protein forms a monotone distribution with the high point at the anterior end.

We consider a rectangular solid continuum whose major axis lies along the x axis, and we let $L_x = 275 \mu\text{m}$, $L_y = 5 \mu\text{m}$, and $L_z = 0.5 \mu\text{m}$ represent the lengths of each side of the system, motivated by a slice of the PV space in *Drosophila* (Umulis et al. 2008). Since $L_x \gg L_y, L_z$, we set $N_y = N_z = 1$, and determine the appropriate discretization defined by $N_x = N_c$ in the x -direction. We suppose that there is one diffusing species, A , and two non-diffusing species, B and C , which represent ligand, receptor with ligand bound, and downstream signal, respectively. Assuming that the number of receptors is large, as it is in many biological systems, receptor–ligand binding is described as a first order reaction. The complete set of reactions is as follows.



Here superscript k denotes the species in the k th compartment.

All reactions are either production from a source, degradation, or conversion, in the terminology of Gadgil et al. (2005); there is no catalytic production from a source. The reaction (20) simply describes a linearized ligand-binding to receptors. The reaction (21) describes production of species A from a source located at the leftmost compartment, and thus A has an input only to the first compartment. The coefficients

Table 3 Deterministic and stochastic parameters in Example 2.2

Deterministic		Stochastic	
k_5	$1 \text{ nM}^{-1} \text{ min}^{-1}$	κ_5	$k_5/(\mathcal{N}_A V_c) \approx 2.42 \times 10^{-3} N_c \text{ min}^{-1}$
k_{-5}	2 min^{-1}	κ_{-5}	2 min^{-1}
k_6	1 min^{-1}	κ_6	1 min^{-1}
k_7	0.03 min^{-1}	κ_7	0.03 min^{-1}
k_8	$250 \text{ nM } \mu\text{m min}^{-1}$	κ_8	$k_8(\mathcal{N}_A \mathbf{V})/L_x \approx 376.38 \text{ min}^{-1}$
k_9	0.03 min^{-1}	κ_9	0.03 min^{-1}
c_R	320 nM	R	$c_R(\mathcal{N}_A V_c) \approx 132484/N_c$
D	$4380 \mu\text{m}^2 \text{ min}^{-1}$	κ_d	$D/(L_x/N_c)^2 \approx 5.79 \times 10^{-2} N_c^2 \text{ min}^{-1}$
L_x	$275 \mu\text{m}$		
L_y	$5 \mu\text{m}$		
L_z	$0.5 \mu\text{m}$		
\mathbf{V}	$687.5 \mu\text{m}^3$		

κ_m , for $m = 5, 6, 7, 8, 9$, are stochastic reaction rate constants and κ_d is the diffusion rate constant for species A . These are derived from the corresponding deterministic rate constants estimated in Umulis et al. (2006), and both the deterministic and the stochastic parameters are given in Table 3.

In the kinetic scheme κ_5 is a stochastic rate constant for ligand–receptor binding, and thus depends on the volume, but since we assume that the receptor density is large compared to the signal, the product of the binding constant and the receptor density is a pseudo-first-order rate constant, and hence independent of the volume. All other reactions except for production of species A are first order, and the deterministic and stochastic rate constants are independent of the volume and hence N_c . To standardize the input as we change N_c , we must hold the total flux of A constant. An estimate of an input on a volumetric basis given in Umulis et al. (2006) is converted to a flux per unit area by multiplying by the length of the longest edge, $L_x = 275 \mu\text{m}$; this yields k_8 . The corresponding stochastic rate, κ_8 , is given as follows:

$$\kappa_8 = \frac{k_8(\mathcal{N}_A \mathbf{V})}{L_x}.$$

Therefore, κ_8 does not depend on N_c .

The stochastic diffusion rate constant κ_d is computed by dividing the continuum deterministic diffusion rate constant by $(L_x/N_c)^2$, via discretization of the Laplacian, and thus scales as N_c^2 .

Let $X(t)$ be the first moment vector for the diffusing species A and $Y(t)$ be the first moment vector for the non-diffusing species B and C . $[X(t)]_{i(k,1)}$ denotes the mean number of molecules of species A in the k th compartment, and $[Y(t)]_{i(q,1)}$ and $[Y(t)]_{i(q,2)}$ represent the mean numbers of species B and C in the q th compartment, respectively. The evolution of the first moments is governed by

$$\frac{dX(t)}{dt} = (\Delta \otimes D + I_{N_c} \otimes \mathcal{R}) X(t) + (I_{N_c} \otimes \mathcal{S}) Y(t) + \mathbf{k}^s \tag{22}$$

$$\frac{dY(t)}{dt} = (I_{N_c} \otimes \mathcal{T}) X(t) + (I_{N_c} \otimes \mathcal{W}) Y(t). \tag{23}$$

The diffusion matrix, reaction matrices, and a matrix for production rate from a source are given as

$$\begin{aligned} \mathcal{D} &= \kappa_d, \quad \mathcal{R} = -\kappa_5 R - \kappa_6, \quad \mathcal{S} = [\kappa_{-5} \quad 0], \quad \mathcal{T} = \begin{bmatrix} \kappa_5 R \\ 0 \end{bmatrix}, \\ \mathcal{W} &= \begin{bmatrix} -\kappa_{-5} - \kappa_7 & 0 \\ \kappa_7 & -\kappa_9 \end{bmatrix}, \quad \mathbf{k}^s = [\kappa_8, 0, \dots, 0]^T. \end{aligned}$$

In this example, the eigenvalues of all principal submatrices of the reaction matrices \mathcal{R} and \mathcal{W} are in the *LHP*.

Let X_∞ be the steady-state first moment vector for the number of molecules of species *A* and let Y_∞ be the steady-state first moment vector for the numbers of molecules of species *B* and *C*. Using the fact that species *B* and *C* do not diffuse, we compute Y_∞ in terms of X_∞ .

$$Y_\infty = - \left(I_{N_c} \otimes (\mathcal{W}^{-1} \mathcal{T}) \right) X_\infty.$$

Then we find that

$$[Y_\infty]_{i(k,1)} = \frac{\kappa_5 R}{\kappa_{-5} + \kappa_7} [X_\infty]_{i(k,1)} \tag{24}$$

$$[Y_\infty]_{i(k,2)} = \frac{\kappa_5 \kappa_7 R}{\kappa_9 (\kappa_{-5} + \kappa_7)} [X_\infty]_{i(k,1)} \tag{25}$$

Converting the steady-state first moment of *B* into that of *A*, the effective reaction rate of species *A* at steady-state becomes

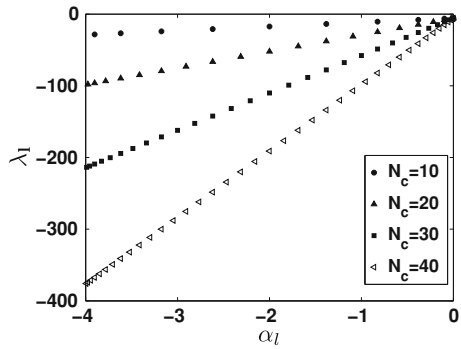
$$\begin{aligned} \mathcal{K} &\equiv \mathcal{R} - \mathcal{S} \mathcal{W}^{-1} \mathcal{T} \\ &= -\frac{\kappa_5 \kappa_7 R}{\kappa_{-5} + \kappa_7} - \kappa_6. \end{aligned}$$

Note that \mathcal{K} is a scalar since there is exactly one diffusing species, *A*. Then, X_∞ satisfies

$$(\Delta \otimes \mathcal{D} + I_{N_c} \otimes \mathcal{K}) X_\infty + \mathbf{k}^s = 0. \tag{26}$$

Define $\overline{X}_\infty \equiv X_\infty / V_c$. To calculate the steady-state first moment for species *A*, we first compute the eigenvalues and corresponding projections of the reaction–diffusion matrix $\Omega = \Delta \otimes \mathcal{D} + I_{N_c} \otimes \mathcal{K}$. As before, let α_l denote an eigenvalue of Δ , let λ_1 be an eigenvalue of Ω , and let P_1 be the corresponding projection of Ω . Then according

Fig. 3 Eigenvalues of Δ and Ω when $N_c = 10, 20, 30, 40$



to (11), the scaled steady-state first moment of A is

$$\bar{X}_\infty = -\frac{1}{V_c} \sum_l \frac{P_l}{\lambda_l} \mathbf{k}^s. \tag{27}$$

In Fig. 3 we show the relation between α_l and λ_l for $N_c = 10, 20, 30, 40$. The range of α_l is fixed at $[-4, 0]$ by the structure of the network and the boundary conditions, but the range of λ_l increases as N_c is increased because higher spatial frequencies are captured with increasing N_c . Since we impose Neumann data on the boundary in the discrete problem, the smallest eigenvalue in magnitude is $\lambda_{N_c,1} \approx -5.73$ corresponding to $\alpha_{N_c} = 0$. The dominant term in (27) corresponds to $\lambda_{N_c,1}$, and is independent of N_c . Using (24) and (25), we compute $\max_k (\bar{C}V_\infty)^{k,i}$ for $i = A, B, C$ in terms of $\min_k [\bar{X}_\infty]_{i(k,1)}$.

$$\max_k (\bar{C}V_\infty)^{k,A} = \sqrt{\frac{1}{\min_k [\bar{X}_\infty]_{i(k,1)}}} \tag{28}$$

$$\max_k (\bar{C}V_\infty)^{k,B} = \sqrt{\frac{\kappa-5+\kappa\gamma}{\kappa_5 R}} \sqrt{\frac{1}{\min_k [\bar{X}_\infty]_{i(k,1)}}} \tag{29}$$

$$\max_k (\bar{C}V_\infty)^{k,C} = \sqrt{\frac{(\kappa-5+\kappa\gamma)\kappa\theta}{\kappa_5\kappa_7 R}} \sqrt{\frac{1}{\min_k [\bar{X}_\infty]_{i(k,1)}}} \tag{30}$$

Also, we have

$$\bar{C}V^* = \sqrt{\frac{1}{\min \left(\min_k [\bar{X}_\infty]_{i(k,1)}, \frac{\kappa_5 R}{\kappa-5+\kappa\gamma} \min_k [\bar{X}_\infty]_{i(k,1)}, \frac{\kappa_5\kappa_7 R}{\kappa\theta(\kappa-5+\kappa\gamma)} \min_k [\bar{X}_\infty]_{i(k,1)} \right)}}.$$

In Appendix D we prove that $\bar{X}_\infty/\mathcal{N}_A$ converges to the concentration satisfying the corresponding continuum model in which the source is located at $x = 0$. Due to the source location at $x = 0$, the steady-state concentration is monotone decreasing in x .

Fig. 4 The evolution of $\ln(\sqrt{V_c}(CV(t))^{N_c,C})$ in time for $N_c = 10, 30, 60$, when production is restricted to the first compartment and initial values are zero

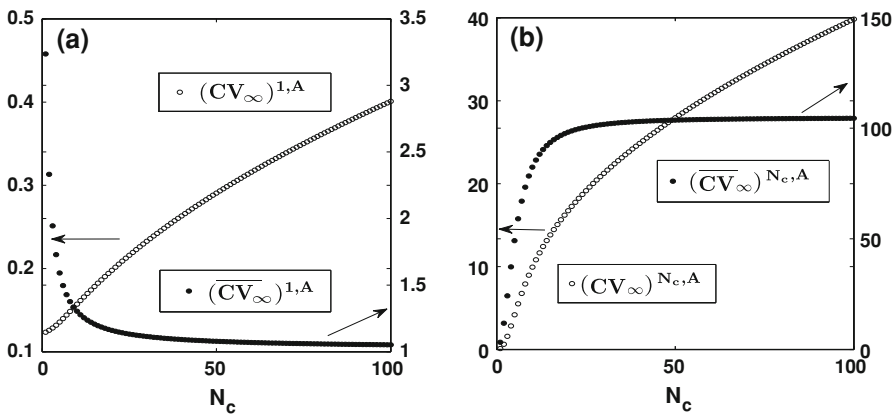
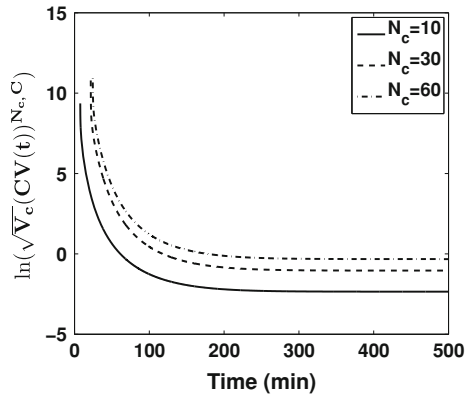


Fig. 5 The CV of species A in the 1-dimensional model

One can show that the same is true in the discrete problem, and the proof is left to the reader.

Since we later only use the steady-state measure for the noise to determine the number of compartments, one has to check that the steady-state is reached rapidly. In Fig. 4 we show the transient evolution of $\sqrt{V_c}(CV(t))^{N_c,C}$ in the last compartment for $N_c = 10, 30, 60$. In this example species C serves as the downstream signal, and as we see in Fig. 4, the noise in the downstream signal stabilizes very quickly, which indicates that a compartment size based on the steady-state noise level is appropriate here. Of course it may not always be.

In Figs. 5 and 6, we display the steady state noise for the kinetic scheme in Example 2.2 for the unscaled and scaled CVs as a function of N_c . In Fig. 5, we show $(CV_\infty)^{k,A}$ for $k = 1, N_c$ as we vary N_c . The values of $(CV_\infty)^{k,B}$ and $(CV_\infty)^{k,C}$ are simply scaled versions of $(CV_\infty)^{k,A}$ and are not shown. $[X_\infty]_{li(k,1)}$ has its maximum and minimum values in the first and the last compartments, respectively, by virtue of the monotonicity of the profile. Therefore, using Proposition 1, $(CV_\infty)^{k,i}$ has its maximum and minimum values in the last and the first compartments, respectively. It is apparent in

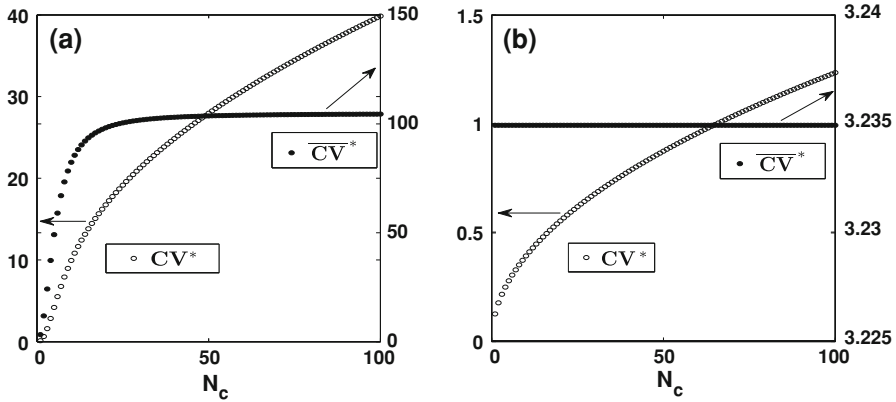


Fig. 6 A comparison of the noise for (a) spatially-nonuniform and (b) spatially-uniform inputs

the figure that as N_c increases, $(CV_\infty)^{k,i}$ gets larger due to the smaller number of molecules in each compartment, but $(\overline{CV}_\infty)^{k,i}$ stabilizes due to convergence of \overline{X}_∞ to the corresponding concentration multiplied by N_A as $N_c \rightarrow \infty$. This indicates that the contribution of diffusion to this scaled measure is dominated by the kinetic contribution for large enough N_c . This explanation could be made rigorous by analyzing the asymptotic behavior of the covariance as $h \rightarrow 0$, but we will not pursue this here.

In Fig. 6 we illustrate the effect of the source location on the global measures CV^* and \overline{CV}^* . In (a) the source for species A is in the first compartment as previously, while in (b) the input is divided amongst all compartments, scaled so that the total input is fixed and independent of N_c . In (a) \overline{CV}^* stabilizes at about $N_c = 30$, while in (b) \overline{CV}^* is constant in N_c , whereas CV^* is monotone increasing in N_c in both cases. The stabilization of \overline{CV}^* with N_c suggests that the minimum number of compartments needed for an accurate representation of the noise is defined by the smallest N_c at which \overline{CV}^* reaches a chosen percentage of the asymptotic value. As we show in the following section, this agrees remarkably well with a criterion based on convergence of solutions to a uniform state. Although it is not shown in (a), an increase of the diffusion constant decreases the value of N_c at which \overline{CV}^* stabilizes, as is to be expected. The results in (b) suggest that distributing the input is an effective way of reducing the noise, but of course this cannot be done if A is a morphogen that is used to determine cell types in a developing tissue. A comparison of $(\overline{CV}_\infty)^{N_c,A}$ in Fig. 5b and \overline{CV}^* in Fig. 6a shows that these two values are equal, since $[X_\infty]_{i(N_c,1)}$ is the smallest among all first moments of species A in all compartments, which is what is used for computing \overline{CV}^* .

In Sect. 1.4 we discussed different criteria to determine the compartment size, and here we apply Bernstein’s criterion to the foregoing example. Denote A_{tot} , B_{tot} , and C_{tot} as the total numbers of molecules of species A , B , and C at steady state, respectively. To compute the reaction timescale we have to compute the propensity of each reaction, for which we use the steady-state first moments for species A , B , and C , and this yields $A_{tot} = 65.69$ and $B_{tot} = C_{tot} = 10356$. Since the propensity of conversion from A to B is the largest, we use this to compute the timescale of the process, τ_r .

Thus

$$\begin{aligned}\tau_r &\approx \frac{1}{320 \text{ min}^{-1} \times \frac{A_{tot}}{N_c}} \\ &= \frac{1}{76.44 \times h_x} \text{ min.}\end{aligned}$$

The diffusion timescale computed using the diffusion coefficient of species A is

$$\frac{h_x^2}{2D} = \frac{h_x \mu\text{m}^2}{2 \times 4380 \mu\text{m}^2 \text{ min}^{-1}} = \frac{h_x^2}{8760} \text{ min.}$$

If we demand that the diffusion timescale be much smaller than the reaction timescale, we obtain

$$\begin{aligned}h_x &\ll \left(\frac{8760}{76.44}\right)^{1/3} \mu\text{m} \\ &\approx 4.86 \mu\text{m}.\end{aligned}$$

In Sect. 3 we derive an upper bound for the compartment size for general systems, and as we show in Sect. 4, this leads to an estimate $h_x < 8.25 \mu\text{m}$ (which corresponds to $N_c > 33$). This result confirms the fact that it is not necessary to discretize in the y or z -direction, since those dimensions are less than the maximum allowable compartment size.

3 An upper bound for the compartment size

As was discussed earlier, current criteria for choosing an appropriate cell or compartment size for discretizing a reaction–diffusion system are based on first estimating the smallest reaction time-scale and then choosing a compartment size to ensure that the diffusion time scale is less than this. Since this is based on the objective of ensuring that all molecules within a cell are accessible to each other, an alternate approach is to ask what conditions guarantee that the solution of the coupled reaction–diffusion system converges to spatially-uniform solutions, whether stationary or time-dependent. This obviously requires that diffusion dominates reaction in an appropriate sense, and that sense was first developed in Othmer (1977) and Ashkenazi and Othmer (1978). There it was shown that every species approaches a spatially-uniform solution at an exponential rate in time when the diffusion constant for each species is sufficiently large relative to a measure of the sensitivity of the kinetic network. More precisely, if c is the vector of species concentrations and \bar{c} is the spatial average of c , then under the assumption that all species diffuse, the authors prove that $\|c(\mathbf{x}, t) - \bar{c}(t)\|_{L_2} \rightarrow 0$ exponentially in t in any bounded domain Ω in 1-, 2-, or 3-dimensional space if $|\alpha_1 \delta| > \hat{r}$. Here δ is the smallest diffusion coefficient, α_1 is the largest non-zero eigenvalue of the Laplacian with homogeneous Neumann conditions on $\partial\Omega$, and \hat{r} is the maximum Euclidean norm, taken over an appropriate set, of the Jacobian of the reaction terms.

That result was generalized in Conway et al. (1978). Here we extend this result to allow non-diffusing species and reactions at the boundary, as described below, and use the result to compute a maximal compartment size for a discretized reaction–diffusion system. We do this in two steps—first we treat homogeneous Neumann boundary data to analyze the effect of non-diffusing species, and then we summarize the results for other boundary conditions.

3.1 Homogeneous Neumann conditions

Let $\Omega \subset R^3$ be a domain with a smooth boundary $\partial\Omega$. Denote generic spatial locations as $\mathbf{x} = (x, y, z)$ and $\boldsymbol{\xi} = (\xi_x, \xi_y, \xi_z)$, where either can lie in the interior of or on the boundary of Ω . Let $u(\mathbf{x}, t) \in R^m$ and $v(\mathbf{x}, t) \in R^n$ denote the concentrations of diffusing and non-diffusing species, respectively, that react in Ω at time t , and let $w(\mathbf{x}, t) \in R^p$ denote the concentrations of non-diffusing species that do not affect the evolution of any species in u and v . We write the governing equations and the boundary conditions for all species as follows.

$$\begin{aligned} \frac{\partial u(\mathbf{x}, t)}{\partial t} &= \mathcal{D}\Delta u(\mathbf{x}, t) + \mathcal{R}(u(\mathbf{x}, t), v(\mathbf{x}, t)), & \mathbf{x} \in \Omega \\ \frac{\partial v(\mathbf{x}, t)}{\partial t} &= \mathcal{S}(u(\mathbf{x}, t), v(\mathbf{x}, t)), & \mathbf{x} \in \Omega \\ \frac{\partial w(\mathbf{x}, t)}{\partial t} &= \mathcal{T}(u(\mathbf{x}, t), v(\mathbf{x}, t), w(\mathbf{x}, t)), & \mathbf{x} \in \Omega \\ \frac{\partial u(\mathbf{x}, t)}{\partial n} &= 0, & \mathbf{x} \in \partial\Omega \\ u(\mathbf{x}, 0) &= u_0(\mathbf{x}), & \mathbf{x} \in \Omega \\ v(\mathbf{x}, 0) &= v_0(\mathbf{x}), & \mathbf{x} \in \Omega \\ w(\mathbf{x}, 0) &= w_0(\mathbf{x}), & \mathbf{x} \in \Omega \end{aligned}$$

Here differentiation with respect to n is along the outward unit normal vector to Ω , and \mathcal{D} is a diagonal matrix of diffusion coefficients. Note that the non-diffusing species in $w(\mathbf{x}, t)$, which do not affect any species in u or v , can be ignored in the following, since they do not affect the convergence to a uniform solution of the diffusing species. Hereafter we exclude the governing equation for $w(\mathbf{x}, t)$ from the system equations, and this leads to the following simplified set of equations that we use for the analysis.³

$$\begin{aligned} \frac{\partial u(\mathbf{x}, t)}{\partial t} &= \mathcal{D}\Delta u(\mathbf{x}, t) + \mathcal{R}(u(\mathbf{x}, t), v(\mathbf{x}, t)), & \mathbf{x} \in \Omega \\ \frac{\partial v(\mathbf{x}, t)}{\partial t} &= \mathcal{S}(u(\mathbf{x}, t), v(\mathbf{x}, t)), & \mathbf{x} \in \Omega \\ \frac{\partial u(\mathbf{x}, t)}{\partial n} &= 0, & \mathbf{x} \in \partial\Omega \end{aligned} \tag{31}$$

³ In fact, as we show in an example later, inclusion of such species can lead to an inappropriate estimate of the compartment size, and for this reason we include it in the above.

$$\begin{aligned} u(\mathbf{x}, 0) &= u_0(\mathbf{x}), & \mathbf{x} \in \Omega \\ v(\mathbf{x}, 0) &= v_0(\mathbf{x}), & \mathbf{x} \in \Omega \end{aligned}$$

We assume that \mathcal{R} and \mathcal{S} are C^1 in the non-negative cone of (u, v) -space, and in general both are nonlinear functions of (u, v) .

Define the vector $c(\mathbf{x}, t) \equiv [u(\mathbf{x}, t)^T, v(\mathbf{x}, t)^T]^T$ of all species concentrations and let $c_0(\mathbf{x})$ be the initial distribution. For a given $c_0(\mathbf{x})$, define $C_0 = \{c_0(\mathbf{x}) | \mathbf{x} \in \bar{\Omega}\}$. In the following theorem we assume that the concentration $c(\mathbf{x}, t)$, which is the image of $c_0(\mathbf{x})$ under the mapping defined by the integral representation given in (43) and (44) is contained in a closed, bounded, convex set $C_\infty \supseteq C_0$, for all $t \in [0, \infty)$. We define the spatial average of the concentrations for diffusing species as

$$\bar{u}(t) \equiv \frac{1}{|\Omega|} \int_{\Omega} u(\mathbf{x}, t) \, d\mathbf{x},$$

and we further assume that for each $t > 0$, there exists a spatially-uniform solution $\bar{v}(t)$ satisfying

$$\begin{aligned} \frac{d\bar{v}(t)}{dt} &= \mathcal{S}(\bar{u}(t), \bar{v}(t)), \\ \bar{v}(0) &= \frac{1}{|\Omega|} \int_{\Omega} v_0(\mathbf{x}) \, d\mathbf{x}. \end{aligned} \tag{32}$$

Given $\bar{u}(t)$, the existence and uniqueness of \bar{v} is guaranteed by the smoothness assumptions, but $\bar{v}(t)$ may not be the spatial average of $v(\mathbf{x}, t)$ when \mathcal{S} is a nonlinear function of either u or v .

We define the L_2 norm

$$\|f(\mathbf{x}, t)\|_{L_2}^2 \equiv (f(\mathbf{x}, t), f(\mathbf{x}, t))_{L_2} \equiv \int_{\Omega} \|f(\mathbf{x}, t)\|_E^2 \, d\mathbf{x}$$

where $\|\cdot\|_E$ is the Euclidean matrix norm, and we define $\bar{c}(t) \equiv [\bar{u}(t)^T, \bar{v}(t)^T]^T$. Then we say that $\|c(\mathbf{x}, t) - \bar{c}(t)\|_{L_2} \rightarrow 0$ if $\|u(\mathbf{x}, t) - \bar{u}(t)\|_{L_2} \rightarrow 0$ and $\|v(\mathbf{x}, t) - \bar{v}(t)\|_{L_2} \rightarrow 0$.

The Jacobians of a function $f : R^m \times R^n \rightarrow R^m \times R^n$ with respect to u and v are denoted

$$D_u f(u, v) \equiv \frac{\partial f(u, v)}{\partial u}, \quad D_v f(u, v) \equiv \frac{\partial f(u, v)}{\partial v}.$$

We define measures of kinetic sensitivity via the Jacobians of the reaction terms as follows

$$\begin{aligned} \hat{r}_u &\equiv \sup_{c \in C_\infty} \|D_u \mathcal{R}(c)\|_E, & \hat{r}_v &\equiv \sup_{c \in C_\infty} \|D_v \mathcal{R}(c)\|_E, \\ \hat{s}_u &\equiv \sup_{c \in C_\infty} \|D_u \mathcal{S}(c)\|_E, & \check{s}_v &\equiv \inf_{c \in C_\infty} |\sigma(W_c D_v \mathcal{S}(c))|. \end{aligned} \tag{33}$$

The matrix W_c is defined in the following.

For a Hermitian operator H , let $\lambda_m(H)$ and $\lambda_M(H)$ be the smallest and the largest eigenvalues of H , which are defined as

$$\lambda_M(H) = \sup_x \{\langle x, Hx \rangle \mid \|x\| = 1\} \quad \text{and} \quad \lambda_m(H) = \inf_x \{\langle x, Hx \rangle \mid \|x\| = 1\}, \tag{34}$$

respectively, and define $\|H\| \equiv \max\{\lambda_M(H), -\lambda_m(H)\}$. An operator H is said to be uniformly positive if $\lambda_m(H) > 0$ (Daleckiĭ and Kreĭn 1974), which we denote as $H \gg 0$. If $H \gg 0$, the norm defined as $\|x\|_H^2 = \langle x, Hx \rangle$ satisfies

$$\lambda_m(H)\|x\|^2 \leq \|x\|_H^2 \leq \lambda_M(H)\|x\|^2 = \|H\|\|x\|^2. \tag{35}$$

In case all species are diffusible, the proof of the convergence result in Othmer (1977) does not require that the spectrum of the Jacobian of the kinetics lies in the *LHP*; only that a norm of the Jacobian can be dominated by the diffusion terms. However this fails when there are non-diffusing species, and this raises several technical difficulties, even when the spectrum of the Jacobian of the kinetics lies in the *LHP* pointwise in time. These are overcome in part by use of a time-dependent metric, but this raises additional difficulties. We assume that for all $c \in C_\infty$,

$$\sigma(D_v \mathcal{S}(c)) \subset LHP, \tag{36}$$

where $\sigma(A)$ denotes the spectrum of A . A generalized Lyapunov theorem (Theorem 5.1 in Daleckiĭ and Kreĭn 1974) states that if A is a real bounded linear operator on a real Hilbert space, and if $\sigma(A) \subset LHP$, then there exists a uniformly positive operator W_A such that $W_A A \ll 0$. Thus in view of (36), for each $t > 0$ there is a uniformly positive operator W_c such that

$$W_c D_v \mathcal{S}(c) \ll 0. \tag{37}$$

Since c is time-dependent W is also, and one cannot apply the standard result which states that for a linear system with a real constant matrix A , the zero solution of

$$\frac{dz}{dt} = Az, \tag{38}$$

is exponentially stable if and only if the Lyapunov equation

$$A^T W + W A = -Q$$

has a positive definite solution W for any positive definite matrix Q (Gantmacher 1974). When A is time-dependent the spectral condition no longer suffices, but it is known that the fundamental solution $U(t, s)$ of the nonautonomous version of (38) is exponentially stable if and only if the Lyapunov equation

$$\frac{dW}{dt} = -(A^T(t)W(t) + W(t)A(t) + Q)$$

has a solution for any positive definite matrix Q (Phat and Nam 2007). Here we do not assume exponential stability, but later we require a bound on the derivative with respect to time of W_c , and one can see that this is equivalent to requiring that the Jacobian $D_v S(c)$ does not vary too rapidly. We define

$$\begin{aligned} \lambda_m &\equiv \inf_{c \in C_\infty} \lambda_m(W_c), \\ \lambda_M &\equiv \sup_{c \in C_\infty} \lambda_M(W_c), \\ w &\equiv \frac{1}{2} \sup_{U \in C_\infty} \left\| \frac{\partial W_c}{\partial t} \right\|_E. \end{aligned} \tag{39}$$

In the definition of w the supremum is taken over all solutions $U = (u(\mathbf{x}, t), v(\mathbf{x}, t), \bar{v}(t))$ where $(u(\mathbf{x}, t), v(\mathbf{x}, t))$ satisfy (31), the third component satisfies (32), and $(\mathbf{x}, t) \in (\Omega, [0, \infty))$.

The following theorem gives conditions for exponential convergence in time of $c(\mathbf{x}, t)$ to a spatially-uniform solution under homogeneous Neumann boundary conditions. In essence the condition requires that the smallest non-zero diffusion coefficient should be large enough compared to some function of the kinetic sensitivities, $\hat{r}_u, \hat{r}_v, \hat{s}_u$, and \check{s}_v , and of the constants, λ_m, λ_M , and w , defined by the positive operator W_c .

Theorem 3 $\|c(\mathbf{x}, t) - \bar{c}(t)\|_{L_2} \rightarrow 0$ exponentially in t if

$$\begin{aligned} \text{(i)} \quad &\sigma(D_v S(c)) \subset LHP \quad \text{for all } c \in C_\infty, \\ \text{(ii)} \quad &\check{s}_v > w, \\ \text{(iii)} \quad &|\alpha_1 \delta| > \hat{r}_u + \frac{\hat{r}_v \hat{s}_u}{\check{s}_v - w} \cdot \frac{\lambda_M^2}{\lambda_m}, \end{aligned} \tag{40}$$

where $\delta = \min_i \mathcal{D}_{ii}$ and α_1 is the largest non-zero eigenvalue of the scalar problem

$$\begin{aligned} \Delta \phi(\mathbf{x}) &= \alpha \phi(\mathbf{x}), \quad \mathbf{x} \in \Omega, \\ \frac{\partial \phi}{\partial n} &= 0, \quad \mathbf{x} \in \partial \Omega. \end{aligned} \tag{41}$$

Proof Define the Green's function $G(\mathbf{x}, \boldsymbol{\xi}, t)$ as the solution of

$$\begin{aligned} \frac{\partial G(\mathbf{x}, \boldsymbol{\xi}, t)}{\partial t} &= \mathcal{D}\Delta G(\mathbf{x}, \boldsymbol{\xi}, t), & \mathbf{x} \in \Omega, \\ \frac{\partial G(\mathbf{x}, \boldsymbol{\xi}, t)}{\partial n} &= 0, & \mathbf{x} \in \partial\Omega, \\ G(\mathbf{x}, \boldsymbol{\xi}, 0) &= \delta(\mathbf{x}, \boldsymbol{\xi}). \end{aligned} \tag{42}$$

G is a diagonal matrix and G_{ii} represents the i th diagonal element. Then for $\mathbf{x} \in \Omega$, u and v satisfy

$$u(\mathbf{x}, t) = \int_{\Omega} G(\mathbf{x}, \boldsymbol{\xi}, t)u_0(\boldsymbol{\xi}) d\boldsymbol{\xi} + \int_0^t \int_{\Omega} G(\mathbf{x}, \boldsymbol{\xi}, t - \tau)\mathcal{R}(u(\boldsymbol{\xi}, \tau), v(\boldsymbol{\xi}, \tau)) d\boldsymbol{\xi} d\tau, \tag{43}$$

$$v(\mathbf{x}, t) = v_0(\mathbf{x}) + \int_0^t \mathcal{S}(u(\mathbf{x}, \tau), v(\mathbf{x}, \tau)) d\tau. \tag{44}$$

The i th diagonal element of G satisfies

$$\int_{\Omega} G_{ii}(\mathbf{x}, \boldsymbol{\xi}, t - \tau) d\boldsymbol{\xi} = 1,$$

and by defining

$$G_{ii}^0(\mathbf{x}, \boldsymbol{\xi}, t) \equiv G_{ii}(\mathbf{x}, \boldsymbol{\xi}, t) - \frac{1}{|\Omega|}, \tag{45}$$

we have

$$\int_{\Omega} G_{ii}^0(\mathbf{x}, \boldsymbol{\xi}, t) d\boldsymbol{\xi} = 0. \tag{46}$$

Therefore

$$\begin{aligned} u(\mathbf{x}, t) &= \int_{\Omega} \left(\frac{1}{|\Omega|} + G^0(\mathbf{x}, \boldsymbol{\xi}, t) \right) u_0(\boldsymbol{\xi}) d\boldsymbol{\xi} \\ &\quad + \int_0^t \int_{\Omega} \left(\frac{1}{|\Omega|} + G^0(\mathbf{x}, \boldsymbol{\xi}, t - \tau) \right) \mathcal{R}(u(\boldsymbol{\xi}, \tau), v(\boldsymbol{\xi}, \tau)) d\boldsymbol{\xi} d\tau, \end{aligned} \tag{47}$$

and it follows that

$$\bar{u}(t) = \frac{1}{|\Omega|} \int_{\Omega} u_0(\xi) d\xi + \frac{1}{|\Omega|} \int_0^t \int_{\Omega} \mathcal{R}(u(\xi, \tau), v(\xi, \tau)) d\xi d\tau \tag{48}$$

and

$$0 = \int_{\Omega} G^0(\mathbf{x}, \xi, t) \bar{u}(0) d\xi + \int_0^t \int_{\Omega} G^0(\mathbf{x}, \xi, t - \tau) \mathcal{R}(\bar{u}(\tau), \bar{v}(\tau)) d\xi d\tau. \tag{49}$$

We define

$$\Psi(\mathbf{x}, t) \equiv u(\mathbf{x}, t) - \bar{u}(t), \quad \Phi(\mathbf{x}, t) \equiv v(\mathbf{x}, t) - \bar{v}(t),$$

and then find that

$$\Psi(\mathbf{x}, t) = \int_{\Omega} G^0(\mathbf{x}, \xi, t) \Psi(\xi, 0) d\xi + \int_0^t \int_{\Omega} G^0(\mathbf{x}, \xi, t - \tau) R(\xi, \tau) d\xi d\tau \tag{50}$$

where

$$R(\xi, \tau) \equiv \mathcal{R}(u(\xi, \tau), v(\xi, \tau)) - \mathcal{R}(\bar{u}(\tau), \bar{v}(\tau)).$$

Consider the diffusion problem

$$\begin{aligned} \frac{\partial \psi(\mathbf{x}, t)}{\partial t} &= \mathcal{D}_{ii} \Delta \psi(\mathbf{x}, t), & \mathbf{x} \in \Omega, \\ \frac{\partial \psi(\mathbf{x}, t)}{\partial n} &= 0, & \mathbf{x} \in \partial \Omega. \end{aligned} \tag{51}$$

The solution of (51) can be written

$$\psi(\mathbf{x}, t) = \sum_l a_l \phi_l(\mathbf{x}) e^{\alpha_l \mathcal{D}_{ii} t}$$

where the eigenvalues α_l are non-positive and the $\phi_l(\mathbf{x})$'s are the corresponding orthogonal eigenfunctions. For those having zero mean over Ω , $\alpha_l < 0$ and $\psi(\mathbf{x}, t)$ satisfies

$$\begin{aligned} \frac{d}{dt} \|\psi\|_{L_2}^2 &= \frac{d}{dt} \langle \psi, \psi \rangle_{L_2} = 2 \left\langle \psi, \frac{\partial \psi}{\partial t} \right\rangle_{L_2} \\ &= 2 \langle \psi, \mathcal{D}_{ii} \Delta \psi \rangle_{L_2} \leq 2\alpha_1 \mathcal{D}_{ii} \|\psi\|_{L_2}^2 \end{aligned}$$

where α_1 is the largest non-zero eigenvalue. It follows that $\psi(\mathbf{x}, t)$ satisfies

$$\|\psi(\mathbf{x}, t)\|_{L_2} \leq e^{-|\alpha_1| \mathcal{D}_{ii} t} \|\psi(\mathbf{x}, 0)\|_{L_2}. \tag{52}$$

The Green's function defined at (42) has an eigenfunction expansion in terms of the $\phi's$, and from this it follows that the first term in (50) satisfies the inequality

$$\left\| \int_{\Omega} G^0(\mathbf{x}, \xi, t) \Psi(\xi, 0) d\xi \right\|_{L_2} \leq e^{-|\alpha_1| \delta t} \|\Psi(\mathbf{x}, 0)\|_{L_2}.$$

Using this, and the inequality

$$\|\mathcal{R}(u(\xi, \tau), v(\xi, \tau)) - \mathcal{R}(\bar{u}(\tau), \bar{v}(\tau))\|_{L_2} \leq \hat{r}_u \|\Psi(\mathbf{x}, \tau)\|_{L_2} + \hat{r}_v \|\Phi(\mathbf{x}, \tau)\|_{L_2}, \tag{53}$$

it follows from (50) that

$$\begin{aligned} e^{|\alpha_1| \delta t} \|\Psi(\mathbf{x}, t)\|_{L_2} &\leq \|\Psi(\mathbf{x}, 0)\|_{L_2} + \hat{r}_u \int_0^t e^{|\alpha_1| \delta \tau} \|\Psi(\mathbf{x}, \tau)\|_{L_2} d\tau \\ &\quad + \hat{r}_v \int_0^t e^{|\alpha_1| \delta \tau} \|\Phi(\mathbf{x}, \tau)\|_{L_2} d\tau. \end{aligned} \tag{54}$$

From (32), we have

$$\bar{v}(t) = \bar{v}(0) + \int_0^t \mathcal{S}(\bar{u}(\tau), \bar{v}(\tau)) d\tau \tag{55}$$

and therefore the difference $\Phi(\mathbf{x}, t) = v(\mathbf{x}, t) - \bar{v}(t)$ satisfies

$$\Phi(\mathbf{x}, t) = \Phi(\mathbf{x}, 0) + \int_0^t \{\mathcal{S}(u(\mathbf{x}, \tau), v(\mathbf{x}, \tau)) - \mathcal{S}(\bar{u}(\tau), \bar{v}(\tau))\} d\tau. \tag{56}$$

Since C_∞ is convex, for each $\mathbf{x} \in \Omega$ and $\tau \in [0, t < \infty)$, there exist $c_1(\mathbf{x}, \tau)$ and $c_2(\mathbf{x}, \tau)$ such that

$$\begin{aligned} \mathcal{S}(u(\mathbf{x}, \tau), v(\mathbf{x}, \tau)) - \mathcal{S}(\bar{u}(\tau), \bar{v}(\tau)) &= D_u \mathcal{S}(c_1(\mathbf{x}, \tau)) (u(\mathbf{x}, \tau) - \bar{u}(\tau)) \\ &\quad + D_v \mathcal{S}(c_2(\mathbf{x}, \tau)) (v(\mathbf{x}, \tau) - \bar{v}(\tau)). \end{aligned}$$

As a result, (56) can be rewritten as

$$\Phi(\mathbf{x}, t) = \Phi(\mathbf{x}, 0) + \int_0^t \{D_u S(c_1(\mathbf{x}, \tau))\Psi(\mathbf{x}, \tau) + D_v S(c_2(\mathbf{x}, \tau))\Phi(\mathbf{x}, \tau)\} d\tau. \tag{57}$$

In view of (36) and (37), for each $c \in C_\infty$ we can define a weighted Euclidean norm by W_c as

$$\|A\|_{E, W_c}^2 \equiv \langle A, W_c A \rangle_E.$$

Since W_c is a uniformly positive operator for each $c \in C_\infty$, $\lambda_m > 0$ in (39). Using (35) and (39), for each $\mathbf{x} \in \Omega$ and $t \in [0, \infty)$, we obtain the upper and lower bounds

$$\lambda_m \|\Phi(\mathbf{x}, t)\|_E^2 \leq \|\Phi(\mathbf{x}, t)\|_{E, W_{c_2(\mathbf{x}, t)}}^2 \leq \lambda_M \|\Phi(\mathbf{x}, t)\|_E^2. \tag{58}$$

Define a weighted L_2 norm as

$$\|f(\mathbf{x}, t)\|_{L_2, W_f}^2 \equiv \int_\Omega \|f(\mathbf{x}, t)\|_{E, W_{f(\mathbf{x}, t)}}^2 d\mathbf{x}.$$

Then,

$$\lambda_m \|\Phi(\mathbf{x}, t)\|_{L_2}^2 \leq \|\Phi(\mathbf{x}, t)\|_{L_2, W_{c_2}}^2 \leq \lambda_M \|\Phi(\mathbf{x}, t)\|_{L_2}^2, \tag{59}$$

and differentiating this we obtain

$$\begin{aligned} \frac{d}{dt} \|\Phi(\mathbf{x}, t)\|_{E, W_{c_2(\mathbf{x}, t)}}^2 &= \langle \Phi(\mathbf{x}, t), D_t W_{c_2(\mathbf{x}, t)} \Phi(\mathbf{x}, t) \rangle_E + \langle \Phi(\mathbf{x}, t), W_{c_2(\mathbf{x}, t)} D_t \Phi(\mathbf{x}, t) \rangle_E \\ &\quad + \langle D_t \Phi(\mathbf{x}, t), W_{c_2(\mathbf{x}, t)} \Phi(\mathbf{x}, t) \rangle_E. \end{aligned} \tag{60}$$

From (57) and (60) it follows that

$$\begin{aligned} \frac{d}{dt} \|\Phi(\mathbf{x}, t)\|_{E, W_{c_2(\mathbf{x}, t)}}^2 &= \langle \Phi(\mathbf{x}, t), D_t W_{c_2(\mathbf{x}, t)} \Phi(\mathbf{x}, t) \rangle_E \\ &\quad + \langle \Phi(\mathbf{x}, t), W_{c_2(\mathbf{x}, t)} D_u S(c_1(\mathbf{x}, \tau))\Psi(\mathbf{x}, t) \rangle_E \\ &\quad + \langle \Phi(\mathbf{x}, t), W_{c_2(\mathbf{x}, t)} D_v S(c_2(\mathbf{x}, \tau))\Phi(\mathbf{x}, t) \rangle_E \\ &\quad + \langle D_u S(c_1(\mathbf{x}, \tau))\Psi(\mathbf{x}, t), W_{c_2(\mathbf{x}, t)} \Phi(\mathbf{x}, t) \rangle_E \\ &\quad + \langle D_v S(c_2(\mathbf{x}, \tau))\Phi(\mathbf{x}, t), W_{c_2(\mathbf{x}, t)} \Phi(\mathbf{x}, t) \rangle_E. \end{aligned}$$

After applying the Cauchy–Schwarz inequality and using the fact that $\sigma(W_c D_v S(c)) \subset LHP$ for all $c \in C_\infty$, we obtain

$$\begin{aligned} \frac{d}{dt} \|\Phi(\mathbf{x}, t)\|_{E, W_{c_2(\mathbf{x}, t)}}^2 &\leq 2w \|\Phi(\mathbf{x}, t)\|_E^2 + 2\hat{s}_u \lambda_M \|\Phi(\mathbf{x}, t)\|_E \|\Psi(\mathbf{x}, t)\|_E \\ &\quad + \left\langle \Phi(\mathbf{x}, t), (W_{c_2(\mathbf{x}, t)} D_v S(c_2(\mathbf{x}, \tau)) + [D_v S(c_2(\mathbf{x}, \tau))]^T \right. \\ &\quad \left. \times W_{c_2(\mathbf{x}, t)} \Phi(\mathbf{x}, t) \right\rangle_E \\ &\leq 2\hat{s}_u \lambda_M \|\Phi(\mathbf{x}, t)\|_E \|\Psi(\mathbf{x}, t)\|_E - (2\check{s}_v - 2w) \|\Phi(\mathbf{x}, t)\|_E^2 \end{aligned} \tag{61}$$

where $[D_v S(c_2(\mathbf{x}, \tau))]^T$ is the transpose of $D_v S(c_2(\mathbf{x}, \tau))$ for fixed $\mathbf{x} \in \Omega$ and $\tau \in [0, \infty)$. From the second condition in (40), we assume that $\check{s}_v - w > 0$. Then using (58) and dividing by $2\|\Phi(\mathbf{x}, t)\|_{E, W_{c_2(\mathbf{x}, t)}}$, (61) becomes

$$\frac{d}{dt} \|\Phi(\mathbf{x}, t)\|_{E, W_{c_2(\mathbf{x}, t)}} \leq \frac{\hat{s}_u \lambda_M}{\sqrt{\lambda_m}} \|\Psi(\mathbf{x}, t)\|_E - \frac{\check{s}_v - w}{\lambda_M} \|\Phi(\mathbf{x}, t)\|_{E, W_{c_2(\mathbf{x}, t)}}. \tag{62}$$

From this one obtains

$$\begin{aligned} e^{|\alpha_1 \delta| t} \|\Phi(\mathbf{x}, t)\|_{E, W_{c_2(\mathbf{x}, t)}} &\leq \|\Phi(\mathbf{x}, 0)\|_{E, W_{c_2(\mathbf{x}, 0)}} + \frac{\hat{s}_u \lambda_M}{\sqrt{\lambda_m}} \int_0^t e^{|\alpha_1 \delta| \tau} \|\Psi(\mathbf{x}, \tau)\|_E d\tau \\ &\quad + \left(|\alpha_1 \delta| - \frac{\check{s}_v - w}{\lambda_M} \right) \int_0^t e^{|\alpha_1 \delta| \tau} \|\Phi(\mathbf{x}, \tau)\|_{E, W_{c_2(\mathbf{x}, \tau)}} d\tau \end{aligned} \tag{63}$$

which the reader can verify by integration by parts. Integrating (63) over $\mathbf{x} \in \Omega$, we get

$$\begin{aligned} e^{|\alpha_1 \delta| t} \|\Phi(\mathbf{x}, t)\|_{L_2, W_{c_2}} &\leq \|\Phi(\mathbf{x}, 0)\|_{L_2, W_{c_2}} + \frac{\hat{s}_u \lambda_M}{\sqrt{\lambda_m}} \int_0^t e^{|\alpha_1 \delta| \tau} \|\Psi(\mathbf{x}, \tau)\|_{L_2} d\tau \\ &\quad + \left(|\alpha_1 \delta| - \frac{\check{s}_v - w}{\lambda_M} \right) \int_0^t e^{|\alpha_1 \delta| \tau} \|\Phi(\mathbf{x}, \tau)\|_{L_2, W_{c_2}} d\tau. \end{aligned} \tag{64}$$

We now have the estimates on the diffusing and non-diffusing species needed, and we combine these as follows. Define

$$g(t) \equiv \left[e^{|\alpha_1 \delta| t} \|\Psi(\mathbf{x}, t)\|_{L_2}, e^{|\alpha_1 \delta| t} \|\Phi(\mathbf{x}, t)\|_{L_2, W_{c_2}} \right]^T;$$

then from (54) and (64) we have

$$g(t) \leq g(0) + \int_0^t \begin{bmatrix} \hat{r}_u & \frac{\hat{r}_v}{\sqrt{\lambda_m}} \\ \frac{\hat{s}_u \lambda_M}{\sqrt{\lambda_m}} & |\alpha_1 \delta| - \frac{\check{s}_v - w}{\lambda_M} \end{bmatrix} g(\tau) d\tau,$$

where the inequality is defined componentwise. Since the off-diagonal elements of the matrix K in the integral are positive, the map defined by the right-hand side preserves the order in the positive cone of R^2 (Smith 1988), and it follows that

$$g(t) \leq e^{Kt} g(0).$$

Therefore

$$\begin{bmatrix} \|\Psi(\mathbf{x}, t)\|_{L_2} \\ \|\Phi(\mathbf{x}, t)\|_{L_2, W_{c_2}} \end{bmatrix} \leq e^{At} \begin{bmatrix} \|\Psi(\mathbf{x}, 0)\|_{L_2} \\ \|\Phi(\mathbf{x}, 0)\|_{L_2, W_{c_2}} \end{bmatrix}$$

where

$$A = \begin{bmatrix} -|\alpha_1 \delta| + \hat{r}_u & \frac{\hat{r}_v}{\sqrt{\lambda_m}} \\ \frac{\hat{s}_u \lambda_M}{\sqrt{\lambda_m}} & -\frac{\check{s}_v - w}{\lambda_M} \end{bmatrix}.$$

Consequently, if all eigenvalues of A have negative real part, then it follows, after using (59), that $\|c(\mathbf{x}, t) - \bar{c}(t)\|_{L_2} \rightarrow 0$ exponentially in t .

We can compute the characteristic equation explicitly and find the factored form

$$(\lambda + |\alpha_1 \delta| - \hat{r}_u) \left(\lambda + \frac{\check{s}_v - w}{\lambda_M} \right) - \frac{\hat{r}_v}{\sqrt{\lambda_m}} \frac{\hat{s}_u \lambda_M}{\sqrt{\lambda_m}} = 0.$$

Therefore the λ 's are negative if

$$\begin{aligned} (|\alpha_1 \delta| - \hat{r}_u) + \frac{\check{s}_v - w}{\lambda_M} &> 0 \\ (|\alpha_1 \delta| - \hat{r}_u) \frac{\check{s}_v - w}{\lambda_M} - \frac{\hat{r}_v \hat{s}_u \lambda_M}{\lambda_m} &> 0. \end{aligned} \tag{65}$$

Since we assume that $\check{s}_v > w$, these conditions are satisfied if

$$|\alpha_1 \delta| > \hat{r}_u + \frac{\hat{r}_v \hat{s}_u}{\check{s}_v - w} \cdot \frac{\lambda_M^2}{\lambda_m}, \tag{66}$$

which then guarantees exponential in t convergence to the uniform solution. This proves the theorem. \square

Remark 1 If all species diffuse, the criterion in (66) reduces to

$$|\alpha_1 \delta| > \hat{r}_u,$$

since $\mathcal{S}(u(\mathbf{x}, t), v(\mathbf{x}, t)) = 0$. This is the condition given in Ashkenazi and Othmer (1978).

Remark 2 If $\Omega = [0, h_x] \times [0, h_y] \times [0, h_z]$,

$$\alpha_i \mathcal{D} = - \left(\frac{l_1 \pi}{h_x} \right)^2 \mathcal{D}_x - \left(\frac{l_2 \pi}{h_y} \right)^2 \mathcal{D}_y - \left(\frac{l_3 \pi}{h_z} \right)^2 \mathcal{D}_z$$

for $l_1, l_2, l_3 = 0, 1, \dots$ where $\mathcal{D}_x, \mathcal{D}_y$, and \mathcal{D}_z are diffusion matrices of diffusing species in x -, y -, and z - directions. If diffusion is isotropic, we have

$$|\alpha_1 \delta| = \min \left\{ \left(\frac{\pi}{h_x} \right)^2, \left(\frac{\pi}{h_y} \right)^2, \left(\frac{\pi}{h_z} \right)^2 \right\} \min_i \mathcal{D}_{ii}.$$

If one adopts the criterion that the largest computational cell size for a stochastic simulation of a reaction–diffusion system should be small enough that the cell is uniform on time scales relevant to the coupled deterministic reaction network, one can apply the criterion in (66) to predict the minimum number of computational cells. We do this in detail for Example 2.2, as later shown in Example 4.1. There we set $W_c = 1$ since $D_v S$ is a scalar, and therefore $\lambda_m = \lambda_M = 1$ and $w = 0$ in (66).

3.2 Other types of boundary conditions

The convergence result in Theorem 3 can be extended in several ways. For example, when there are no non-diffusing species, exponential convergence to a uniform state under homogeneous Robin boundary conditions on $\partial\Omega$ was proven in Conway et al. (1978). That result can be extended to allow homogeneous Robin conditions on $\partial\Omega_1 \subset \partial\Omega$ and homogeneous Neumann data on $\partial\Omega/\partial\Omega_1$, since it is easy to show that the principal eigenvalue for the spectral problem with mixed data is strictly less than zero.

When there are non-diffusing species, the Neumann conditions in (31) are replaced by

$$\begin{aligned} \mathcal{D} \frac{\partial u(\mathbf{x}, t)}{\partial n} &= -\mathcal{B}u(\mathbf{x}, t), \quad \mathbf{x} \in \partial\Omega_1, \\ \frac{\partial u(\mathbf{x}, t)}{\partial n} &= 0, \quad \mathbf{x} \in \partial\Omega/\partial\Omega_1. \end{aligned} \tag{67}$$

We assume that \mathcal{B} is a diagonal matrix with positive diagonal elements, and thus the reactions represent degradation or sequestration on the boundary, or transfer through

the boundary. In any case, the flux of diffusing species to $\partial\Omega_1$ balances reactions of diffusing species on $\partial\Omega_1$.

We could allow a slightly more general boundary condition by replacing the term $-\mathcal{B}u(\mathbf{x}, t)$ in (67) with $-\mathcal{B}(u(\mathbf{x}, t) - u^s)$, where u^s is a solution of

$$\mathcal{R}(u^s, v^s) = 0 \quad \text{and} \quad \mathcal{S}(u^s, v^s) = 0,$$

but by translating the steady state, we can assume that $(u^s, v^s) = (0, 0)$, which we do hereafter.

We then have the following.

Theorem 4 Consider the system (31) with boundary conditions replaced by (67). Further, suppose that the system admits the uniform steady state $(u^s, v^s) = (0, 0)$.

Let α_{i1} be the principal eigenvalue of the scalar problem

$$\begin{aligned} \Delta\phi(\mathbf{x}) &= \alpha_i\phi(\mathbf{x}), & \mathbf{x} \in \Omega, \\ \frac{\partial\phi}{\partial n} &= \frac{\mathcal{B}_{ii}}{\mathcal{D}_{ii}}\phi, & \mathbf{x} \in \partial\Omega_1, \\ \frac{\partial\phi}{\partial n} &= 0, & \mathbf{x} \in \partial\Omega/\partial\Omega_1, \end{aligned} \tag{68}$$

and suppose that

- (i) $\sigma(D_v\mathcal{S}(c)) \subset LHP$ for all $c \in C_\infty$,
- (ii) $\check{s}_v > w$,
- (iii) $\delta_1 > \hat{r}_u + \frac{\hat{r}_v\hat{s}_u}{\check{s}_v - w} \cdot \frac{\lambda_M^2}{\lambda_m}$,

where $\delta_1 \equiv \min_i(|\alpha_{i1}|\mathcal{D}_{ii})$. Then $\|c(\mathbf{x}, t)\|_{L_2} \rightarrow 0$ exponentially in t .

Proof The proof follows along the same lines as that of Theorem 3. The equations are cast into integral form using a Green’s function for the Robin problem. From the analog of (51) one finds that since the principal eigenvalue $\alpha_{i1} < 0$ (Smoller 1982), $\psi(\mathbf{x}, t)$ satisfies the inequality

$$\|\psi(\mathbf{x}, t)\|_{L_2} \leq e^{-|\alpha_{i1}|\mathcal{D}_{ii}t} \|\psi(\mathbf{x}, 0)\|_{L_2}, \tag{69}$$

where α_{i1} is the largest eigenvalue of the scalar problem analogous to (51). This leads to the estimates

$$\begin{aligned}
 e^{\delta_1 t} \|u(\mathbf{x}, t)\|_{L_2} &\leq \|u_0(\mathbf{x})\|_{L_2} + \hat{r}_u \int_0^t e^{\delta_1 \tau} \|u(\mathbf{x}, \tau)\|_{L_2} d\tau \\
 &\quad + \frac{\hat{r}_v}{\sqrt{\lambda_m}} \int_0^t e^{\delta_1 \tau} \|v(\mathbf{x}, \tau)\|_{L_2, W_{c_4}} d\tau, \tag{70}
 \end{aligned}$$

$$\begin{aligned}
 e^{\delta_1 t} \|v(\mathbf{x}, t)\|_{L_2, W_{c_4}} &\leq \|v_0(\mathbf{x})\|_{L_2, W_{c_4}} + \frac{\hat{s}_u \lambda_M}{\sqrt{\lambda_m}} \int_0^t e^{\delta_1 \tau} \|u(\mathbf{x}, \tau)\|_{L_2} d\tau \\
 &\quad + \left(\delta_1 - \frac{\check{s}_v - w}{\lambda_M} \right) \int_0^t e^{\delta_1 \tau} \|v(\mathbf{x}, \tau)\|_{L_2, W_{c_4}} d\tau, \tag{71}
 \end{aligned}$$

and from these it follows that $\|c(\mathbf{x}, t)\|_{L_2} \rightarrow 0$ exponentially in t under the hypotheses in the statement of the theorem. Here W_{c_4} in (70) and (71) is analogous to W_{c_2} in (64). This is used to estimate $\mathcal{S}(u(\mathbf{x}, \tau), v(\mathbf{x}, \tau))$, rather than $\mathcal{S}(u(\mathbf{x}, \tau), v(\mathbf{x}, \tau)) - \mathcal{S}(\bar{u}(\tau), \bar{v}(\tau))$ as in Theorem 3. The functions c_3 and c_4 are defined as follows: for each $\mathbf{x} \in \Omega$ and τ where $0 \leq \tau \leq t < \infty$, there exist $c_3(\mathbf{x}, \tau)$ in $(0, u(\mathbf{x}, \tau))$ and $c_4(\mathbf{x}, \tau)$ in $(0, v(\mathbf{x}, \tau))$ satisfying

$$\mathcal{S}(u(\mathbf{x}, \tau), v(\mathbf{x}, \tau)) = D_u \mathcal{S}(c_3(\mathbf{x}, \tau))u(\mathbf{x}, \tau) + D_v \mathcal{S}(c_4(\mathbf{x}, \tau))v(\mathbf{x}, \tau).$$

The details of the proof are left to the reader. □

Other types of boundary conditions can be treated under suitable constraints on the boundary values. For example, if non-homogeneous Dirichlet conditions of the form $u(\mathbf{x}, t) = u^B$ for $\mathbf{x} \in \partial\Omega$ are imposed, then a uniform steady state exists only if there is a constant vector v^s such that

$$\mathcal{R}(u^B, v^s) = 0 \quad \text{and} \quad \mathcal{S}(u^B, v^s) = 0.$$

In other words, the boundary values must coincide with the u -component of a constant, spatially-uniform steady state of the governing reaction–diffusion equations. In this case, as in the above, the proof of convergence to a uniform solution follows that from Robin data, since the principal eigenvalue of the associated spectral problem is negative (Smoller 1982).

4 Applications

In this section we apply the results in Sects. 2 and 3 to Example 2.2 and to a simple nonlinear reaction–diffusion system with the bimolecular reaction $2A \rightleftharpoons C$. We compute \overline{CV}^* as a function of N_c and determine at what number of compartments, \overline{CV}^* stabilizes, so as to determine the number of compartments in the stochastic model. We also compute the upper bound for the computational cell size by applying Theorem

3 to obtain the minimal number of compartments, and we compare this number to the one determined by \overline{CV}^* . Erban and Chapman (2009) also analyzed a system with bimolecular reaction, $2A \rightarrow C$, but their reaction is irreversible and there is production of A from a source in their model. They consider both the compartment-based model using a master equation and the molecular-based model using stochastic differential equations. We consider a multi-compartment model to illustrate another aspect of how the criterion of Theorem 3 can be used.

4.1 Example 2.2 revisited

Consider the reactions involving species A , B , and C in Example 2.2 with corresponding deterministic rate constants given in Table 3. Species A can diffuse, species B and C do not, and species C does not affect species A and B . Let $u(x, t)$, $v(x, t)$, and $w(x, t)$ be the concentrations of species A , B , and C , respectively. Since C does not affect the dynamics of A or B , we first consider the system with only A and B . The domain is $\Omega = [0, h_x]$ and $\partial\Omega = \{0, h_x\}$. $u(x, t)$ and $v(x, t)$ satisfy (31) with

$$\begin{aligned}\mathcal{R}(u(x, t), v(x, t)) &= \begin{bmatrix} -(k_5 c_R + k_6) & k_{-5} \\ k_5 c_R & -(k_{-5} + k_7) \end{bmatrix} \begin{bmatrix} u(x, t) \\ v(x, t) \end{bmatrix}, \\ \mathcal{S}(u(x, t), v(x, t)) &= \begin{bmatrix} k_5 c_R & -(k_{-5} + k_7) \end{bmatrix} \begin{bmatrix} u(x, t) \\ v(x, t) \end{bmatrix}, \\ \mathcal{D} &= D.\end{aligned}$$

Since $D_v \mathcal{S}$ is a scalar, we may set $W_c = 1$. Then, the variables defined by Jacobian of the reaction terms are found to be

$$\hat{r}_u = k_5 c_R + k_6, \quad \hat{r}_v = k_{-5}, \quad \hat{s}_u = k_5 c_R, \quad \hat{s}_v = k_{-5} + k_7.$$

After computing the convergence criterion given in Theorem 3, we obtain the following upper bound for the computational cell size that guarantees convergence to a spatially-uniform solution in the deterministic calculation.

$$h_x < \sqrt{\frac{D\pi^2}{\left(\frac{k_5 c_R(2k_{-5} + k_7)}{k_{-5} + k_7} + k_6\right)}} \approx 8.25 \text{ } \mu\text{m}$$

We then use h_x as the compartment size for the corresponding stochastic model, apply the fact that $h_x = L_x/N_c$, and replace the deterministic reaction rate constants by stochastic reaction rate constants. As a result we obtain the following lower bound for the number of compartments,

$$N_c > \sqrt{\frac{\left(\frac{\kappa_5 R(2\kappa_{-5} + \kappa_7)}{\kappa_{-5} + \kappa_7} + \kappa_6\right) L_x^2}{D\pi^2}} \approx 33. \quad (72)$$

Comparing this lower bound for N_c to the number at which the \overline{CV}^* in Fig. 6a stabilizes, we conclude that (72) gives a good estimate for the maximum allowable compartment size. This shows that Theorem 3, applied appropriately, provides a rational basis for computing the minimum number of compartments. However, some thought is required, as the following illustrates.

Suppose that we had not recognized that C does not affect the upstream reactions. Now w becomes v_2 and the reaction matrices are

$$\begin{aligned} \mathcal{R}(u(x, t), v(x, t)) &= \begin{bmatrix} -(k_5c_R + k_6) & k_{-5} & 0 \end{bmatrix} \begin{bmatrix} u(x, t) \\ v_1(x, t) \\ v_2(x, t) \end{bmatrix}, \\ \mathcal{S}(u(x, t), v(x, t)) &= \begin{bmatrix} k_5c_R & -(k_{-5} + k_7) & 0 \\ 0 & k_7 & -k_9 \end{bmatrix} \begin{bmatrix} u(x, t) \\ v_1(x, t) \\ v_2(x, t) \end{bmatrix}, \\ \mathcal{D} &= D. \end{aligned}$$

Since $\sigma((D_v\mathcal{S}(c) + [D_v\mathcal{S}(c)]^T)/2) \subset LHP$ for all $c \in C_\infty$, we can take W_c to be the identity matrix. The sensitivities defined by the Jacobians of the reaction terms are found to be

$$\begin{aligned} \hat{r}_u &= k_5c_R + k_6, \quad \hat{r}_v = k_{-5}, \\ \hat{s}_u &= k_5c_R, \quad \check{s}_v = \frac{(k_{-5} + k_7 + k_9) - \sqrt{(k_{-5} + k_7 - k_9)^2 + k_7^2}}{2}. \end{aligned}$$

Using $\alpha_l = -\left(\frac{l\pi}{h_x}\right)^2$ and applying Theorem 3, we find that

$$h_x < \sqrt{\frac{D\pi^2}{\left(\frac{k_5c_R(k_{-5} + \check{s}_v)}{\check{s}_v} + k_6\right)}} \approx 1.41 \mu\text{m}.$$

Treating $[0, h_x]$ as one compartment, we obtain a lower bound for the number of compartments,

$$N_c > \sqrt{\frac{\left(\frac{\kappa_5 R(k_{-5} + \check{s}_v)}{\check{s}_v} + \kappa_6\right) L_x^2}{D\pi^2}} \approx 195. \tag{73}$$

Comparing (72) and (73), we see that the condition in Theorem 3 overestimates a lower bound for the number of compartments if we include the non-diffusing species which do not affect the diffusing species. The difference between (72) and (73) arises from the fact that $\kappa_{-5} + \kappa_7 \approx 2.03 \text{ min}^{-1}$ in (72), whereas $\check{s}_v \approx 0.03 \text{ min}^{-1}$ appears in (73). The difference reflects the fact that the relaxation time of the non-diffusible species (more generally, a measure of the sensitivity of the non-diffusible species) enters into the calculation of the overall relaxation time, and this is much longer when C

is included. Clearly if downstream uncoupled components relax faster than upstream components their inclusion will not have this effect.

4.2 Why network properties must be considered

Condition (i) in Theorem 3 is very important, since without it diffusive instabilities (such as the Turing instability) can arise (Othmer 1977, 1980). In fact, if a self-activating species is also immobile, instabilities of arbitrarily-short wavelengths can arise (Othmer 1969), which precludes establishing a minimum non-zero compartment size. To illustrate some of the effects of violating this condition, we investigate a simple reaction–diffusion network which does not satisfy this condition.

Example 1 Consider a model for the glycolytic reactions, which involves positive feedback and leads to a generic back-activation oscillator (Ashkenazi and Othmer 1978). The kinetic steps are



and assuming that the enzyme is far from saturation, these can be described via polynomials. To illustrate some of the problems as simply as possible, we consider a two-compartment model, since the deterministic case for that system has been analyzed in detail (Ashkenazi and Othmer 1978). We assume that Y does not diffuse and therefore the governing equations are

$$\begin{aligned} \frac{du_1(t)}{dt} &= \frac{D_x}{(L_x/2)^2} (u_2(t) - u_1(t)) + k_0 - k_1 u_1(t) v_1(t)^2 - k_2 u_1(t), \\ \frac{dv_1(t)}{dt} &= k_1 u_1(t) v_1(t)^2 + k_2 u_1(t) - k_3 v_1(t), \\ \frac{du_2(t)}{dt} &= \frac{D_x}{(L_x/2)^2} (u_1(t) - u_2(t)) + k_0 - k_1 u_2(t) v_2(t)^2 - k_2 u_2(t), \\ \frac{dv_2(t)}{dt} &= k_1 u_2(t) v_2(t)^2 + k_2 u_2(t) - k_3 v_2(t), \end{aligned}$$

where $u_k(t)$ and $v_k(t)$ are concentrations of species X and Y in the k th compartment at time t for $k = 1, 2$. The term $k_1 u_k(t) v_k(t)^2$ comes from the positive feedback step in which Y activates its production. The uniform steady state is

$$\begin{aligned} u^* = u_1^* = u_2^* &= \frac{\frac{k_0}{k_3}}{\frac{k_2}{k_3} + \left(\frac{k_0}{k_3} \sqrt{\frac{k_1}{k_3}}\right)^2}, \\ v^* = v_1^* = v_2^* &= \frac{k_0}{k_3}. \end{aligned}$$

Table 4 Deterministic and stochastic parameters in Example 1

Deterministic		Stochastic	
k_0	5.25 nM min^{-1}	κ_0	$k_0 \times (\mathcal{N}_A V_c) \approx 158.22 \text{ min}^{-1}$
k_1	$1 \text{ nM}^{-2} \text{ min}^{-1}$	κ_1	$k_1 / (\mathcal{N}_A V_c)^2 \approx 0.0011 \text{ min}^{-1}$
k_2	0.005 min^{-1}	κ_2	$k_2 = 0.005 \text{ min}^{-1}$
k_3	5 min^{-1}	κ_3	$k_3 = 5 \text{ min}^{-1}$
D_x	$1000 \mu\text{m}^2 \text{ min}^{-1}$	$\kappa_{d,x}$	$D_x / (L_x/2)^2 = 0.4 \text{ min}^{-1}$
$u_1(0)$	2 nM	$N^{(1,1)}(0)$	$2 \text{ nM} \times \frac{6.022 \times 10^{-1} \mu\text{m}^{-3}}{1 \text{ nM}} \times 50 \mu\text{m}^3 \approx 60$
$u_2(0)$	2 nM	$N^{(2,1)}(0)$	$2 \text{ nM} \times \frac{6.022 \times 10^{-1} \mu\text{m}^{-3}}{1 \text{ nM}} \times 50 \mu\text{m}^3 \approx 60$
$v_1(0)$	7 nM	$N^{(1,2)}(0)$	$7 \text{ nM} \times \frac{6.022 \times 10^{-1} \mu\text{m}^{-3}}{1 \text{ nM}} \times 50 \mu\text{m}^3 \approx 210$
$v_2(0)$	0 nM	$N^{(2,2)}(0)$	$0 \text{ nM} \times \frac{6.022 \times 10^{-1} \mu\text{m}^{-3}}{1 \text{ nM}} \times 50 \mu\text{m}^3 \approx 0$
L_x	100 μm		
L_y	1 μm		
L_z	1 μm		
V	100 μm^3		

The diffusion matrix and the Jacobian of the kinetic terms are

$$\mathcal{D} = \begin{bmatrix} \frac{D_x}{(L_x/2)^2} & 0 \\ 0 & 0 \end{bmatrix},$$

$$\mathcal{K}(u_k(t), v_k(t)) = \begin{bmatrix} -(k_2 + k_1 v_k(t)^2) & -2k_1 u_k(t) v_k(t) \\ k_2 + k_1 v_k(t)^2 & 2k_1 u_k(t) v_k(t) - k_3 \end{bmatrix}.$$

The stability of the uniform steady state to spatially uniform disturbance is determined by the eigenvalues of $\mathcal{K}(u^*, v^*)$ and the stability of the uniform steady state to non-uniform disturbance is determined by the eigenvalues of $\mathcal{K}(u^*, v^*) - 2\mathcal{D}$ (Ashkenazi and Othmer 1978).

We choose parameter values so that the uniform steady state is unstable, in which case a well-mixed system evolves to a unique periodic solution. This solution is also a solution of the coupled systems, since both cells are identical, and therefore a stochastic simulation should be expected to exhibit periodic behavior if averaged over many realizations. Using the stochastic and deterministic parameters given in Table 4, we compare the time evolution of X and Y in the two compartment model. Let $N^{(k,1)}(t)$ and $N^{(k,2)}(t)$ represent the numbers of molecules of X and Y in the k th compartment at time t , respectively.

Note that in Table 4, we multiply k_0 by the volume of each compartment (V_c) to obtain the corresponding stochastic rate constant, since the corresponding reaction is production from a source occurring in both compartments. Similarly, we divide k_1 by square of the volume of each compartment to obtain the stochastic rate constant, since the corresponding reaction, $X + 2Y \rightarrow 3Y$, is trimolecular. Diffusion coefficients in both the deterministic and the stochastic two-compartment model are scaled by the square of each compartment size due to the discretization of the Laplacian.

For the parameter values chosen, the second diagonal element of $\mathcal{K}(u^*, v^*)$, corresponding to the non-diffusing species Y , is positive, which reflects the self-activation of that species. Thus a deterministic spatially-continuous system with these kinetics does not satisfy condition (i) in Theorem 3, and thus we cannot apply the criterion to determine an appropriate discretization. Furthermore, we have

$$\begin{aligned} \text{Tr}(\mathcal{K}(u^*, v^*)) &> 0, \\ \det(\mathcal{K}(u^*, v^*)) &> 0, \\ \text{Tr}(\mathcal{K}(u^*, v^*) - 2\mathcal{D}) &> 0, \\ \det(\mathcal{K}(u^*, v^*) - 2\mathcal{D}) &> 0, \end{aligned}$$

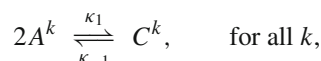
and therefore the eigenvalues of $\mathcal{K}(u^*, v^*)$ and $\mathcal{K}(u^*, v^*) - 2\mathcal{D}$ are positive and the uniform steady state is unstable to both uniform and nonuniform disturbances.

In Fig. 7 we compare the stochastic and deterministic simulations of the two-compartment model. In (a) and (b), we show the uniform periodic solution of the deterministic two-compartment model for initial values given in Table 4. One sees that when $u_k(t)$ approaches zero, $v_k(t)$ approaches to its maximum. In (c)–(f) and (g)–(j) we give two realizations of stochastic simulations of the two-compartment model. Clearly there is no hint of periodicity in the stochastic simulations, despite running for a long time compared to that needed for relaxation to the uniform periodic solution in the deterministic case, and the compartments are certainly not synchronized. As in (a) and (b), when X peaks, Y in the same compartment has a local minimum value. However, the local minimum and maximum values of the numbers of molecules for the same species vary, and the burst times of the same species in two compartments are not synchronized. One reason for the discrepancy between the deterministic and stochastic solutions is that there is also a stable non-uniform periodic solution in the deterministic system, and though the initial data lies in the domain of attraction of the uniform solution for the deterministic problem, the non-uniform solution appears to exert a significant influence on the stochastic evolution. A detailed analysis of the deterministic case is done on (Ashkenazi and Othmer 1978), where the reader can see the full complexity of the solution set for this simple system.

The complexity of the solution set is solely the result of the self-activation in the local dynamics—without that the system would not show oscillations and the condition (i) in Theorem 3 would be satisfied. Thus a full understanding of the local dynamics is needed to determine whether a sufficiently small compartment size will produce meaningful results in a stochastic simulation.

4.3 The reaction $2A \rightleftharpoons C$ in a distributed setting

Consider a multi-compartment system of N_c compartments. Let A^k and C^k denote species A and C in the k th compartment for $k = 1, \dots, N_c$. The system has the following reactions



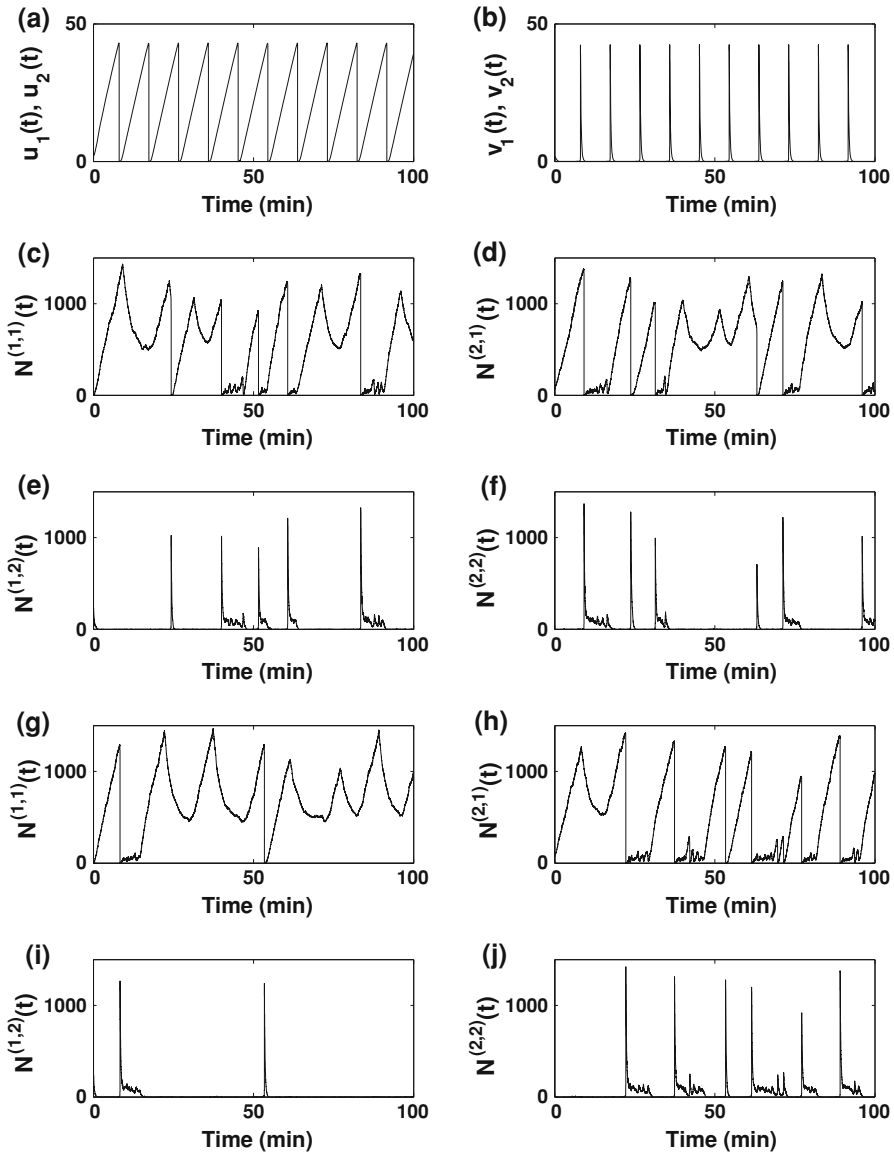
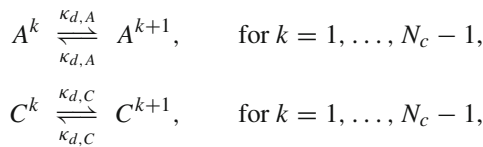


Fig. 7 Deterministic and stochastic simulation for the two-compartment model. $u_k(t)$ and $v_k(t)$ are concentrations of species X and Y in the k th compartment at time t . $N^{(k,1)}(t)$ and $N^{(k,2)}(t)$ are the numbers of molecules of species X and Y in the k th compartment at time t



wherein the parameter values are as given in Table 5.

Table 5 Deterministic and stochastic parameters in Example 4.3

Deterministic		Stochastic	
k_1	$0.05 \text{ nM}^{-1} \text{ min}^{-1}$	κ_1	$k_1/(\mathcal{N}_A V_c) \approx 1.21 \times 10^{-4} N_c \text{ min}^{-1}$
k_{-1}	0.05 min^{-1}	κ_{-1}	0.05 min^{-1}
$D_A = D_C$	$73 \mu\text{m}^2 \text{ s}^{-1}$	$\kappa_{d,A} = \kappa_{d,C}$	$D_A/(L_x/N_c)^2 \approx 9.65 \times 10^{-4} N_c^2 \text{ s}^{-1}$
	$0.73 \mu\text{m}^2 \text{ s}^{-1}$		$D_A/(L_x/N_c)^2 \approx 9.65 \times 10^{-6} N_c^2 \text{ s}^{-1}$
L_x	$275 \mu\text{m}$		
L_y	$5 \mu\text{m}$		
L_z	$0.5 \mu\text{m}$		
V	$687.5 \mu\text{m}^3$		

In Table 5, k_1 is divided by the volume of the compartment (V_c) to obtain the stochastic rate constant κ_1 . As before, we assume that $L_x \gg L_y, L_z$, and discretize L_x into N_c compartments. Since this system is closed, the components are strongly connected, the deficiency is zero, and the steady-state probability density function has a product form (Anderson et al. 2009). (Zero-deficiency of the network means that ν does not annihilate any elements in the range of \mathcal{E} , Othmer 1981.)

Let $N^{(k,1)}(t)$ and $N^{(k,2)}(t)$ represent the numbers of molecules of species A and C in the k th compartment at time t , respectively. Then, $\sum_{k=1}^{N_c} (N^{(k,1)}(t) + 2N^{(k,2)}(t))$ is conserved and equal to its initial value N_0 . The steady-state probability density function can be expressed as (Anderson et al. 2009)

$$\begin{aligned}
 P_\infty(n^{(1,1)}, n^{(1,2)}, \dots, n^{(k,1)}, n^{(k,2)}, \dots, n^{(N_c,1)}, n^{(N_c,2)}) \\
 = M \prod_{k=1}^{N_c} \frac{(w_A^k)^{n^{(k,1)}} (w_C^k)^{n^{(k,2)}}}{(n^{(k,1)})! (n^{(k,2)})!}
 \end{aligned} \tag{74}$$

where w_A^k and w_C^k for $k = 1, \dots, N_c$ are the components of the steady-state solution of the following deterministic system.

$$\begin{aligned}
 \frac{dw_A^k(t)}{dt} = & -2\kappa_1 w_A^k(t)^2 + 2\kappa_{-1} w_C^k(t) \\
 & + \kappa_{d,A} \left[(w_A^{k-1}(t) - w_A^k(t)) I_{\{k \neq 1\}} + (w_A^{k+1}(t) - w_A^k(t)) I_{\{k \neq N_c\}} \right]
 \end{aligned} \tag{75}$$

$$\begin{aligned}
 \frac{dw_C^k(t)}{dt} = & \kappa_1 w_A^k(t)^2 - \kappa_{-1} w_C^k(t) \\
 & + \kappa_{d,C} \left[(w_C^{k-1}(t) - w_C^k(t)) I_{\{k \neq 1\}} + (w_C^{k+1}(t) - w_C^k(t)) I_{\{k \neq N_c\}} \right]
 \end{aligned} \tag{76}$$

Here I is the indicator function, w_A^k and w_C^k satisfy the conservation law, $\sum_{k=1}^{N_c} (w_A^k + 2w_C^k) = 1$, and in (74), M is a normalizing constant that depends on

Table 6 CV^* and \overline{CV}^* when $N_0 = 6$

N_c	CV^*	\overline{CV}^*
1	3.7164	97.4456
2	5.3659	99.4871
3	6.5719	99.4871
4	7.5886	99.4871
5	8.4843	99.4871
6	9.2941	99.4871
7	10.0387	99.4871
8	10.7319	99.4871
9	11.3829	99.4871
10	11.9986	99.4871

N_c . The steady-state solution of (75) and (76) is spatially uniform and given by

$$w_A^k = Kd, \quad w_C^k = \frac{K}{2}d^2,$$

where

$$K = \frac{\kappa_{-1}}{2\kappa_1}, \quad d = \frac{-1 + \sqrt{1 + \frac{4}{KN_c}}}{2}.$$

Since d and K do not depend on the diffusion coefficients of species A and C , the steady-state probability density function does not depend on them neither. (Compare the earlier example of diffusion only in Sect. 1.4, which led to a multinomial distribution independent of the diffusion constant.) Using $P_\infty(\cdot)$ in (74) and parameters given in Table 5, the computed CV^* and \overline{CV}^* for $N_0 = 6$ is given in Table 6. For $N_c \geq 2$, \overline{CV}^* is approximately constant. Thus the results suggest that the number of compartments should be at least 2 in a multi-compartment stochastic model.

Next, we apply Theorem 3 to estimate an upper bound for each compartment size in the stochastic model. Let $u_1(\mathbf{x}, t)$ and $u_2(\mathbf{x}, t)$ be concentrations of species A and C on \mathbf{x} at time t , and denote $u(\mathbf{x}, t) \equiv [u_1(\mathbf{x}, t), u_2(\mathbf{x}, t)]^T$. The reaction and diffusion matrices are given as

$$\mathcal{R}(u(\mathbf{x}, t)) = \begin{bmatrix} -2k_1u_1(\mathbf{x}, t)^2 + 2k_{-1}u_2(\mathbf{x}, t) \\ k_1u_1(\mathbf{x}, t)^2 - k_{-1}u_2(\mathbf{x}, t) \end{bmatrix},$$

$$\mathcal{D} = \begin{bmatrix} D_A & 0 \\ 0 & D_C \end{bmatrix}.$$

Since we assume that both species A and C diffuse, (40) is reduced to

$$|\alpha_1\delta| > \hat{r}_u \tag{77}$$

where $\alpha_1 = -(\pi/h_x)^2$ and $\delta = D_A$. The Jacobian matrix for the kinetic terms is

$$D_u\mathcal{R}(u(\mathbf{x}, t)) = \begin{bmatrix} -4k_1u_1(\mathbf{x}, t) & 2k_{-1} \\ 2k_1u_1(\mathbf{x}, t) & -k_{-1} \end{bmatrix}.$$

Using $\|D_u \mathcal{R}(u(\mathbf{x}, t))\|_E = \sqrt{20(k_1 u_1(\mathbf{x}, t))^2 + 5(k_{-1})^2}$, we have

$$\hat{r}_u = \max_{u_1(\mathbf{x}, t) \in C_\infty} \sqrt{20(k_1 u_1(\mathbf{x}, t))^2 + 5(k_{-1})^2}.$$

For fixed volume V_c , \hat{r}_u has a maximum value when all molecules of species A are located in one compartment. Therefore, we approximate the maximum value of $u_1(\mathbf{x}, t)$ by $N_0/(\mathcal{N}_A V_c) = N_0/(\mathcal{N}_A h_x L_y L_z)$ where $N_0 = 6$ is the conserved number of molecules. Using the upper bound of \hat{r}_u , we find the following is a sufficient condition to satisfy (77):

$$\frac{D_A \pi^2}{h_x^2} > \sqrt{20 \left(\frac{k_1 N_0}{\mathcal{N}_A h_x L_y L_z} \right)^2 + 5(k_{-1})^2}.$$

It follows that h_x must be chosen so that

$$5(k_{-1})^2 h_x^4 + 20 \left(\frac{k_1 N_0}{\mathcal{N}_A L_y L_z} \right)^2 h_x^2 - D_A^2 \pi^4 < 0,$$

which leads to the following condition on h_x .

$$\begin{aligned} h_x < 621.79 \mu\text{m} & \quad \text{when } D_A = D_C = 73 \mu\text{m}^2 \text{ s}^{-1} \\ h_x < 61.93 \mu\text{m} & \quad \text{when } D_A = D_C = 0.73 \mu\text{m}^2 \text{ s}^{-1} \end{aligned}$$

Said otherwise, a single compartment suffices if $L_x < 622 \mu\text{m}$, which compares well with the result in Table 6, which depends on L_x through the rate constants, and are computed for $L_x = 275 \mu\text{m}$. However when $D_A = D_C = 0.73 \mu\text{m}^2 \text{ s}^{-1}$, the upper bound for the compartment size gives $N_c > 4$ which overestimates the number of compartments needed according to Table 6. This is not surprising, since the theoretical estimate is based on the relaxation rate to the uniform solution, and for the second case, in which diffusion is 100-fold slower, the approach to the uniform solution takes much longer and at least four compartments are needed to capture the temporal evolution. Once again, care is needed in applying the criterion.

Finally, we compare our result to the one using Bernstein’s criterion for the compartment size introduced in Sect. 1.4. Consider the case when $D_A = D_C = 73 \mu\text{m}^2 \text{ s}^{-1}$. To compute the reaction timescale, we use the reaction with the largest propensity, since Bernstein sets the reaction time as the reciprocal of the propensity. Denote A_{tot} and C_{tot} as the total numbers of molecules of species A and C , respectively. Using $A_{tot} + 2C_{tot} = 6$, we compute

$$\begin{aligned} \kappa_1 \frac{A_{tot}}{N_c} \left(\frac{A_{tot}}{N_c} - 1 \right) &\approx (1.21 \times 10^{-4} N_c) \frac{6}{N_c} \left(\frac{6}{N_c} - 1 \right) \approx 0.0044 \left(\frac{1}{N_c} - \frac{1}{6} \right), \\ \kappa_{-1} \frac{C_{tot}}{N_c} &\approx 0.05 \frac{3}{N_c} = 0.15 \left(\frac{1}{N_c} \right). \end{aligned}$$

Therefore, the propensity of the first-order reaction, $C \xrightarrow{\kappa-1} 2A$, is the largest. Based on the conservation law, we assume that the total number of molecules of species C is 3. The reaction time-scale is given as

$$\begin{aligned} \tau_r &\approx \frac{1}{0.05 \text{ min}^{-1} \times \frac{3}{N_c}} \\ &= \frac{1833.33}{h_x} \text{ min.} \end{aligned}$$

The diffusion time-scale is computed using the diffusion coefficient of species A .

$$\frac{h_x^2}{2D_A} \approx \frac{h_x^2 \mu\text{m}^2}{2 \times 4380 \mu\text{m}^2 \text{ min}^{-1}} = \frac{h_x^2}{8760} \text{ min}$$

Since the diffusion time-scale should be much faster than the reaction time-scale, we have

$$\begin{aligned} h_x &\ll (8760 \times 1833.33)^{1/3} \mu\text{m} \\ &\approx 252.30 \mu\text{m.} \end{aligned}$$

Similarly, when $D_A = D_C = 0.73 \mu\text{m}^2 \text{ s}^{-1}$, Bernstein's criterion yields $h_x \ll 54.36 \mu\text{m}$. Therefore, in both cases the upper bound for the compartment size using our criterion is larger than the one obtained from Bernstein's criterion.

5 Discussion

A number of criteria have been suggested for determining the appropriate compartment size for a stochastic treatment of a reaction–diffusion system, but none incorporates measures of the noise in the process, nor do they account for the properties of the integrated reaction network. We incorporate those factors here and develop a criterion for choosing the compartment size.

We first define a suitably scaled, generalized coefficient of variation as an appropriate measure for the noise level of the system, and use this scaled measure, \overline{CV}^* , to determine a lower bound for the number of compartments based on simulations of a particular network. Using results from [Gadgil et al. \(2005\)](#), we compute the asymptotic mean M_∞ and variance V_∞ , and we express \overline{CV}^* in terms of M_∞ for specific cases of a linear reaction–diffusion network. We show the convergence of each component in \overline{M}_∞ multiplied by some constant to the corresponding concentration in the continuum model for an open linear network with production from a source, and for a closed linear network with no inputs and no degradation (in case there is exactly one zero eigenvalue in the reaction matrix). We then show computationally that the scaled measure converges for a sufficiently large number of compartments in a linear network, which suggests the minimum value for the number of compartments.

However, it is not easy in general to compute the minimum value of the number of compartments using \overline{CV}^* analytically, and therefore we developed an alternate criterion based on convergence of solutions of the deterministic reaction–diffusion system to a spatially-uniform solution. In previous work, conditions for this convergence were derived for closed systems in which all species diffuse (Othmer 1977; Ashkenazi and Othmer 1978), and we extend this here to allow both non-diffusing species and degradation of diffusing species on the boundary of the domain. Of course the system size plays a role in the convergence, and this leads to an estimate of the minimal compartment size by requiring that the dynamics converge to a spatially-uniform solution for that compartment size. The exponential convergence condition involved is applicable to the nonlinear reaction–diffusion networks for which it is known that solutions are bounded in L_2 , which include the majority of biologically-realistic systems. We apply the results to a simple dimerization reaction that illustrates some of the issues that must be considered in general.

Acknowledgments This work was supported by NIH grant GM29123, NSF grant DMS-0817529 and the University of Minnesota Supercomputing Institute. We would like to thank the reviewers for their helpful suggestions for this paper.

Appendices

A Proof of the mean first passage time for N walkers

Consider the first passage time for annihilation beginning on a spherical surface of radius $r \in (a, b)$. Define $P_i(R, t|r, s)$ as the probability that the i th particle starts on a spherical surface of radius r at time s and ends on a spherical surface of radius R at time t . Define $\tau_i(r) \equiv \tau_i$ as the first passage time for annihilation of the i th particle when it begins on the spherical surface of radius r and $\tau(r_1, r_2, \dots, r_N) \equiv \tau$ as the first passage time for the first annihilation of the one particle among the N particles, where for $i = 1, 2, \dots, N$, the i th particle begins on a spherical surface of radius r_i . Define a cumulative distribution function for τ_i as

$$\begin{aligned} F_i(r, t) &\equiv P(\tau_i \leq t), \\ &= \int_0^t -\frac{d}{ds} \int_a^b P_i(R, s|r, 0) dR ds = 1 - \int_a^b P_i(R, t|r, 0) dR, \end{aligned}$$

and define the operator Δ_r as

$$\begin{aligned} \Delta_r f(r, t) &= \frac{1}{r^2} \frac{\partial}{\partial r} \left(r^2 \frac{\partial f(r, t)}{\partial r} \right), \\ \Delta_r g(r) &= \frac{1}{r^2} \frac{d}{dr} \left(r^2 \frac{dg(r)}{dr} \right). \end{aligned}$$

Then, for $i = 1, \dots, N$, $F_i(r, t)$ is a solution of

$$\begin{aligned} \frac{\partial}{\partial t} F_i(r, t) &= D \Delta_r F_i(r, t), \\ F_i(r, t)|_{\{r=a\}} &= 1, \\ \frac{\partial}{\partial r} F_i(r, t)|_{\{r=b\}} &= 0. \end{aligned} \tag{78}$$

Let $F(r_1, r_2, \dots, r_N, t)$ be the cumulative distribution function of τ when N particles are initially located on spherical surface of radius $r_i \in (a, b)$ for $i = 1, \dots, N$. Then

$$\begin{aligned} P(\tau > t) &= 1 - F(r_1, r_2, \dots, r_N, t) \\ &= \prod_{i=1}^N (1 - F_i(r_i, t)). \end{aligned}$$

The mean first passage time of N particles is defined as $\lambda \equiv E[\tau]$, and is computed in terms of the cumulative distribution function of the first passage time of each particle.

$$\begin{aligned} \lambda(r_1, r_2, \dots, r_N) &= \int_0^\infty P(\tau > s) ds \\ &= \int_0^\infty \prod_{i=1}^N (1 - F_i(r_i, s)) ds \end{aligned}$$

Using (78), λ satisfies

$$\begin{aligned} D \Delta_{r_i} \lambda(r_1, r_2, \dots, r_N) &= - \int_0^\infty (D \Delta_{r_i} F_i(r_i, s)) \prod_{j \neq i} (1 - F_j(r_j, s)) ds \\ &= - \int_0^\infty \frac{\partial F_i(r_i, s)}{\partial s} \prod_{j \neq i} (1 - F_j(r_j, s)) ds. \end{aligned} \tag{79}$$

Summing (79) over $i = 1, \dots, N$, we find that

$$\begin{aligned} \sum_{i=1}^N D \Delta_{r_i} \lambda(r_1, r_2, \dots, r_N) &= \int_0^\infty \frac{\partial \prod_{i=1}^N (1 - F_i(r_i, s))}{\partial s} ds \\ &= \lim_{t \rightarrow \infty} \prod_{i=1}^N (1 - F_i(r_i, t)) - \prod_{i=1}^N (1 - F_i(r_i, 0)) \\ &= -1. \end{aligned}$$

λ also satisfies the boundary conditions

$$\begin{aligned} \lambda(r_1, r_2, \dots, r_N)|_{\{r_i=a\}} &= 0, \\ \frac{\partial}{\partial r_i} \lambda(r_1, r_2, \dots, r_N)|_{\{r_i=b\}} &= 0, \end{aligned}$$

for each $i = 1, \dots, N$. Substituting $r_0 = a, r_1 = b$, and $\tau = \tau_i$ in (7) in Sect. 1.4, for each $i = 1, \dots, N, E[\tau_i(r)]$ satisfies

$$\begin{aligned} D\Delta_r E[\tau_i(r)] &= -1, \\ E[\tau_i(a)] &= 0, \\ E[\tau_i'(b)] &= 0. \end{aligned}$$

Thus, λ is given as

$$\lambda(r_1, r_2, \dots, r_N) = \frac{1}{N} \sum_{i=1}^N E[\tau_i(r_i)] \prod_{j \neq i} (1 - \delta(r_j - a)).$$

B Spectral representation of the reaction–diffusion matrix Ω

In this section, we give the explicit form of the eigenvalues and eigenvectors of the reaction–diffusion matrix Ω , which are used in Sect. 2.1. Consider the first-order chemical reaction–diffusion network in the 3-dimensional parallelepiped with dimension $L_x \times L_y \times L_z$. Δ_n is a finite difference approximation of the 1-dimensional Laplacian with homogeneous Neumann conditions. Then, modulo terms in h_x^{-2} , the entries of Δ_n are

$$(\Delta_n)_{ij} = \begin{cases} -1 & \text{when } i = j = 1 \text{ or } i = j = n, \\ -2 & \text{when } i = j, i \neq 1, \text{ and } i \neq n, \\ 1 & \text{when } |i - j| = 1, \\ 0 & \text{otherwise.} \end{cases}$$

Let $\mathcal{D}_x, \mathcal{D}_y$, and \mathcal{D}_z be diagonal matrices whose diagonal elements are the scaled diffusion coefficients for diffusion along the x, y , and z directions, respectively. The reaction–diffusion matrix Ω is expressed as

$$\Omega = \bar{\Delta}_z \otimes \mathcal{D}_z + \bar{\Delta}_y \otimes \mathcal{D}_y + \bar{\Delta}_x \otimes \mathcal{D}_x + (I_{N_z} \otimes I_{N_y} \otimes I_{N_x}) \otimes \mathcal{K}$$

where

$$\begin{aligned} \overline{\Delta}_x &\equiv I_{N_z} \otimes I_{N_y} \otimes \Delta_{N_x}, \\ \overline{\Delta}_y &\equiv I_{N_z} \otimes \Delta_{N_y} \otimes I_{N_x}, \\ \overline{\Delta}_z &\equiv \Delta_{N_z} \otimes I_{N_y} \otimes I_{N_x}. \end{aligned}$$

Define an index for compartments as $l = (l_1, l_2, l_3)$. Let $\mathbf{l} = (l, \mu)$ for $l_1, l_2, l_3 = 1, \dots, N_x, N_y, N_z$, respectively, and for $\mu = 1, \dots, s$. Denote by α_{l_1} , α_{l_2} and α_{l_3} the eigenvalues of Δ_{N_x} , Δ_{N_y} , and Δ_{N_z} given as

$$\begin{aligned} \alpha_{l_1} &= -4 \sin^2 \left(\frac{\pi l_1}{2N_x} \right) (1 - \delta_{l_1 N_x}), \\ \alpha_{l_2} &= -4 \sin^2 \left(\frac{\pi l_2}{2N_y} \right) (1 - \delta_{l_2 N_y}), \\ \alpha_{l_3} &= -4 \sin^2 \left(\frac{\pi l_3}{2N_z} \right) (1 - \delta_{l_3 N_z}), \end{aligned}$$

where δ_{ij} is the Kronecker delta. Denote ϕ_{l_1} , ϕ_{l_2} , and ϕ_{l_3} as the corresponding eigenvectors of Δ_{N_x} , Δ_{N_y} , and Δ_{N_z} with elements given as

$$\begin{aligned} (\phi_{l_1})_{l'_1} &= \sqrt{\frac{2}{N_x}} \cos \left(\frac{\pi l_1 (l'_1 - 1/2)}{N_x} \right) (1 - \delta_{l_1 N_x}) + \sqrt{\frac{1}{N_x}} \delta_{l_1 N_x}, \\ (\phi_{l_2})_{l'_2} &= \sqrt{\frac{2}{N_y}} \cos \left(\frac{\pi l_2 (l'_2 - 1/2)}{N_y} \right) (1 - \delta_{l_2 N_y}) + \sqrt{\frac{1}{N_y}} \delta_{l_2 N_y}, \\ (\phi_{l_3})_{l'_3} &= \sqrt{\frac{2}{N_z}} \cos \left(\frac{\pi l_3 (l'_3 - 1/2)}{N_z} \right) (1 - \delta_{l_3 N_z}) + \sqrt{\frac{1}{N_z}} \delta_{l_3 N_z}, \end{aligned} \tag{80}$$

for $l'_1, l'_2, l'_3 = 1, \dots, N_x, N_y, N_z$, respectively. Then, the eigenvalue of $\overline{\Delta}_x + \overline{\Delta}_y + \overline{\Delta}_z$ is expressed as $\alpha_l \equiv \alpha_{l_1} + \alpha_{l_2} + \alpha_{l_3}$ and the corresponding eigenvector and adjoint eigenvector are given as $\phi_l \equiv \phi_{l_3} \otimes \phi_{l_2} \otimes \phi_{l_1}$ and ϕ_l^* .

Define the complete diffusion matrix as $\alpha_l \mathcal{D} \equiv \alpha_{l_1} \mathcal{D}_x + \alpha_{l_2} \mathcal{D}_y + \alpha_{l_3} \mathcal{D}_z$, and then the eigenvalue λ_1 of Ω is a solution of

$$|\mathcal{K} + \alpha_l \mathcal{D} - \lambda_1 I_s| = 0.$$

Let φ_1 and φ_1^* be the eigenvector and the adjoint eigenvector of $\mathcal{K} + \alpha_l \mathcal{D}$ corresponding to the eigenvalue λ_1 . Then, $\phi_l \otimes \varphi_1$ is an eigenvector of Ω corresponding to λ_1 , and the projection P_1 associated with λ_1 is

$$P_1 = (\phi_l * \overline{\phi_l^*}) \otimes (\varphi_1 * \overline{\varphi_1^*}) \tag{81}$$

where $*$ is the dyad product and $\overline{\phi_l^*}$ is the complex conjugate of ϕ_l^* .

In Example 2.2, $N_y = N_z = 1$ and we set $N_x = N_c$. The eigenvalues of Δ are

$$\alpha_l = \begin{cases} -4 \sin^2 \left(\frac{\pi l}{2N_c} \right), & l \neq N_c, \\ 0, & l = N_c, \end{cases} \tag{82}$$

and the corresponding eigenvectors are

$$\phi_l = \begin{cases} \sqrt{\frac{2}{N_c}} \left(\cos \left(\frac{\pi l}{2N_c} \right), \dots, \cos \left(\frac{(2l'-1)\pi l}{2N_c} \right), \dots, \cos \left(\frac{(2N_c-1)\pi l}{2N_c} \right) \right)^T, & l \neq N_c, \\ \sqrt{\frac{1}{N_c}} (1, 1, \dots, 1)^T, & l = N_c. \end{cases} \tag{83}$$

In Example 2.2,

$$\mathcal{K} + \alpha_l \mathcal{D} = -\frac{\kappa_5 \kappa_7 R}{\kappa_{-5} + \kappa_7} - \kappa_6 + \alpha_l \frac{D}{(L_x/N_c)^2},$$

and the eigenvalue of $\mathcal{K} + \alpha_l \mathcal{D}$ is

$$\lambda_1 = -\frac{\kappa_5 \kappa_7 R}{\kappa_{-5} + \kappa_7} - \kappa_6 + \alpha_l \frac{D}{(L_x/N_c)^2}.$$

The corresponding eigenvector and adjoint eigenvector of $\mathcal{K} + \alpha_l \mathcal{D}$ are $\phi_1 = 1, \phi_1^* = 1$. In Example 2.2, we only need the first column of P_1 to compute the first and the second moments, since we assume that production from a source only occurs in the first compartment. Thus we have

$$P_1 \mathbf{k}^s = \kappa_8 P_1^{(1)}$$

where $P_1^{(1)}$ represents the first column of P_1 . From (81), we obtain the first column of the projection as

$$\begin{aligned} P_1^{(1)} &= (\phi_l * \overline{\phi_l^*})^{(1)} \otimes (\phi_1 * \overline{\phi_1^*})^{(1)} \\ &= (\phi_l * \overline{\phi_l^*})^{(1)}. \end{aligned}$$

Using $\phi_l = \overline{\phi_l^*}$, we compute

$$P_1^{(1)} = \begin{cases} \frac{2}{N_c} \cos \left(\frac{\pi l}{2N_c} \right) \left(\cos \left(\frac{\pi l}{2N_c} \right), \dots, \cos \left(\frac{(2l'-1)\pi l}{2N_c} \right), \dots, \cos \left(\frac{(2N_c-1)\pi l}{2N_c} \right) \right)^T, & l \neq N_c, \\ \frac{1}{N_c} (1, 1, \dots, 1)^T, & l = N_c. \end{cases}$$

C Proof of Proposition 1

In this section, we prove Proposition 1 in Sect. 2.1. Using (10) in Sect. 2.1, we have

$$\begin{aligned} \frac{d(M(t)M(t)^T)}{dt} &= \frac{dM(t)}{dt}M(t)^T + M(t)\frac{dM(t)^T}{dt} \\ &= (\Omega M(t) + \mathbf{k}^s)M(t)^T + M(t)(\Omega M(t) + \mathbf{k}^s)^T \\ &= \Omega M(t)M(t)^T + [\Omega M(t)M(t)^T]^T + C(t) \\ &\quad + C(t)^T - W(t) - W(t)^T. \end{aligned} \tag{84}$$

where $C(t) = W(t) + \mathbf{k}^s M(t)^T$ and $W(t)$ is a block-diagonal matrix with elements defined as

$$[W(t)]_{i(\eta),i(\zeta)} = \begin{cases} K_{ij}^{cat}[M(t)]_{i(\zeta)}, & \text{if } k = q, \\ 0, & \text{otherwise.} \end{cases}$$

Recall that $M_d(t) = \text{diag}[M(t)]$. Using (84), (10), and

$$\text{Cov}(t) = V(t) - M(t)M(t)^T + M_d(t),$$

we have

$$\begin{aligned} \frac{d\text{Cov}(t)}{dt} &= \frac{dV(t)}{dt} - \frac{d(M(t)M(t)^T)}{dt} + \frac{dM_d(t)}{dt} \\ &= \left\{ \Omega V(t) + [\Omega V(t)]^T + C(t) + C(t)^T \right\} \\ &\quad - \left\{ \Omega M(t)M(t)^T + [\Omega M(t)M(t)^T]^T + C(t) + C(t)^T - W(t) - W(t)^T \right\} \\ &\quad + \frac{dM_d(t)}{dt} \\ &= \Omega \text{Cov}(t) + [\Omega \text{Cov}(t)]^T - \Omega M_d(t) - (\Omega M_d(t))^T + W(t) + W(t)^T \\ &\quad + \frac{dM_d(t)}{dt}. \end{aligned} \tag{85}$$

From this we obtain

$$\begin{aligned} \frac{d(\text{Cov}(t) - M_d(t))}{dt} &= \Omega(\text{Cov}(t) - M_d(t)) + [\Omega(\text{Cov}(t) - M_d(t))]^T \\ &\quad + W(t) + W(t)^T. \end{aligned} \tag{86}$$

Define $\text{col}(A)$ as a vector by concatenating all columns of A in order, i.e. $\text{col}(A) = [(A^{(1)})^T, (A^{(2)})^T, \dots, (A^{(m)})^T]^T$ where $A^{(l)}$ is the l th column of A . Define $v(t) = \text{col}(\text{Cov}(t) - M_d(t))$, $\mathcal{V} = \Omega \otimes I_{s_{N_c}} + I_{s_{N_c}} \otimes \Omega$, and $\gamma(t) = \text{col}(W(t) + W(t)^T)$.

We change matrices in (86) to column vectors, and obtain (Gadgil et al. 2005),

$$\frac{dv(t)}{dt} = \mathcal{V}v(t) + \gamma(t). \tag{87}$$

The solution of (87) is

$$\begin{aligned} v(t) &= e^{\mathcal{V}t}v(0) + \int_0^t e^{\mathcal{V}(t-\tau)}\gamma(\tau) d\tau \\ &= \sum_{\mathbf{l}, \mathbf{m}} e^{(\lambda_{\mathbf{l}}+\lambda_{\mathbf{m}})t} P_{\mathbf{l}} \otimes P_{\mathbf{m}}v(0) \\ &\quad + \sum_{\mathbf{l}, \mathbf{m}} \int_0^t e^{(\lambda_{\mathbf{l}}+\lambda_{\mathbf{m}})(t-\tau)} \left(P_{\mathbf{l}}K^{cat} \otimes P_{\mathbf{m}} + P_{\mathbf{l}} \otimes P_{\mathbf{m}}K^{cat} \right) col(M_d(\tau)) d\tau. \end{aligned} \tag{88}$$

Reverting to the matrix form in (88), we find that

$$\begin{aligned} &(Cov(t) - M_d(t)) \\ &= \sum_{\mathbf{l}, \mathbf{m}} e^{(\lambda_{\mathbf{l}}+\lambda_{\mathbf{m}})t} P_{\mathbf{m}}(Cov(0) - M_d(0)) P_{\mathbf{l}}^T \\ &\quad + \sum_{\mathbf{l}, \mathbf{m}} \int_0^t e^{(\lambda_{\mathbf{l}}+\lambda_{\mathbf{m}})(t-\tau)} \left(P_{\mathbf{m}}M_d(\tau)(P_{\mathbf{l}}K^{cat})^T + P_{\mathbf{m}}K^{cat}M_d(\tau)P_{\mathbf{l}}^T \right) d\tau. \end{aligned} \tag{89}$$

Next we compute $M_d(t)$. Following Gadgil et al. (2005), the evolution of the mean matrix is expressed as

$$M(t) = \sum_{\mathbf{n}} e^{\lambda_{\mathbf{n}}t} P_{\mathbf{n}}M(0) - \sum_{\mathbf{n}} \frac{1 - e^{\lambda_{\mathbf{n}}t}}{\lambda_{\mathbf{n}}} P_{\mathbf{n}}\mathbf{k}^s. \tag{90}$$

Define $L(t)$ and S as $sN_c \times sN_c$ matrices satisfying

$$\begin{aligned} L(t) &= [M(t)|M(t)|\dots|M(t)]^T, \\ S &= [\mathbf{k}^s|\mathbf{k}^s|\dots|\mathbf{k}^s]. \end{aligned}$$

Define $diag[b_1, b_2, \dots, b_n]$ as an $n \times n$ diagonal matrix with the i th diagonal element equal to b_i . Define diagonalization of matrices and of vectors as

$$\begin{aligned} diag[A] &\equiv diag[a_{11}, a_{22}, \dots, a_{nn}], \\ diag[X] &\equiv diag[x_1, x_2, \dots, x_n], \end{aligned}$$

where A is an $n \times n$ matrix with each element a_{ij} and X is an n -dimensional vector with each element x_i . Diagonalizing both sides in (90), we have

$$M_d(t) = \sum_{\mathbf{n}} e^{\lambda_{\mathbf{n}}t} \text{diag}[P_{\mathbf{n}}L(0)^T] - \sum_{\mathbf{n}} \frac{1 - e^{\lambda_{\mathbf{n}}t}}{\lambda_{\mathbf{n}}} \text{diag}[P_{\mathbf{n}}S]. \tag{91}$$

In (89), we first calculate $\int_0^t e^{(\lambda_1 + \lambda_m)(t-\tau)} P_{\mathbf{m}} M_d(\tau) (P_1 K^{cat})^T d\tau$ using (91), and find that

$$\begin{aligned} & \int_0^t e^{(\lambda_1 + \lambda_m)(t-\tau)} P_{\mathbf{m}} M_d(\tau) (P_1 K^{cat})^T d\tau \\ &= \int_0^t e^{(\lambda_1 + \lambda_m)(t-\tau)} P_{\mathbf{m}} \left\{ \sum_{\mathbf{n}} e^{\lambda_{\mathbf{n}}\tau} \text{diag}[P_{\mathbf{n}}L(0)^T] \right. \\ & \quad \left. - \sum_{\mathbf{n}} \frac{1 - e^{\lambda_{\mathbf{n}}\tau}}{\lambda_{\mathbf{n}}} \text{diag}[P_{\mathbf{n}}S] \right\} (P_1 K^{cat})^T d\tau \\ &= \sum_{\lambda_{\mathbf{n}} \neq \lambda_1 + \lambda_m} \frac{e^{\lambda_{\mathbf{n}}t} - e^{(\lambda_1 + \lambda_m)t}}{-(\lambda_1 + \lambda_m) + \lambda_{\mathbf{n}}} P_{\mathbf{m}} \text{diag}[P_{\mathbf{n}}L(0)^T] (P_1 K^{cat})^T \\ & \quad + \sum_{\lambda_{\mathbf{n}} = \lambda_1 + \lambda_m} (t e^{\lambda_{\mathbf{n}}t}) P_{\mathbf{m}} \text{diag}[P_{\mathbf{n}}L(0)^T] (P_1 K^{cat})^T \\ & \quad - \sum_{\lambda_{\mathbf{n}} \neq \lambda_1 + \lambda_m} \frac{1}{\lambda_{\mathbf{n}}} \left[\frac{1 - e^{(\lambda_1 + \lambda_m)t}}{-(\lambda_1 + \lambda_m)} - \frac{e^{\lambda_{\mathbf{n}}t} - e^{(\lambda_1 + \lambda_m)t}}{-(\lambda_1 + \lambda_m) + \lambda_{\mathbf{n}}} \right] P_{\mathbf{m}} \text{diag}[P_{\mathbf{n}}S] (P_1 K^{cat})^T \\ & \quad - \sum_{\lambda_{\mathbf{n}} = \lambda_1 + \lambda_m} \frac{1}{\lambda_{\mathbf{n}}} \left[\frac{e^{\lambda_{\mathbf{n}}t} - 1}{\lambda_{\mathbf{n}}} - t e^{\lambda_{\mathbf{n}}t} \right] P_{\mathbf{m}} \text{diag}[P_{\mathbf{n}}S] (P_1 K^{cat})^T, \tag{92} \end{aligned}$$

and $\int_0^t e^{(\lambda_1 + \lambda_m)(t-\tau)} P_{\mathbf{m}} K^{cat} M_d(\tau) P_1^T d\tau$ as

$$\begin{aligned} & \int_0^t e^{(\lambda_1 + \lambda_m)(t-\tau)} P_{\mathbf{m}} K^{cat} M_d(\tau) P_1^T d\tau \\ &= \sum_{\lambda_{\mathbf{n}} \neq \lambda_1 + \lambda_m} \frac{e^{\lambda_{\mathbf{n}}t} - e^{(\lambda_1 + \lambda_m)t}}{-(\lambda_1 + \lambda_m) + \lambda_{\mathbf{n}}} P_{\mathbf{m}} K^{cat} \text{diag}[P_{\mathbf{n}}L(0)^T] P_1^T \\ & \quad + \sum_{\lambda_{\mathbf{n}} = \lambda_1 + \lambda_m} (t e^{\lambda_{\mathbf{n}}t}) P_{\mathbf{m}} K^{cat} \text{diag}[P_{\mathbf{n}}L(0)^T] P_1^T \end{aligned}$$

$$\begin{aligned}
 & - \sum_{\lambda_n \neq \lambda_l + \lambda_m} \frac{1}{\lambda_n} \left[\frac{1 - e^{(\lambda_l + \lambda_m)t}}{-(\lambda_l + \lambda_m)} - \frac{e^{\lambda_n t} - e^{(\lambda_l + \lambda_m)t}}{-(\lambda_l + \lambda_m) + \lambda_n} \right] P_m K^{cat} \text{diag}[P_n S] P_1^T \\
 & - \sum_{\lambda_n = \lambda_l + \lambda_m} \frac{1}{\lambda_n} \left[\frac{e^{\lambda_n t} - 1}{\lambda_n} - t e^{\lambda_n t} \right] P_m K^{cat} \text{diag}[P_n S] P_1^T. \tag{93}
 \end{aligned}$$

Now we prove the second and the third cases in Proposition 1, using the results of the previous computations. First, consider the open system with $\sigma(\Omega) \subset LHP$. Using (89), (92), and (93) and letting $t \rightarrow \infty$, we get

$$\begin{aligned}
 Cov_\infty - M_{d,\infty} &= \sum_{l,m} \sum_{\lambda_n \neq \lambda_l + \lambda_m} \frac{P_m \left\{ \text{diag}[P_n S](K^{cat})^T + K^{cat} \text{diag}[P_n S] \right\} P_1^T}{\lambda_n(\lambda_l + \lambda_m)} \\
 &+ \sum_{l,m} \sum_{\lambda_n = \lambda_l + \lambda_m} \frac{P_m \left\{ \text{diag}[P_n S](K^{cat})^T + K^{cat} \text{diag}[P_n S] \right\} P_1^T}{\lambda_n^2} \\
 &= \sum_{l,m,n} \frac{P_m \left\{ \text{diag}[P_n S](K^{cat})^T + K^{cat} \text{diag}[P_n S] \right\} P_1^T}{\lambda_n(\lambda_l + \lambda_m)}. \tag{94}
 \end{aligned}$$

From (94), either if there is no production from a source or if there is no catalytic inputs, which is $K^S = 0$ ($S = 0$) or $K^{cat} = 0$, we have $Cov_\infty = M_{d,\infty}$.

Second, consider a closed system for which $\sigma(\Omega)$ is in the closed left-half plane. We only consider the case in which there is exactly one zero eigenvalue of Ω and no inputs. Then (89) becomes

$$(Cov(t) - M_d(t)) = \sum_{l,m} e^{(\lambda_l + \lambda_m)t} P_m (Cov(0) - M_d(0)) P_1^T. \tag{95}$$

Letting $t \rightarrow \infty$ in (95) and using the fact that there is exactly one zero eigenvalue of Ω and that the remaining eigenvalues are negative, we get

$$Cov_\infty - M_{d,\infty} = P_s (Cov(0) - M_d(0)) P_s^T$$

where P_s is the projection corresponding to the zero eigenvalue. Assuming that initial values are deterministic, $Cov(0) = 0$. As a result, Cov_∞ can be expressed in terms of $M_{d,\infty}$, $M_d(0)$, and P_s as follows.

$$Cov_\infty = M_{d,\infty} - P_s M_d(0) P_s^T$$

D Proof of Theorem 1

To prove the theorem, we first introduce and prove a lemma. The proof of the theorem is given at the end of this appendix. In the following lemma we show that as

$N_c \rightarrow \infty$, each component of $X_\infty/(\mathcal{N}_A V_c)$ converges to the corresponding value of the steady-state concentration in the continuum deterministic reaction–diffusion system.

Let $u_\infty(\mathbf{x})$ and $v_\infty(\mathbf{x})$ be the steady-state solution of the corresponding continuum model. $u_\infty(\mathbf{x})$ and $v_\infty(\mathbf{x})$ represent concentration vectors for diffusing and non-diffusing species, respectively, which satisfy

$$\begin{aligned} \tilde{\mathcal{D}}\Delta u_\infty(\mathbf{x}) + \mathcal{R}u_\infty(\mathbf{x}) + \mathcal{S}v_\infty(\mathbf{x}) + \delta(\mathbf{x}, 0)\tilde{k}^s &= 0, \\ \mathcal{T}u_\infty(\mathbf{x}) + \mathcal{W}v_\infty(\mathbf{x}) &= 0. \end{aligned} \tag{96}$$

In (96), each component of \tilde{k}^s is defined as

$$\tilde{k}_i^s \equiv \mathbf{k}_{\mathbf{i}(1,i)}^s \frac{L_x}{\mathcal{N}_A \mathbf{V}},$$

where \mathbf{V} is the volume of the system. Letting $[\mathbf{k}^s]^{(1)} \equiv [\mathbf{k}_{\mathbf{i}(1,i)}^s, \dots, \mathbf{k}_{\mathbf{i}(1,m)}^s]^T$, \tilde{k}^s is written as

$$\tilde{k}^s = \frac{L_x}{\mathcal{N}_A \mathbf{V}} [\mathbf{k}^s]^{(1)}. \tag{97}$$

In (96), $\tilde{\mathcal{D}}$ is a diagonal matrix with diagonal elements which are the diffusion coefficients in the continuum description, while diagonal elements of \mathcal{D} in (18) are the corresponding diffusion coefficients in the discretized system. The two are related by

$$\mathcal{D} = \frac{\tilde{\mathcal{D}}}{(L_x/N_c)^2}.$$

Lemma 1 *Let X_∞ be the solution of (18) and $u_\infty(\mathbf{x})$ be the solution of (96). Define $U_\infty(\mathbf{x})$ as a vector with each element satisfying*

$$(U_\infty(\mathbf{x}))_i \equiv \sum_{k=1}^{N_c} \frac{1}{\mathcal{N}_A V_c} [X_\infty \mathbf{i}(k,i) I_{\{[\frac{(k-1)L_x}{N_c}, \frac{kL_x}{N_c}]\}}(\mathbf{x})], \quad i = 1, \dots, m,$$

where m is the number of diffusing species. Then, $\|U_\infty(\mathbf{x}) - u_\infty(\mathbf{x})\|_{L_2} = O\left(\frac{\ln N_c}{N_c}\right)$ and converges to 0 as $N_c \rightarrow \infty$.

Note that for $\mathbf{x} \in [\frac{(k-1)L_x}{N_c}, \frac{kL_x}{N_c})$, $(U_\infty(\mathbf{x}))_i$ gives the concentration of the i th species in the k th compartment.

Proof The proof of the Lemma 1 is lengthy, and we split it into 6 steps:

- **Step 1** Express $U_\infty(\mathbf{x})$ and $u_\infty(\mathbf{x})$ in terms of the discrete and continuous Green’s functions;

- **Step 2** Split the error between $U_\infty(\mathbf{x})$ and $u_\infty(\mathbf{x})$ into three parts, (I) , (II) , and (III) and split (I) into four parts, (i) , (ii) , (iii) , and (iv) ;
- **Step 3** To get an upper bound for (ii) , we prove $\|Q_1\|_E \leq O(1)$;
- **Step 4** Prove $\sum_\mu |\tilde{\lambda}_1^{-1}| \leq O\left(\frac{1}{l^2}\right)$ and finish showing $\|(ii)\|_E, \|(iii)\|_E \leq O\left(\frac{\ln N_c}{N_c}\right)$;
- **Step 5** Show $\|(i)\|_E, \|(iv)\|_E \leq o\left(\frac{1}{N_c}\right)$;
- **Step 6** Show $\|(II)\|_E, \|(III)\|_E \leq O\left(\frac{1}{N_c}\right)$.

Step 1:

First, we show that $U_\infty(\mathbf{x})$, which is defined in terms of X_∞ , is expressed in the form with a discrete version of Green’s function. X_∞ is a solution of (18) and is given as

$$X_\infty = \sum_{\mathbf{l}} \frac{1}{\lambda_{\mathbf{l}}} \left(\phi_{\mathbf{l}} * \overline{\phi_{\mathbf{l}}^*}\right) \otimes \left(\varphi_{\mathbf{l}} * \overline{\varphi_{\mathbf{l}}^*}\right) \mathbf{k}^s.$$

Recall that $\mathbf{l} = (l, \mu)$ where $l = (l_1, l_2, l_3)$ is an index for the compartment and μ is an index for the species. Also, recall from Sect. 2.1 that α_l and ϕ_l are the eigenvalue and eigenvector of Δ and λ_l and φ_l are the eigenvalue and eigenvector of $\mathcal{K} + \alpha_l \mathcal{D}$. ϕ_l^* and φ_l^* are the corresponding adjoint eigenvectors. Denote

$$Q_{\mathbf{l}} \equiv \varphi_{\mathbf{l}} * \overline{\varphi_{\mathbf{l}}^*}$$

and define a spatial variable $q_l(\mathbf{x})$ as

$$q_l(\mathbf{x}) \equiv \sqrt{\frac{N_c}{L_x}} \sum_{l'=1}^{N_c} (\phi_l)_{l'} I_{\left\{ \left[\frac{(l'-1)L_x}{N_c}, \frac{l'L_x}{N_c} \right] \right\}}(\mathbf{x}), \quad l = 1, 2, \dots, N_c. \tag{98}$$

Then, define each element of a spatial vector for the production rates from a source as

$$\begin{aligned} k_i^s(\mathbf{x}) &\equiv \sum_{k=1}^{N_c} \frac{\mathbf{k}_{\mathbf{l}(k,i)}^s}{\mathcal{N}_A V_c} I_{\left\{ \left[\frac{(k-1)L_x}{N_c}, \frac{kL_x}{N_c} \right] \right\}}(\mathbf{x}), \quad i = 1, \dots, m, \\ &= \frac{\mathbf{k}_{\mathbf{l}(1,i)}^s}{\mathcal{N}_A V_c} I_{\left\{ \left[0, \frac{L_x}{N_c} \right] \right\}}(\mathbf{x}). \end{aligned}$$

Using $[\mathbf{k}^s]^{(1)}$, $k^s(\mathbf{x})$ is written as

$$k^s(\mathbf{x}) = \frac{1}{\mathcal{N}_A V_c} [\mathbf{k}^s]^{(1)} I_{\left\{ \left[0, \frac{L_x}{N_c} \right] \right\}}(\mathbf{x}). \tag{99}$$

Using the fact that $\phi_l = \overline{\phi_l^*}$, define a matrix for a discrete Green's function as

$$G(\mathbf{x}, \xi) \equiv \sum_1 \frac{1}{\lambda_1} q_l(\mathbf{x}) q_l(\xi) Q_1. \tag{100}$$

Then, the vector for the scaled species numbers in different locations is expressed as

$$U_\infty(\mathbf{x}) = \int_0^{L_x} G(\mathbf{x}, \xi) k^s(\xi) d\xi. \tag{101}$$

Next, we show that $u_\infty(\mathbf{x})$, which corresponds to $U_\infty(\mathbf{x})$ in the deterministic reaction–diffusion equations, can also be expressed in terms of a Green's function. Using our assumption that $\sigma(\mathcal{W}) \subset LHP$, the steady-state concentration of non-diffusing species is expressed in terms of the steady-state concentration of diffusing species and (96) is reduced to

$$\tilde{D} \Delta u_\infty(\mathbf{x}) + \mathcal{K} u_\infty(\mathbf{x}) + \delta(\mathbf{x}, 0) \tilde{k}^s = 0, \quad \mathbf{x} \in [0, L_x], \tag{102}$$

where $\mathcal{K} = \mathcal{R} - S\mathcal{W}^{-1}\mathcal{T}$. Consider an eigenvalue problem related to (102).

$$\begin{aligned} \tilde{D} \Delta \Upsilon(\mathbf{x}) + (\mathcal{K} - \lambda I_m) \Upsilon(\mathbf{x}) &= 0, & \mathbf{x} \in [0, L_x], \\ \Upsilon'(\mathbf{x}) &= 0, & \mathbf{x} = 0, L_x \end{aligned} \tag{103}$$

Let $\tilde{\lambda}_1$ and $\tilde{\varphi}_1$ be a solution of the algebraic eigenvalue problem

$$(\mathcal{K} + \tilde{\alpha}_1 \tilde{D} - \tilde{\lambda}_1 I_m) \tilde{\varphi}_1 = 0,$$

and let $\tilde{\varphi}_1^*$ be the solution in the adjoint algebraic eigenvalue problem. We find that the solution of the scalar problem in (19) is

$$\tilde{\alpha}_l = - \left(\frac{l\pi}{L_x} \right)^2, \quad l = 0, 1, \dots, \tag{104}$$

and

$$\tilde{q}_l(\mathbf{x}) = \begin{cases} \sqrt{\frac{1}{L_x}}, & l = 0, \\ \sqrt{\frac{2}{L_x}} \cos\left(\frac{l\pi \mathbf{x}}{L_x}\right), & l \neq 0. \end{cases} \tag{105}$$

Then, the eigenfunction of (103) is written as $\Upsilon_1(\mathbf{x}) \equiv \tilde{q}_l(\mathbf{x}) \tilde{\varphi}_1$. Using our assumption that $\mathcal{K} + \tilde{\alpha}_l \tilde{D}$ is semi-simple, the eigenfunctions are complete and the solution of (103)

is given as

$$\Upsilon(\mathbf{x}) = \sum_{\mathbf{l}} \frac{1}{\tilde{\lambda}_{\mathbf{l}}} \tilde{q}_{\mathbf{l}}(\mathbf{x}) \tilde{\varphi}_{\mathbf{l}}.$$

Define

$$\tilde{Q}_{\mathbf{l}} \equiv \tilde{\varphi}_{\mathbf{l}} * \overline{\tilde{\varphi}_{\mathbf{l}}^*}.$$

Since we assume that $\sigma(\mathcal{K} + \tilde{\alpha}_{\mathbf{l}} \tilde{\mathcal{D}}) \subset LHP$, we have $\tilde{\lambda}_{\mathbf{l}} \neq 0$ for all \mathbf{l} and the Green's function of the operator $\tilde{\mathcal{D}}\Delta + \mathcal{K}$ is given as

$$\tilde{G}(\mathbf{x}, \boldsymbol{\xi}) \equiv \sum_{\mathbf{l}} \frac{1}{\tilde{\lambda}_{\mathbf{l}}} \tilde{q}_{\mathbf{l}}(\mathbf{x}) \tilde{q}_{\mathbf{l}}(\boldsymbol{\xi}) \tilde{Q}_{\mathbf{l}}.$$

Then, the steady-state concentration vector which is a solution of (102) is written as

$$u_{\infty}(\mathbf{x}) = \int_0^{L_x} \tilde{G}(\mathbf{x}, \boldsymbol{\xi}) \delta(\boldsymbol{\xi}, 0) \tilde{k}^s d\boldsymbol{\xi}. \tag{106}$$

Step 2:

Now, we estimate the error between $U_{\infty}(\mathbf{x})$ and $u_{\infty}(\mathbf{x})$ and show that $\|U_{\infty}(\mathbf{x}) - u_{\infty}(\mathbf{x})\|_{L_2}$ is $O\left(\frac{\ln N_c}{N_c}\right)$. Define a projection of the Green's function onto the space with a finite number of frequencies and its remainder as

$$\pi_{N_c} \tilde{G}(\mathbf{x}, \boldsymbol{\xi}) \equiv \sum_{\mathbf{l} < N_c, \mathbf{l}} \frac{1}{\tilde{\lambda}_{\mathbf{l}}} \tilde{q}_{\mathbf{l}}(\mathbf{x}) \tilde{q}_{\mathbf{l}}(\boldsymbol{\xi}) \tilde{Q}_{\mathbf{l}}, \tag{107}$$

$$(I_m - \pi_{N_c}) \tilde{G}(\mathbf{x}, \boldsymbol{\xi}) \equiv \sum_{\mathbf{l} \geq N_c, \mathbf{l}} \frac{1}{\tilde{\lambda}_{\mathbf{l}}} \tilde{q}_{\mathbf{l}}(\mathbf{x}) \tilde{q}_{\mathbf{l}}(\boldsymbol{\xi}) \tilde{Q}_{\mathbf{l}}. \tag{108}$$

Subtracting (106) from (101) and breaking $U_{\infty}(\mathbf{x}) - u_{\infty}(\mathbf{x})$ into three parts, we get

$$\begin{aligned} U_{\infty}(\mathbf{x}) - u_{\infty}(\mathbf{x}) &= \int_0^{L_x} \left(G(\mathbf{x}, \boldsymbol{\xi}) - \pi_{N_c} \tilde{G}(\mathbf{x}, \boldsymbol{\xi}) \right) k^s(\boldsymbol{\xi}) d\boldsymbol{\xi} \quad \dots \text{(I)} \\ &+ \int_0^{L_x} \pi_{N_c} \tilde{G}(\mathbf{x}, \boldsymbol{\xi}) \left(k^s(\boldsymbol{\xi}) - \tilde{k}^s \delta(\boldsymbol{\xi}, 0) \right) d\boldsymbol{\xi} \quad \dots \text{(II)} \\ &- \int_0^{L_x} (I_m - \pi_{N_c}) \tilde{G}(\mathbf{x}, \boldsymbol{\xi}) \tilde{k}^s \delta(\boldsymbol{\xi}, 0) d\boldsymbol{\xi} \quad \dots \text{(III)}. \tag{109} \end{aligned}$$

Using (100) and (107), the first part in (109) is computed as

$$\begin{aligned}
 (I) &= \int_0^{L_x} \left(G(\mathbf{x}, \xi) - \pi_{N_c} \tilde{G}(\mathbf{x}, \xi) \right) k^s(\xi) d\xi \\
 &= \int_0^{L_x} \sum_{1,0 < l < N_c} \left(\frac{1}{\lambda_l} q_l(\mathbf{x}) q_l(\xi) Q_1 - \frac{1}{\tilde{\lambda}_l} \tilde{q}_l(\mathbf{x}) \tilde{q}_l(\xi) \tilde{Q}_1 \right) k^s(\xi) d\xi. \quad (110)
 \end{aligned}$$

In (110), the first term in the parenthesis with $l = N_c$ is canceled out by the second term in the parenthesis with $l = 0$. Using (99), (I) is computed as

$$\begin{aligned}
 (I) &= \int_0^{L_x} \sum_{1,0 < l < N_c} \left(\frac{1}{\lambda_l} q_l(\mathbf{x}) q_l(\xi) Q_1 - \frac{1}{\tilde{\lambda}_l} \tilde{q}_l(\mathbf{x}) \tilde{q}_l(\xi) \tilde{Q}_1 \right) \frac{1}{N_A V_c} [\mathbf{k}^s]^{(1)} I_{\left\{ \left[0, \frac{L_x}{N_c} \right] \right\}}(\xi) d\xi \\
 &= \frac{1}{N_A V} \max_i \mathbf{k}_{i(1,i)}^s \int_0^{\frac{L_x}{N_c}} \sum_{1,0 < l < N_c} N_c \left(\frac{1}{\lambda_l} q_l(\mathbf{x}) q_l(\xi) Q_1 - \frac{1}{\tilde{\lambda}_l} \tilde{q}_l(\mathbf{x}) \tilde{q}_l(\xi) \tilde{Q}_1 \right) \mathbf{u}_m d\xi,
 \end{aligned}$$

where \mathbf{u}_m is an m -dimensional vector with each element equal to 1. We break (I) into four parts by adding and subtracting terms as

$$ABCD - \tilde{A}\tilde{B}\tilde{C}\tilde{D} = (A - \tilde{A})BCD + \tilde{A}(B - \tilde{B})CD + \tilde{A}\tilde{B}(C - \tilde{C})D + \tilde{A}\tilde{B}\tilde{C}(D - \tilde{D}).$$

Then, we get

$$\begin{aligned}
 (I) &= \frac{1}{N_A V} \max_i \mathbf{k}_{i(1,i)}^s \\
 &\times \left[\int_0^{\frac{L_x}{N_c}} \sum_{1,0 < l < N_c} N_c \left(\frac{1}{\lambda_l} - \frac{1}{\tilde{\lambda}_l} \right) q_l(\mathbf{x}) q_l(\xi) Q_1 \mathbf{u}_m d\xi \quad \dots (i) \right. \\
 &+ \int_0^{\frac{L_x}{N_c}} \sum_{1,0 < l < N_c} N_c \frac{1}{\lambda_l} (q_l(\mathbf{x}) - \tilde{q}_l(\mathbf{x})) q_l(\xi) Q_1 \mathbf{u}_m d\xi \quad \dots (ii) \\
 &+ \int_0^{\frac{L_x}{N_c}} \sum_{1,0 < l < N_c} N_c \frac{1}{\tilde{\lambda}_l} \tilde{q}_l(\mathbf{x}) (q_l(\xi) - \tilde{q}_l(\xi)) Q_1 \mathbf{u}_m d\xi \quad \dots (iii) \\
 &\left. + \int_0^{\frac{L_x}{N_c}} \sum_{1,0 < l < N_c} N_c \frac{1}{\tilde{\lambda}_l} \tilde{q}_l(\mathbf{x}) \tilde{q}_l(\xi) (Q_1 - \tilde{Q}_1) \mathbf{u}_m d\xi \right] \quad \dots (iv).
 \end{aligned}$$

Step 3:

We will show that $\|(ii)\|_E \leq O\left(\frac{\ln N_c}{N_c}\right)$.

Using (98) and (83), for each l where $0 < l < N_c$ we get

$$|q_l(\mathbf{x})| = \left| \sqrt{\frac{2}{L_x}} \sum_{l'=1}^{N_c} \cos\left(\frac{(2l'-1)\pi l}{2N_c}\right) I_{\left[\frac{(l'-1)L_x}{N_c}, \frac{l'L_x}{N_c}\right]}(\mathbf{x}) \right| \leq O(1). \tag{111}$$

Next, using (98) and (105), for each l where $0 < l < N_c$ and for $\mathbf{x} \in \left[\frac{(k-1)L_x}{N_c}, \frac{kL_x}{N_c}\right)$, a difference between $q_l(\mathbf{x})$ and $\tilde{q}_l(\mathbf{x})$ is estimated as

$$\begin{aligned} |q_l(\mathbf{x}) - \tilde{q}_l(\mathbf{x})| &= \left| \sqrt{\frac{2}{L_x}} \sum_{l'=1}^{N_c} \cos\left(\frac{(2l'-1)\pi l}{2N_c}\right) I_{\left[\frac{(l'-1)L_x}{N_c}, \frac{l'L_x}{N_c}\right]}(\mathbf{x}) - \sqrt{\frac{2}{L_x}} \cos\left(\frac{l\pi \mathbf{x}}{L_x}\right) \right| \\ &= \sqrt{\frac{2}{L_x}} \left| \cos\left(\frac{(2k-1)\pi l}{2N_c}\right) - \cos\left(\frac{l\pi \mathbf{x}}{L_x}\right) \right| \\ &= \sqrt{\frac{2}{L_x}} \left| \left(\frac{(2k-1)\pi l}{2N_c} - \frac{l\pi \mathbf{x}}{L_x}\right) \sin b \right| \end{aligned} \tag{112}$$

$$\begin{aligned} &\leq \sqrt{\frac{2}{L_x}} \cdot \frac{l\pi}{2N_c} \cdot |\sin b| \\ &\equiv O\left(\frac{1}{N_c}\right) \times l. \end{aligned} \tag{113}$$

(112) is obtained by the Mean value theorem where b is between $\frac{(2k-1)\pi l}{2N_c}$ and $\frac{l\pi \mathbf{x}}{L_x}$. Then using (111) and (113), $\|(ii)\|_E$ is estimated as

$$\begin{aligned} \|(ii)\|_E &= \left\| \int_0^{\frac{L_x}{N_c}} \sum_{1,0 < l < N_c} N_c \frac{1}{\tilde{\lambda}_1} (q_l(\mathbf{x}) - \tilde{q}_l(\mathbf{x})) q_l(\xi) Q_1 \mathbf{u} \, d\xi \right\|_E \\ &\leq \left\| \sum_{1,0 < l < N_c} |\tilde{\lambda}_1^{-1}| \int_0^{\frac{L_x}{N_c}} N_c \times O\left(\frac{1}{N_c}\right) \times l \times O(1) \, d\xi \right\|_E \max_1 \|Q_1 \mathbf{u}_m\|_E \\ &\leq O\left(\frac{1}{N_c}\right) \sum_{1,0 < l < N_c} l \cdot |\tilde{\lambda}_1^{-1}| \max_1 \|Q_1\|_E. \end{aligned} \tag{114}$$

Now, we will show that $\max_1 \|Q_1\|_E \leq O(1)$ by showing $\max_1 \|\tilde{Q}_1\|_E \leq O(1)$, because $\tilde{Q}_1 - Q_1 = o\left(\frac{1}{N_c}\right)$ as we will show later in (118). To estimate difference between Q_1 and \tilde{Q}_1 , we use a perturbation theory of the linear operator in a finite-dimensional space (Theorem 5.4, p. 111 Kato 1966). Define the operator $A = \mathcal{K} + \tilde{\alpha}_l \tilde{D}$,

and express $\mathcal{K} + \alpha_l \mathcal{D}$ as a series of perturbed operators from A . Using (82) and (104), we obtain

$$\begin{aligned} A(\epsilon) &= A - \tilde{\alpha}_l \tilde{\mathcal{D}} + \alpha_l \mathcal{D} \\ &= A - \tilde{\alpha}_l \tilde{\mathcal{D}} + \alpha_l \frac{\tilde{\mathcal{D}}}{(L_x/N_c)^2} \\ &= A + \left(\frac{l\pi}{L_x}\right)^2 \tilde{\mathcal{D}} - \left(\frac{2N_c \sin\left(\frac{l\pi}{2N_c}\right)}{L_x}\right)^2 \tilde{\mathcal{D}} \\ &= A + \left(\frac{l\pi}{L_x}\right)^2 \tilde{\mathcal{D}} - \left(\frac{\sin\left(\frac{l\pi\epsilon}{2}\right)}{\left(\frac{L_x\epsilon}{2}\right)}\right)^2 \tilde{\mathcal{D}} \end{aligned}$$

where $\epsilon = \frac{1}{N_c}$. We can show that $A(\epsilon)$ is differentiable at $\epsilon = 0$ and $A'(0) = 0$. Let λ be the semi-simple eigenvalue of A and let Q be the projection of A corresponding to λ . Then, using Theorem 5.4 in Kato (1966), we get

$$\lambda(\epsilon) = \lambda + o(\epsilon), \tag{115}$$

$$Q(\epsilon) = Q + o(\epsilon), \tag{116}$$

where $\lambda(\epsilon)$ and $Q(\epsilon)$ are eigenvalues and projections of $A(\epsilon)$. From (115) and (116), $\frac{\lambda(\epsilon)-\lambda}{\epsilon}$ and $\left\|\frac{Q(\epsilon)-Q}{\epsilon}\right\|_E$ go to zero as $\epsilon \rightarrow 0$. In our setting, $\lambda = \tilde{\lambda}_1$ and $\lambda(\epsilon) = \lambda_1$. Similarly, $Q = \tilde{Q}_1$ and $Q(\epsilon) = Q_1$. Since we assume that $A = \mathcal{K} + \tilde{\alpha}_l \tilde{\mathcal{D}}$ is semi-simple, the condition that λ is the semi-simple eigenvalue of A is satisfied. Then, (115) and (116) yields

$$\tilde{\lambda}_1 - \lambda_1 = o\left(\frac{1}{N_c}\right), \tag{117}$$

$$\tilde{Q}_1 - Q_1 = o\left(\frac{1}{N_c}\right). \tag{118}$$

Using (118) and $\|Q_1 \mathbf{u}_m\|_E \leq \|Q_1\|_E \|\mathbf{u}_m\|_E = \sqrt{m} \|Q_1\|_E$ where m is the number of diffusing species, we only need to show that

$$\max_{\mathbf{1}} \left\| \tilde{Q}_1 \right\|_E = O(1).$$

Define the operator $B = \tilde{\alpha}_l \tilde{\mathcal{D}}$ and consider $\mathcal{K} + \tilde{\alpha}_l \tilde{\mathcal{D}}$ as perturbation of B as follows:

$$B(\epsilon) = \left(-\mathcal{K} \left(\frac{L_x\epsilon}{\pi}\right)^2 \tilde{\mathcal{D}}^{-1} + I\right) \tilde{\alpha}_l \tilde{\mathcal{D}}$$

where $\epsilon = \frac{1}{l}$. As $\epsilon \rightarrow 0$, $B(\epsilon) \rightarrow B$ and $B'(0) = 0$. Therefore, using Theorem 5.4 in Kato (1966),

$$J(\epsilon) - J = o(\epsilon)$$

where $J(\epsilon)$ and J are projections of $B(\epsilon)$ and B . Define $M > 0$ large enough so that $\epsilon = \frac{1}{l}$ is small for $l \geq M$. e_μ denotes an m -dimensional vector with its μ th entry equal to 1 and all others equal to zero. Since $B(\frac{1}{l}) = \mathcal{K} + \tilde{\alpha}_l \tilde{\mathcal{D}}$, $J(\frac{1}{l}) = \tilde{Q}_1$, and $J = e_\mu * e_\mu$, for $l \geq M$ we estimate the upper bound of $\|\tilde{Q}_1\|_E$ as

$$\begin{aligned} \|\tilde{Q}_1\|_E &\leq \|\tilde{Q}_1 - Q\|_E + \|Q\|_E \\ &= o\left(\frac{1}{l}\right) + \|e_\mu * e_\mu\|_E \\ &\leq o\left(\frac{1}{M}\right) + 1, \quad \text{for } l \geq M. \end{aligned}$$

Since \tilde{Q}_1 and M do not depend on N_c where $\mathbf{l} = (l, \mu)$, we get

$$\begin{aligned} \max_{\mathbf{l}} \|\tilde{Q}_1\|_E &\leq \max\left(\max_{l < M, \mu} \|\tilde{Q}_{(l, \mu)}\|_E, o\left(\frac{1}{M}\right) + 1\right) \\ &= O(1). \end{aligned} \tag{119}$$

Step 4:

Next, we estimate $\sum_{\mu} |\tilde{\lambda}_1^{-1}|$. Since $\tilde{\lambda}_1$ is an eigenvalue of $\mathcal{K} + \tilde{\alpha}_l \tilde{\mathcal{D}}$, $\tilde{\lambda}_1^{-1}$ is an eigenvalue of $(\mathcal{K} + \tilde{\alpha}_l \tilde{\mathcal{D}})^{-1}$. For $l > 0$, $\tilde{\alpha}_l \neq 0$ and we expand the inverse matrix as

$$\begin{aligned} (\mathcal{K} + \tilde{\alpha}_l \tilde{\mathcal{D}})^{-1} &= \left[(\tilde{\alpha}_l \tilde{\mathcal{D}}) \left(I + (\tilde{\alpha}_l \tilde{\mathcal{D}})^{-1} \mathcal{K} \right) \right]^{-1} \\ &= \left(I + (\tilde{\alpha}_l \tilde{\mathcal{D}})^{-1} \mathcal{K} \right)^{-1} (\tilde{\alpha}_l \tilde{\mathcal{D}})^{-1} \\ &= \left[\sum_{p=0}^{\infty} \left(-(\tilde{\alpha}_l \tilde{\mathcal{D}})^{-1} \mathcal{K} \right)^p \right] (\tilde{\alpha}_l \tilde{\mathcal{D}})^{-1}. \end{aligned} \tag{120}$$

We estimate the upper and lower bounds of the spectrum of $-(\tilde{\alpha}_l \tilde{\mathcal{D}})^{-1} \mathcal{K}$ to show convergence of the matrix series in (120). Using the fact that all diagonal elements of

\tilde{D} are positive and using the definition of $\tilde{\alpha}_l$, we get

$$\begin{aligned} \left| \sigma \left(- \left(\tilde{\alpha}_l \tilde{D} \right)^{-1} \mathcal{K} \right) \right| &\leq \left| \tilde{\alpha}_l^{-1} \right| \frac{1}{\min_x \tilde{D}_{xx}} |\sigma(\mathcal{K})| \\ &= \left(\frac{L_x}{l\pi} \right)^2 \frac{1}{\min_x \tilde{D}_{xx}} |\sigma(\mathcal{K})|. \end{aligned}$$

Therefore, there exists $A > 0$ such for $l \geq A$

$$\left| \sigma \left(- \left(\tilde{\alpha}_l \tilde{D} \right)^{-1} \mathcal{K} \right) \right| \leq 1.$$

Since the spectrum of $-\left(\tilde{\alpha}_l \tilde{D}\right)^{-1} \mathcal{K}$ is bounded by ± 1 for $l \geq A$, the matrix series in (120) converges. From Levy–Hadamard theorem (Bodwig 1959), each eigenvalue, $\tilde{\lambda}_1^{-1}$, of $\left(\mathcal{K} + \tilde{\alpha}_l \tilde{D}\right)^{-1}$ satisfies

$$\left| \tilde{\lambda}_1^{-1} - \left[\left(\mathcal{K} + \tilde{\alpha}_l \tilde{D} \right)^{-1} \right]_{xx} \right| < \sum_{\gamma \neq x} \left| \left[\left(\mathcal{K} + \tilde{\alpha}_l \tilde{D} \right)^{-1} \right]_{x\gamma} \right|$$

and the inequality can be rewritten as

$$\begin{aligned} &\left| \left[\left(\mathcal{K} + \tilde{\alpha}_l \tilde{D} \right)^{-1} \right]_{xx} - \sum_{\gamma \neq x} \left| \left[\left(\mathcal{K} + \tilde{\alpha}_l \tilde{D} \right)^{-1} \right]_{x\gamma} \right| \right| \\ &< \left| \tilde{\lambda}_1^{-1} \right| < \left| \left[\left(\mathcal{K} + \tilde{\alpha}_l \tilde{D} \right)^{-1} \right]_{xx} + \sum_{\gamma \neq x} \left| \left[\left(\mathcal{K} + \tilde{\alpha}_l \tilde{D} \right)^{-1} \right]_{x\gamma} \right| \right|. \end{aligned} \tag{121}$$

Using (121) and (120), for each $l \geq A$ we get

$$\begin{aligned} \sum_{\mu} \left| \tilde{\lambda}_1^{-1} \right| &< \sum_{\mu=1}^m \max_x \sum_{\gamma} \left| \left[\left(\mathcal{K} + \tilde{\alpha}_l \tilde{D} \right)^{-1} \right]_{x\gamma} \right| \\ &< m \left(\frac{L_x}{l\pi} \right)^2 \max_x \sum_{\gamma} \sum_{p=0}^{\infty} \left| \left[\left(\left(\frac{L_x}{l\pi} \right)^2 \tilde{D}^{-1} \mathcal{K} \right)^p \right]_{x\gamma} \right| \tilde{D}_{\gamma\gamma}^{-1} \\ &\leq m \left(\frac{L_x}{l\pi} \right)^2 \max_x \sum_{\gamma} \left[I + O \left(\frac{1}{l^2} \right) \right]_{x\gamma} \tilde{D}_{\gamma\gamma}^{-1} \\ &\leq \tilde{C} \left(\frac{1}{l} \right)^2, \end{aligned}$$

where m is the number of diffusing species. Define $C \equiv \max\left(\tilde{C}, \max_{l < A} \left(mA^2 \left|\tilde{\lambda}_1^{-1}\right|\right)\right)$. Then, for each $l > 0$ the eigenvalues are bounded as

$$\sum_{\mu} |\tilde{\lambda}_1^{-1}| \leq \frac{C}{l^2} = o\left(\frac{1}{l^2}\right). \quad (122)$$

Therefore, using (119) and (122) in (114), we get

$$\begin{aligned} \|(ii)\|_E &\leq o\left(\frac{1}{N_c}\right) \sum_{l, 0 < l < N_c} l \cdot |\tilde{\lambda}_1^{-1}| \max_1 \|Q_1\|_E \\ &\leq o\left(\frac{1}{N_c}\right) \sum_{l, 0 < l < N_c} l \times o\left(\frac{1}{l^2}\right) \times o(1) \\ &\leq o\left(\frac{1}{N_c}\right) \sum_{l, 0 < l < N_c} o\left(\frac{1}{l}\right) \\ &\leq o\left(\frac{1}{N_c}\right) o\left(1 + \int_1^{N_c-1} \frac{1}{y} dy\right) \\ &\leq o\left(\frac{\ln N_c}{N_c}\right). \end{aligned} \quad (123)$$

Now, we estimate an upper bound for $\|(iii)\|_E$. Using (105), for $l > 0$ we get

$$\begin{aligned} |\tilde{q}_l(\mathbf{x})| &= \left| \sqrt{\frac{2}{L_x}} \cos\left(\frac{l\pi\mathbf{x}}{L_x}\right) \right| \\ &\leq o(1). \end{aligned} \quad (124)$$

Since the estimates in (111), (113), and (124) do not depend on \mathbf{x} and since the integrands in (ii) and (iii) are the same vice versa when we exchange \mathbf{x} and ξ , using (123) we can get

$$\|(iii)\|_E \leq o\left(\frac{\ln N_c}{N_c}\right). \quad (125)$$

Step 5:

We will show that $\|(i)\|_E \leq o\left(\frac{1}{N_c}\right)$. Using (111), (118), and (119), we get

$$\begin{aligned}
 \|(i)\|_E &= \left\| \int_0^{\frac{L_x}{N_c}} \sum_{1,0 < l < N_c} N_c \left(\frac{1}{\lambda_l} - \frac{1}{\tilde{\lambda}_l} \right) q_l(\mathbf{x}) q_l(\xi) Q_l \mathbf{u}_m d\xi \right\|_E \\
 &\leq \left| \int_0^{\frac{L_x}{N_c}} N_c \times O(1) d\xi \sum_{1,0 < l < N_c} \frac{\tilde{\lambda}_l - \lambda_l}{\lambda_l \tilde{\lambda}_l} \right| \times O(1) \\
 &= O(1) \times \sum_{1,0 < l < N_c} \left| \frac{\tilde{\lambda}_l - \lambda_l}{\lambda_l \tilde{\lambda}_l} \right|. \tag{126}
 \end{aligned}$$

Then using (117) and (122) in (126), we get

$$\begin{aligned}
 \|(i)\|_E &\leq \sum_{1,0 < l < N_c} \left| \frac{o\left(\frac{1}{N_c}\right)}{\tilde{\lambda}_l \left(\tilde{\lambda}_l + o\left(\frac{1}{N_c}\right)\right)} \right| \\
 &\leq \sum_{0 < l < N_c} \left| \frac{o\left(\frac{1}{N_c}\right)}{\left(l^4 + o\left(\frac{1}{N_c}\right)\right)} \right| \\
 &\leq \frac{o\left(\frac{1}{N_c}\right)}{\left(1 + o\left(\frac{1}{N_c}\right)\right)} + \int_1^{N_c-1} \frac{o\left(\frac{1}{N_c}\right)}{\left(y^4 + o\left(\frac{1}{N_c}\right)\right)} dy \\
 &\leq \frac{o\left(\frac{1}{N_c}\right)}{\left(1 + o\left(\frac{1}{N_c}\right)\right)} + \frac{o\left(\frac{1}{N_c}\right)}{(N_c - 1)^3} \leq o\left(\frac{1}{N_c}\right). \tag{127}
 \end{aligned}$$

Next, we will show that $\|(iv)\|_E \leq o\left(\frac{1}{N_c}\right)$. Using (111), (124), and (118), we get

$$\begin{aligned}
 \|(iv)\|_E &= \left\| \int_0^{\frac{L_x}{N_c}} \sum_{1,0 < l < N_c} N_c \frac{1}{\tilde{\lambda}_l} \tilde{q}_l(\mathbf{x}) \tilde{q}_l(\xi) \left(Q_l - \tilde{Q}_l\right) \mathbf{u}_m d\xi \right\|_E \\
 &= \left| \int_0^{\frac{L_x}{N_c}} N_c \times O(1) d\xi \sum_{1,0 < l < N_c} \frac{1}{\tilde{\lambda}_l} \right| \times o\left(\frac{1}{N_c}\right) \\
 &= \sum_{1,0 < l < N_c} \left| \tilde{\lambda}_l^{-1} \right| \times o\left(\frac{1}{N_c}\right). \tag{128}
 \end{aligned}$$

Using (122) in (128), we get

$$\begin{aligned} \|(iv)\|_E &\leq \sum_{l,0 < l < N_c} o\left(\frac{1}{l^2}\right) \times o\left(\frac{1}{N_c}\right) \\ &\leq O\left(1 + \int_1^{N_c-1} \frac{1}{y^2} dy\right) \times o\left(\frac{1}{N_c}\right) \\ &\leq o\left(\frac{1}{N_c}\right). \end{aligned} \tag{129}$$

Step 6:

We will show that $\|(II)\|_E \leq O\left(\frac{1}{N_c}\right)$. Using (107), (99), and (97), we get

$$\begin{aligned} (II) &= \int_0^{L_x} \pi_{N_c} \tilde{G}(\mathbf{x}, \xi) \left(k^s(\xi) - \tilde{k}^s \delta(\xi, 0)\right) d\xi \\ &= \int_0^{L_x} \sum_{l, l < N_c} \frac{1}{\tilde{\lambda}_l} \tilde{q}_l(\mathbf{x}) \tilde{q}_l(\xi) \tilde{Q}_l \left(\frac{1}{\mathcal{N}_A V_c} [\mathbf{k}^s]^{(1)} I_{\left\{ \left[0, \frac{L_x}{N_c} \right] \right\}}(\xi) - \frac{L_x}{\mathcal{N}_A V} [\mathbf{k}^s]^{(1)} \delta(\xi, 0) \right) d\xi. \end{aligned} \tag{130}$$

In (130), the term with $l = 0$ in the series becomes zero. Using (122), (124), (119) in (130), we get

$$\begin{aligned} \|(II)\|_E &\leq \sum_{l,0 < l < N_c} o\left(\frac{1}{l^2}\right) \times O(1) \times \frac{L_x}{\mathcal{N}_A V} \max_i \mathbf{k}_i^s \\ &\quad \times \left| \int_0^{L_x} \tilde{q}_l(\xi) \left(\frac{N_c}{L_x} I_{\left\{ \left[0, \frac{L_x}{N_c} \right] \right\}}(\xi) - \delta(\xi, 0) \right) d\xi \right| \\ &\leq \sum_{l,0 < l < N_c} o\left(\frac{1}{l^2}\right) \times \left| \int_0^{L_x} \tilde{q}_l(\xi) \left(\frac{N_c}{L_x} I_{\left\{ \left[0, \frac{L_x}{N_c} \right] \right\}}(\xi) - \delta(\xi, 0) \right) d\xi \right|. \end{aligned} \tag{131}$$

Using (105) in (131), we estimate

$$\|(II)\|_E \leq \sum_{l,0 < l < N_c} o\left(\frac{1}{l^2}\right) \times \sqrt{\frac{2}{L_x}} \left| \frac{N_c}{l\pi} \sin\left(\frac{l\pi}{N_c}\right) - 1 \right|. \tag{132}$$

By approximating the series in (132), we get

$$\begin{aligned} \|(II)\|_E &\leq O(1) \times \sum_{l, 0 < l < N_c} \frac{\left| 1 - \frac{\sin\left(\frac{l\pi}{N_c}\right)}{\left(\frac{l\pi}{N_c}\right)} \right|}{l^2} \\ &\leq O(1) \times \sum_{l, 0 < l < N_c} \frac{1 - \frac{\left(\frac{l\pi}{N_c}\right) - \frac{\left(\frac{l\pi}{N_c}\right)^3}{3!}}{\left(\frac{l\pi}{N_c}\right)}}{l^2} \\ &\leq O\left(\frac{1}{N_c}\right). \end{aligned} \tag{133}$$

Now, we will show that $\|(III)\|_E \leq O\left(\frac{1}{N_c}\right)$. Using (108) and (97), we compute

$$\begin{aligned} (III) &= \int_0^{L_x} \left(I_m - \pi_{N_c} \tilde{G}(\mathbf{x}, \boldsymbol{\xi}) \right) \tilde{k}^s \delta(\boldsymbol{\xi}, 0) d\boldsymbol{\xi} \\ &= \int_0^{L_x} \left(\sum_{l, l \geq N_c} \frac{1}{\tilde{\lambda}_l} \tilde{q}_l(\mathbf{x}) \tilde{q}_l(\boldsymbol{\xi}) \tilde{Q}_l \right) \frac{L_x}{N_A \mathbf{V}} [\mathbf{k}^s]^{(1)} \delta(\boldsymbol{\xi}, 0) d\boldsymbol{\xi} \\ &= \sum_{l, l \geq N_c} \left(\frac{1}{\tilde{\lambda}_l} \tilde{q}_l(\mathbf{x}) \tilde{q}_l(0) \tilde{Q}_l \right) \frac{L_x}{N_A \mathbf{V}} [\mathbf{k}^s]^{(1)}. \end{aligned} \tag{134}$$

Using (124), (122), and (119) in (134), we get

$$\begin{aligned} \|(III)\|_E &\leq \sum_{l \geq N_c} O\left(\frac{1}{l^2}\right) \times O(1) \times \max_i \mathbf{k}_{i(1,i)}^s \\ &\leq O(1) \times \int_{N_c-1}^{\infty} \frac{1}{y^2} dy \\ &\leq O\left(\frac{1}{N_c}\right). \end{aligned} \tag{135}$$

In conclusion, we prove that for any $\mathbf{x} \in [0, L_x]$, $\|U_\infty(\mathbf{x}) - u_\infty(\mathbf{x})\|_E \leq O\left(\frac{\ln N_c}{N_c}\right)$ as shown in (123), (125), (127), (129), (133), and (135). Since the upper bound is independent of \mathbf{x} , we get $\|U_\infty(\mathbf{x}) - u_\infty(\mathbf{x})\|_{L_2} = O\left(\frac{\ln N_c}{N_c}\right)$. \square

Using Lemma 1, we prove the convergence of $U_\infty(\mathbf{x})$ to $u_\infty(\mathbf{x})$, and this implies the convergence of $\frac{1}{N_A V_c} X_\infty$ as $N_c \rightarrow \infty$. Since Y_∞ is expressed in terms of X_∞ , \overline{M}_∞ converges as $N_c \rightarrow \infty$, and this implies the convergence of \overline{CV}^* .

E Proof of Theorem 2

Before proving the theorem, we first state and prove a lemma which is used to prove the theorem. The proof of the theorem is given at the end of this appendix. In the following lemma, we prove that each component of $\bar{M}_\infty/\mathcal{N}_A$ converges to the corresponding value of the steady-state concentration in the continuum deterministic reaction–diffusion system.

The mean vector of the stochastic system with no inputs is governed by

$$\frac{dM(t)}{dt} = \Omega M(t), \tag{136}$$

where $\Omega = \Delta \otimes \mathcal{D} + I_{N_c} \otimes \mathcal{K}$.

The corresponding deterministic reaction–diffusion system is governed by

$$\begin{aligned} \frac{\partial u(\mathbf{x}, t)}{\partial t} &= \tilde{D} \Delta u(\mathbf{x}, t) + \mathcal{K}u(\mathbf{x}, t), \quad \mathbf{x} \in [0, L_x], \\ \frac{\partial u(\mathbf{x}, t)}{\partial x} &= 0, \quad \mathbf{x} = 0, L_x, \\ u(\mathbf{x}, 0) &= u_0(\mathbf{x}), \end{aligned} \tag{137}$$

where $u(\mathbf{x}, t)$ is a concentration vector for species in $\mathbf{x} \in [0, L_x]$ at time t . In (137), the diffusion matrix is given as $\tilde{D} = (L_x/N_c)^2 \mathcal{D}$. The integrated initial concentration, $u_0(\mathbf{x})$, between $\mathbf{x} \in \left[\frac{(k-1)L_x}{N_c}, \frac{kL_x}{N_c} \right)$ is expressed in terms of $M(0)$ as follows:

$$\int_{\frac{(k-1)L_x}{N_c}}^{\frac{kL_x}{N_c}} (u_0(\boldsymbol{\xi}))_i \, d\boldsymbol{\xi} = \frac{L_x}{\mathcal{N}_A V} [M(0)]_{\mathbf{i}(k,i)}. \tag{138}$$

Lemma 2 *Let M_∞ be the steady-state solution of (136) and let $u_\infty(\mathbf{x})$ be the steady-state solution of (137). Define $U_\infty(\mathbf{x})$ as a vector with each component satisfying*

$$(U_\infty(\mathbf{x}))_i \equiv \sum_{k=1}^{N_c} \frac{1}{\mathcal{N}_A V_c} [M_\infty]_{\mathbf{i}(k,i)} I\left\{ \left[\frac{(k-1)L_x}{N_c}, \frac{kL_x}{N_c} \right) \right\}(\mathbf{x}), \quad i = 1, \dots, s,$$

where s is the number of species. Then, $\|U_\infty(\mathbf{x}) - u_\infty(\mathbf{x})\|_{L_2} = O\left(\frac{1}{N_c}\right)$ and converges to 0 as $N_c \rightarrow \infty$.

Proof The proof of Lemma 2 is given in 2 steps:

- **Step 1** Express $U_\infty(\mathbf{x})$ and $u_\infty(\mathbf{x})$ in terms of the Green’s function;
- **Step 2** Show $\|U_\infty(\mathbf{x}) - u_\infty(\mathbf{x})\|_{L_2} = O\left(\frac{1}{N_c}\right)$.

Step 1:

We first express $U_\infty(\mathbf{x})$ in terms of the Green's function. Recall that ϕ_{N_c} and $\phi_{N_c}^*$ are the eigenvector and the adjoint eigenvector of Δ corresponding to $\alpha_{N_c} = 0$. Rearrange the order of species in the mean vector, $M(t)$, so that that $\varphi_{(N_c,s)}$ and $\varphi_{(N_c,s)}^*$ become an eigenvector and an adjoint eigenvector corresponding to the zero eigenvalue of Ω . Define

$$Q_{(N_c,s)} \equiv \varphi_{(N_c,s)} * \overline{\varphi_{(N_c,s)}^*}. \tag{139}$$

Then, the projection corresponding to the zero eigenvalue is expressed as

$$P_s = \left(\phi_{N_c} * \overline{\phi_{N_c}^*} \right) \otimes Q_{(N_c,s)}. \tag{140}$$

Letting $t \rightarrow \infty$ in (90) and using (140), the steady-state mean vector for species numbers is expressed as

$$\begin{aligned} M_\infty &= P_s M(0) \\ &= \left(\phi_{N_c} * \overline{\phi_{N_c}^*} \right) \otimes Q_{(N_c,s)} M(0). \end{aligned}$$

Here, note that

$$\begin{aligned} \phi_{N_c} &= \overline{\phi_{N_c}^*} \\ &= \sqrt{\frac{1}{N_c}} [1, 1, \dots, 1]^T. \end{aligned} \tag{141}$$

We define a spatial variable $q_{N_c}(\mathbf{x})$ as

$$\begin{aligned} q_{N_c}(\mathbf{x}) &\equiv \sqrt{\frac{N_c}{L_x}} \sum_{l'=1}^{N_c} (\phi_{N_c})_{l'} I_{\left\{ \left[\frac{(l'-1)L_x}{N_c}, \frac{l'L_x}{N_c} \right] \right\}}(\mathbf{x}) \\ &= \sqrt{\frac{1}{L_x}}. \end{aligned} \tag{142}$$

where the last equality comes from (141). Define a matrix for a discrete Green's function as follows, and using (142) we get

$$\begin{aligned} G(\mathbf{x}, \xi) &\equiv q_{N_c}(\mathbf{x}) q_{N_c}(\xi) Q_{(N_c,s)} \\ &= \frac{1}{L_x} Q_{(N_c,s)} \equiv G. \end{aligned} \tag{143}$$

Then, $U_\infty(\mathbf{x})$ is expressed as

$$U_\infty(\mathbf{x}) = G U_0(\mathbf{x}). \tag{144}$$

Here, $U_0(\mathbf{x})$ is defined as follows:

$$(U_0(\mathbf{x}))_i \equiv \sum_{k=1}^{N_c} \frac{1}{\mathcal{N}_A V_c} [M(0)]_{\mathbf{i}(k,i)} I_{\left\{ \left[\frac{(k-1)L_x}{N_c}, \frac{kL_x}{N_c} \right] \right\}}(\mathbf{x}), \quad 1 = 1, \dots, s. \quad (145)$$

Using (138), (145) is written as

$$(U_0(\mathbf{x}))_i = \sum_{k=1}^{N_c} \left(\frac{N_c}{L_x} \int_{\frac{(k-1)L_x}{N_c}}^{\frac{kL_x}{N_c}} (u_0(\boldsymbol{\xi}))_i d\boldsymbol{\xi} \right) I_{\left\{ \left[\frac{(k-1)L_x}{N_c}, \frac{kL_x}{N_c} \right] \right\}}(\mathbf{x}), \quad 1 = 1, \dots, s. \quad (146)$$

Next, we express $u_\infty(\mathbf{x})$ in terms of the Green's function. Let $\tilde{\alpha}_0 = 0$ and $\tilde{q}_0(\mathbf{x})$ be a solution of the scalar problem

$$\begin{aligned} \Delta \tilde{q}(\mathbf{x}) &= \tilde{\alpha} \tilde{q}(\mathbf{x}), & \mathbf{x} &\in [0, L_x], \\ \tilde{q}'(\mathbf{x}) &= 0, & \mathbf{x} &= 0, L_x, \end{aligned}$$

satisfying $\|\tilde{q}(\mathbf{x})\|_{L_2} = 1$. Then, we get

$$\tilde{q}_0(\mathbf{x}) = \sqrt{\frac{1}{L_x}}. \quad (147)$$

Let $\tilde{\lambda}_{(0,s)} = 0$ and $\tilde{\varphi}_{(0,s)}$ be a solution of the algebraic eigenvalue problem

$$\left(\mathcal{K} + \tilde{\alpha}_l \tilde{\mathcal{D}} - \tilde{\lambda}_1 I_s \right) \tilde{\varphi}_1 = 0,$$

and let $\tilde{\varphi}_{(0,s)}^*$ be the solution of the corresponding adjoint eigenvalue problem. Define

$$\tilde{Q}_{(0,s)} \equiv \tilde{\varphi}_{(0,s)} * \overline{\tilde{\varphi}_{(0,s)}^*},$$

and the Green's function as

$$\begin{aligned} \tilde{G}(\mathbf{x}, \boldsymbol{\xi}) &\equiv \tilde{q}_0(\mathbf{x}) \tilde{q}_0(\boldsymbol{\xi}) \tilde{Q}_{(0,s)} \\ &= \frac{1}{L_x} \tilde{Q}_{(0,s)} \equiv \tilde{G}, \end{aligned}$$

where (147) is used to compute $\tilde{G}(\mathbf{x}, \boldsymbol{\xi})$. Note that

$$\begin{aligned} Q_{(N_c,s)} &= \tilde{Q}_{(0,s)}, \\ G &= \tilde{G}. \end{aligned} \quad (148)$$

Then, the steady-state concentration vector is given as

$$u_\infty(\mathbf{x}) = \tilde{G}u_0(\mathbf{x}). \tag{149}$$

Step 2:

We will show that $\|U_\infty(\mathbf{x}) - u_\infty(\mathbf{x})\|_{L_2}$ is $O\left(\frac{1}{N_c}\right)$. Subtracting (149) from (144) and using (148), we get

$$\begin{aligned} \|U_\infty(\mathbf{x}) - u_\infty(\mathbf{x})\|_{L_2} &= \left(\int_0^{L_x} \|GU_0(\mathbf{x}) - \tilde{G}u_0(\mathbf{x})\|_E^2 d\mathbf{x} \right)^{1/2} \\ &\leq \|G\|_E \left(\int_0^{L_x} \|U_0(\mathbf{x}) - u_0(\mathbf{x})\|_E^2 d\mathbf{x} \right)^{1/2}. \end{aligned} \tag{150}$$

Using (143) and (139) we get

$$\begin{aligned} \|G\|_E &= \left\| \frac{1}{L_x} Q_{(N_c,s)} \right\|_E \\ &= \left\| \frac{1}{L_x} \left(\varphi_{(N_c,s)} * \overline{\varphi_{(N_c,s)}^*} \right) \right\|_E \\ &\leq O(1), \end{aligned} \tag{151}$$

where the last inequality comes from the fact that $\varphi_{(N_c,s)}$ and $\varphi_{(N_c,s)}^*$ do not depend on N_c , which are the eigenvector and adjoint eigenvector of $\mathcal{K} + \alpha_l \mathcal{D}$ corresponding to $\alpha_{N_c} = 0$. Using (146) for $\mathbf{x} \in \left[\frac{(k-1)L_x}{N_c}, \frac{kL_x}{N_c} \right)$, we have

$$\begin{aligned} |(U_0(\mathbf{x}))_i - (u_0(\mathbf{x}))_i|^2 &\leq \left| \frac{1}{L_x/N_c} \int_{\frac{(k-1)L_x}{N_c}}^{\frac{kL_x}{N_c}} [(u_0(\boldsymbol{\xi}))_i - (u_0(\mathbf{x}))_i] d\boldsymbol{\xi} \right|^2 \\ &\leq \max_{b \in \left[\frac{(k-1)L_x}{N_c}, \frac{kL_x}{N_c} \right)} (u_0(b))_i^2 \left(\frac{L_x}{N_c} \right)^2 \\ &= O\left(\frac{1}{N_c^2} \right). \end{aligned} \tag{152}$$

When A is an $m \times n$ matrix, $\|A\|_E \leq \sqrt{mn} \|A\|_{\max}$. Therefore, using (152) we get

$$\begin{aligned} \|U_0(\mathbf{x}) - u_0(\mathbf{x})\|_E &\leq \sqrt{s} \|U_0(\mathbf{x}) - u_0(\mathbf{x})\|_{\max} \\ &= \sqrt{s} \max_i |(U_0(\mathbf{x}))_i - (u_0(\mathbf{x}))_i| \\ &\leq O\left(\frac{1}{N_c} \right). \end{aligned} \tag{153}$$

Using (150), (151), and (153), we get

$$\|U_\infty(\mathbf{x}) - u_\infty(\mathbf{x})\|_{L_2} = O\left(\frac{1}{N_c}\right).$$

□

In Lemma 2, we prove the convergence of $U_\infty(\mathbf{x})$ to $u_\infty(\mathbf{x})$. Now, we show the convergence of \overline{CV}^* as $N_c \rightarrow \infty$. Define $M_d(0)^{(k)}$ and $M_{d,\infty}^{(k)}$ be $s \times s$ diagonal matrices where diagonal elements are given as

$$\begin{aligned} \left(M_d(0)^{(k)}\right)_{ii} &= [M_d(0)]_{i(k,i)}, \\ \left(M_{d,\infty}^{(k)}\right)_{ii} &= [M_{d,\infty}]_{i(k,i)}, \end{aligned}$$

for $k = 1, \dots, N_c$ and for $i = 1, \dots, s$. Among the terms in (15), we first compute $P_s M_d(0) P_s^T$ using (140) and (141) as follows:

$$\begin{aligned} P_s M_d(0) P_s^T &= \left((\phi_{N_c} * \overline{\phi_{N_c}^*}) \otimes Q_{(N_c,s)} \right) M_d(0) \left((\phi_{N_c} * \overline{\phi_{N_c}^*}) \otimes Q_{(N_c,s)}^T \right) \\ &= \frac{1}{N_c^2} (\mathbf{u}_{N_c} * \mathbf{u}_{N_c}) \otimes \sum_{p=1}^{N_c} Q_{(N_c,s)} M_d(0)^{(p)} Q_{(N_c,s)}^T, \end{aligned}$$

where \mathbf{u}_{N_c} is an N_c -dimensional vector with each element equal to 1. Then, each component of $M_{d,\infty}^{-1} P_s M_d(0) P_s^T M_{d,\infty}^{-1}$ is written as

$$\begin{aligned} &\left[M_{d,\infty}^{-1} P_s M_d(0) P_s^T M_{d,\infty}^{-1} \right]_{i(k,i),i(q,j)} \\ &= \frac{1}{N_c^2} \left[\left(M_{d,\infty}^{(k)} \right)^{-1} \left(\sum_{p=1}^{N_c} Q_{(N_c,s)} M_d(0)^{(p)} Q_{(N_c,s)}^T \right) \left(M_{d,\infty}^{(q)} \right)^{-1} \right]_{ij}. \end{aligned} \tag{154}$$

Using the fact that sum of the initial mean species numbers in all compartments is bounded and using (151), we get

$$\left\| \sum_{p=1}^{N_c} Q_{(N_c,s)} M_d(0)^{(p)} Q_{(N_c,s)}^T \right\|_E \leq \left\| \sum_{p=1}^{N_c} M_d(0)^{(p)} \right\|_E \left\| Q_{(N_c,s)} \right\|_E \left\| Q_{(N_c,s)}^T \right\|_E \leq O(1). \tag{155}$$

Since each component of $\left(M_{d,\infty}^{(k)} \right)^{-1}$ is bounded by $O(N_c)$, using (155), (154) is bounded by $O(1)$. Therefore, we get

$$\begin{aligned} \overline{CV}^* &= \sqrt{V_c \times \lambda_{\max} \left(M_{d,\infty}^{-1} - M_{d,\infty}^{-1} P_s M_d(0) P_s^T M_{d,\infty}^{-1} \right)} \\ &= \sqrt{\sigma \left(\left(\frac{M_{d,\infty}}{V_c} \right)^{-1} - O \left(\frac{1}{N_c} \right) \mathbf{u}_{sN_c} * \mathbf{u}_{sN_c} \right)} \\ &\rightarrow \sqrt{\frac{1}{\min_{i,\mathbf{x}} (u_{\infty}(\mathbf{x}))_i}} \end{aligned}$$

as $N_c \rightarrow \infty$ where \mathbf{u}_{sN_c} is an sN_c -dimensional vector with each element equal to 1. Therefore, this gives the convergence of \overline{CV}^* .

References

- Anderson DF, Craciun G, Kurtz TG (2009) Product-form stationary distributions for deficiency zero chemical reaction networks. *Bull Math Biol* 72(8):1947–1970
- Andrews SS, Bray D (2004) Stochastic simulation of chemical reactions with spatial resolution and single molecule detail. *Phys Biol* 1(3–4):137–151
- Ashkenazi M, Othmer HG (1978) Spatial patterns in coupled biochemical oscillators. *J Math Biol* 5:305–350
- Austin RH, Beeson KW, Eisenstein L, Frauenfelder H, Gunsalus IC (1975) Dynamics of ligand binding to myoglobin. *Biochemistry* 14(24):5355–5373
- Bamford CH, Tipper CFH, Compton RG (1985) Diffusion limited reactions. *Comprehensive chemical kinetics*, vol 25. Elsevier, Amsterdam
- Baras F, Mansour MM (1996) Reaction-diffusion master equation: a comparison with microscopic simulations. *Phys Rev E* 54:6139–6148
- Bernstein D (2005) Simulating mesoscopic reaction-diffusion systems using the Gillespie algorithm. *Phys Rev E* 71(4 Pt 1):041103
- Bodwig E (1959) *Matrix calculus*. Interscience, New York
- Bokinsky G, Rueda D, Misra VK, Rhodes MM, Gordus A, Babcock HP, Walter NG, Zhuang X (2003) Single-molecule transition-state analysis of RNA folding. *Proc Natl Acad Sci* 100(16):9302–9307
- Conway E, Hoff D, Smoller J (1978) Large time behavior of solutions of systems of nonlinear reaction-diffusion equations. *SIAM J Appl Math* 35(1):1–16
- Crick FH (1970) Diffusion in embryogenesis. *Nature* 225:420–422
- Daleckiĭ JL, Kreĭn MG (1974) Stability of solutions of differential equations in Banach space. Series: translations of mathematical monographs. Providence, RI, AMS
- Delbrück M (1940) Statistical fluctuations in autocatalytic reactions. *J Chem Phys* 8:120–124
- Di Iorio EE, Hiltbold UR, Filipovic D, Winterhalter KH, Gratton E, Vitrano E, Cupane A, Leone M, Cordone L (1991) Protein dynamics. Comparative investigation on heme-proteins with different physiological roles. *Biophys J* 59(3):742–754
- Dobrzyński M, Rodríguez JV, Kaandorp JA, Blom JG (2007) Computational methods for diffusion-influenced biochemical reactions. *Bioinformatics* 23(15):1969–1977
- Erban R, Chapman SJ (2009) Stochastic modelling of reaction–diffusion processes: algorithms for bimolecular reactions. *Phys Biol* 6:046001
- Fange D, Berg OG, Sjöberg P, Elf J (2010) Stochastic reaction-diffusion kinetics in the microscopic limit. *Proc Natl Acad Sci* 107(46):19820
- Gadgil C, Lee CH, Othmer HG (2005) A stochastic analysis of first-order reaction networks. *Bull Math Biol* 67:901–946
- Gantmacher FR (1974) *The theory of matrices*, vol 2. Chelsea, New York
- Gillespie DT (1976) A general method for numerically simulating the stochastic time evolution of coupled chemical reactions. *J Comput Phys* 22:403–434

- Isaacson SA (2009) The reaction-diffusion master equation as an asymptotic approximation of diffusion to a small target. *SIAM J Appl Math* 70(1):77–111
- Isaacson SA, Isaacson D (2009) Reaction-diffusion master equation, diffusion-limited reactions, and singular potentials. *Phys Rev E* 80(6):066106
- Isaacson SA, Peskin CS (2007) Incorporating diffusion in complex geometries into stochastic chemical kinetics simulations. *SIAM J Sci Comput* 28(1):47–74
- Kato T (1966) *Perturbation theory for linear operators*, vol 132. Springer, Berlin
- Kurtz TG (1972) The relationship between stochastic and deterministic models for chemical reactions. *J Chem Phys* 57(7):2976
- Kuthan H (2001) Self-organisation and orderly processes by individual protein complexes in the bacterial cell. *Prog Biophys Mol Biol* 75(1-2):1–17
- Lauffenburger DA, Linderman JJ (1993) *Receptors: models for binding, trafficking, and signaling*. Oxford University Press, New York
- Lee CH, Othmer HG (2010) A multi-time-scale analysis of chemical reaction networks: I. Deterministic systems. *J Math Biol* 60(3):387–450
- Levsky JM, Singer RH (2003) Gene expression and the myth of the average cell. *Trends Cell Biol* 13(1):4–6
- Mayor U, Guydosh NR, Johnson CM, Grossmann JG, Sato S, Jas GS, Freund SM, Alonso DO, Daggett V, Fersht AR (2003) The complete folding pathway of a protein from nanoseconds to microseconds. *Nature* 421(6925):863–867
- Othmer HG (1977) Current problems in pattern formation. In: *Some mathematical questions in biology*, vol VIII. American Mathematical Society, Providence, pp 57–85
- Othmer HG (1980) Synchronized and differentiated modes of cellular dynamics. In: Haken H (ed) *Dynamics of synergetic systems*
- Othmer HG (1981) The interaction of structure and dynamics in chemical reaction networks. In: Ebert KH, Deuffhard P, Jager W (eds) *Modelling of chemical reaction systems*. Springer, New York, pp 1–19
- Othmer HG, Scriven LE (1969) Interactions of reaction and diffusion in open systems. *Ind Eng Chem Fundam* 8:302–315
- Othmer HG, Scriven LE (1971) Instability and dynamic pattern in cellular networks. *J Theor Biol* 32:507–537
- Ozbudak EM, Thattai M, Kurtser I, Grossman AD, van Oudenaarden A (2002) Regulation of noise in the expression of a single gene. *Nat Genet* 31(1):69–73
- Phat VN, Nam PT (2007) Exponential stability and stabilization of uncertain linear time-varying systems using parameter dependent Lyapunov function. *Int J Control* 80(8):1333–1341
- Serpe M, Umulis DM, Ralston A, Chen J, Olson DJ, Avanesov A, Othmer HG, O'Connor MB, Blair SS (2008) The BMP-binding protein Crossveinless 2 is a short-range, concentration-dependent, biphasic modulator of BMP signaling in *Drosophila*. *Dev Cell* 14:940–953
- Shimmi O, O'Connor MB (2003) Physical properties of Tld, Sog, Tsg and Dpp protein interactions are predicted to help create a sharp boundary in BMP signals during dorsoventral patterning of the *Drosophila* embryo. *Development* 130(19):4673–4682
- Smith HL (1988) Systems of ordinary differential equations which generate an order preserving flow. A survey of results. *SIAM Rev* 30(1):87–113
- Smoller J (1982) *Shock waves and reaction-diffusion equations*. Springer, Berlin
- Smoluchowski M (1917) Versuch einer mathematischen Theorie der Koagulationskinetik kolloider Lösungen. *Zeitschrift für physikalische Chemie* 92:129–168
- Spudich JL, Koshland DE (1976) Non-genetic individuality: chance in the single cell. *Nature* 262:467–471
- Stundzia AB, Lumsden CJ (1996) Stochastic simulation of coupled reaction-diffusion processes. *J Comput Phys* 127(0168):196–207
- Sung J, Shin KJ, Lee S (1997) Many-particle effects on the relaxation kinetics of fast reversible reactions of the type $A + B \rightleftharpoons C$. *J Chem Phys* 107:9418
- Thattai M, van Oudenaarden A (2001) Intrinsic noise in gene regulatory networks. *Proc Natl Acad Sci* 98:8614–8619
- Tomioka R, Kimura H, Kobayashi TJ, Aihara K (2004) Multivariate analysis of noise in genetic regulatory networks. *J Theor Biol* 229(4):501–521
- Umulis DM, Serpe M, O'Connor MB, Othmer HG (2006) Robust, bistable patterning of the dorsal surface of the *Drosophila* embryo. *Proc Natl Acad Sci* 103(31):11613–11618
- Umulis DM, O'Connor MB, Othmer HG (2008) Robustness of embryonic spatial patterning in *Drosophila melanogaster*. *Curr Topics Dev Biol* 81:65–111

- Wang X, Harris RE, Bayston LJ, Ashe HL (2008) Type IV collagens regulate BMP signalling in *Drosophila*. *Nature* 455:72–77
- Wolpert L (1969) Positional information and the spatial pattern of cellular differentiation. *J Theor Biol* 25:1–47
- Wolpert L (1971) Positional information and pattern formation. *Curr Topics Dev Biol* 6:183–224
- Zheng L, Kang H-W, Othmer HG (2011) The role of stochastic fluctuations in biological pattern formation (in preparation)